REPUBLIQUE DU CAMEROUN
Paix-Travail-Patrie
****
UNIVERSITE DE YAOUNDE I
****
CENTRE DE RECHERCHE ET DE FORMATION DOCTORALE EN SCIENES, TECHNOLOGIES ET GEOSCIENCES
****
UNITE DE RECHERCHE ET DE FORMATION
DOCTORALE EN PHYSIQUES ET APPLICATIONS
****
B.P 812 Yaoundé
Email: crfd_stg@uy1.uninet.cm

REPUBLIC OF CAMEROON
Peace-Work-Fatherland
****
THE UNIVERSITY OF YAOUNDE I
****
POSTGRADUATE SCHOOL OF SCIENCES, TECHNOLOGY AND GEOSCIENCES
****
RESEARCH AND POSTGRADUATE TRAINING UNIT FOR PHYSICS AND
APPLICATIONS
****
P.O. Box 812 Yaoundé
Email: crfd_stg@uy1.uninet.cm

LABORATOIRE DE MECANIQUE, MATERIAUX ET STRUCTURES

LABORATORY OF MECHANICS, MATERIALS AND STRUCTURES

Fractional Dynamics and Transport of Nerve Impulses in Neurons

Thesis submitted and defended in fulfillment of the requirements for the awards of a Doctor of Philosophy (Ph. D) degree in Physics

Option: Fundamental Mechanics and Complex Systems

By

BITANG A ZIEM Daniel Cassidi

Registration Number: **06W062**

Masters of Science in Physics

Under the supervision of
KOFANE Timoléon Crépin
Professor

UNIVERSITÉ DE YAOUNDÉ I
UNIVERSITY OF YAOUNDE I

FACULTÉ DES SCIENCES
FACULTY OF SCIENCE

DÉPARTEMENT DE PHYSIQUE
DEPARTMENT OF PHYSICS

ATTESTATION DE CORRECTION DE LA THÈSE DE DOCTORAT/Ph.D

Nous, Professeur **KENFACK JIOTSA Aurélien** et Professeur **BOUETOU BOUETOU Thomas**, respectivement Examinateur et Président du jury de la Thèse de Doctorat/Ph.D de Monsieur **BITANG A ZIEM Daniel Cassidi**, Matricule **06W062**, préparée sous la supervision du Professeur **KOFANE Timoléon Crépin,** intitulée : « **Fractional Dynamics and Transport of Nerve Impulses in Neuron**», soutenue le **Mardi 14 septembre 2021**, en vue de l'obtention du grade de Docteur/Ph.D en Physique, Spécialité **Mécanique, Matériaux et Structures,** Option **Mécanique Fondamentale et Systèmes Complexes,** attestons que toutes les corrections demandées par le jury de soutenance ont été effectuées.

En foi de quoi, la présente attestation lui est délivrée pour servir et valoir ce que de droit.

Fait à Yaoundé le 28 SEP 2021

Examinateur	Le Chef de Département de Physique	Le Président du jury
Pr. KENFACK JIOTSA Aurélien	Pr. NDJAKA Jean-Marie Bienvenue	Pr. BOUETOU BOUETOU Thomas

University of Yaoundé I

Faculty of Sciences

Department of Physics

FRACTIONAL DYNAMICS AND TRANSPORT OF NERVE IMPULSES IN NEURONS

Submitted and defended in Fulfillment of the Requirements for the Degree of Doctor of Philosophy/PhD in Physics

Option: Fundamental Mechanics and Complex Systems

By

BITANG A ZIEM Daniel Cassidi

Registration number: 06W062

Master in Physics

Director

Prof. KOFANE Timoléon Crépin

Professor, University of Yaoundé I (Cameroon)

Laboratory of Mechanics, Materials and Structures

Dedication

✠ To Jesus-Christ, which wealth, wisdom and science are so deep; the one of who, by who, and for who are all things.

✠ To my friend and late father ZIEM A BITANG Abel who would have liked to be physically present on this day, but so the fate of the morning of july 3, 2016 had decided otherwise. Wherever you are, I know that you guide my steps. Thanks for all.

✠ To my mother Mrs. KEEMAN A NJERE who always supported me, giving me the possible necessary, allowing thus the realization of this work.

Acknowledgements

At the end of the PhD study, I am deeply grateful for the opportunity to have learned from and worked with so many brilliant teachers, collaborators and students. I am happy to express my sincere gratitude to all those from who near or far have accompanied me during these doctoral years and have directly or indirectly contributed to the completion of this document. Nevertheless, I will do my best to condense my thoughts about this.

★ Firstly, I would like to express my sincere gratitude to God almighty who gave me the life, the opportunity and the knowledge to reach and to end with the PhD study level.

★ I have furthermore to thank the persons responsible of the Faculty of Sciences, and the Research and postgraduate training unit for physics and applications who gave and confirmed the permission to go ahead with my thesis.

★ I would like to express my sincere gratitude to my director **Professor KOFANE Timoléon Crépin** who, despite his multiple academic and family occupations, accepted to guide this work. This thesis would not have been possible without his pernickety vision in nonlinear physics. I want to thank him for the advices he has provided me and the expertise that he has enabled me to acquire.

★ I would like to deeply thanks the honorable **members of the Jury**, who agreed to put aside their multitude occupations so as to evaluate this work. I express to them all my greatest respect.

★ I would like to thank **Professor NDJAKA Jean Marie**, Head of the Department of Physics. I am very grateful for his administrative contribution and encouragement.

★ I would like to thank **Professor BOUETOU BOUETOU Thomas** for his teaching specially in mathematical technics.

★ I would like to thank **Professor BEN-BOLIE** for his support.

★ I would like to thank **Professor WOAFO Paul**, Chairman of the Cameroon Physical Society for his teaching specially in numerical methods.

★ I would like to specially thank **Professor WAKATA Annie Sylvie**, for her advices, her constructive discussions and her flawless support.

★ It would be very pleasing to recognize trade and constructive discussions com-

bined with great moments of sharing with all the teachers of the Department of Physics in general and of the laboratory of Mechanics, Materials and Structures in particular. I have named **Professor TCHAWOUA Clément**; **Germain**; **Professor NANA NBENDJO Blaise Roméo**; **Professor ZEKENG Serge**; **Professor DJUIDJE Germaine**; **Professor BODO Bertrand**; **Professor FEWO Serge**; **Professor SAIDOU**; **Professor HONA Jacques**; **Professor VONDOU Derbetini**; I would like to thank **Doctor TABI Conrad**; **Doctor**
ENYEGUE ANYAM wife **BELINGA F.**; **Doctor TOGUEU MOTCHEYO Alain**, **Doctor ABOBDA Théo**, **Doctor METSEBO Jules**, **Doctor DEMANOU Buris Peguy**, **Doctor DJOMO MBONG T.M.L.**, **Doctor MANDENG Lucien**, **Doctor NWAGOUM Peguy Russel**, **Doctor NDJOMATCHOUA Thomas Frank** for their kindness, availabilities and their encouragements and for many fruitful discussions. Despite their multiple occupations, they initiated me and gave me a taste of research.

★ Special thanks to **NGNINZALONG Carlos**, **MOKEM FOKOU Igor Simplice**, **KEPNANG PEUBEU Maxime Fabrice**, **FOPOSSI MBEMMO André Marie**, **WADOP NGOUONGO Yannick Joel** and **ZANGA Dieudonné**, **HEUTEU Crépin**, **MUNDIH Schazt** for the multitude exchanges and helps.

★ My sincere thanks go to the official editors and referees of Physica A, for their detailed review, constructive criticism and excellent advice during the preparation of my different publications.

★ My sincere thanks go to **Reverent DR NKOLO FANGA Jean Patrick**, pastors of the Cameroonian Presbyterian Chuch located at Manguiers. I thank him for his permanent prayers and actions that he done and continue to do for my life, my family and my studies.

★ The fulfillment of my thesis is the work of the good atmosphere in my family. I would like to thank:

• My mother **KEEMAN A NJERE** for her love for me and for her material, financial and moral supports.

• My brothers and sisters **BEB A ZIEM Hyacinthe**, **BONG A ZIEM Eleonora**, **AZAB A ZIEM Marie**, **MPEY Anne A.**, **MOUBITANG A ZIEM Friedrich**, **BEDIANG Véronique**. I thank all of them for their moral and financial supports and for all their prayers for me.

• I thank all my uncles, aunts, cousins, nephews and nieces for their encouragements.

★ I thank my father **AMANG Laurent** and his wife, my brother and friend **BIDIA A KEDI Achille** and his wife **Sandrine**, and my father

KIBONG EDOUARD for their supports, prayers and encouragements.

★ I thank my lovely **NDOMBI KWATO Elodie Alice** for her love for me and her prayers and all types of supports that she gave me continuously, as well as my daugther **Alycia Katelyn KEEMAN Hoth** . I would also thanks some of my friends like **MATSANG OMOLENE Patrick** and his wife, **Clarisse, JIOKOU Gino, TCHAPI Raoul, TELLA Thierry , MONEPIMB Valdes, KAMENI Marina, PESNDJOCK Mathieu, FOSSI NEUMOGNE Rodrigue, NGADJOU Ariane** and **NGOM GWEM Joseph**.

★ I say thank you to all those that I certainly forget to mention the names here.

Contents

List of Figures

List of Abbreviations

ATP: **A**denosine **T**riphosphate
CRISPR : **C**lustered **R**egularly **I**nterspaced **S**hort **P**alindromic **R**epeats
DDE : **D**elay **D**ifferential **E**quations
DNA : **D**eoxyribonucleic **A**cid
FDCs : **F**ractional **D**erivative **C**onstraints
GABA : **G**amma **A**minobutyric **A**cid
RNA : **R**ibonucleic **A**cid
RNAi : **R**ibonucleic **A**cid interference
RFDE : **R**etarded **F**unctional **D**iferential **E**quation
NDDE : **N**eutral **D**elay **D**ifferential **E**quation
NFDEs : **N**eutral **F**unctional **D**iferential **E**quation
NGS : **N**ext-**G**eneration **S**equencing
PCR : **P**olimerase **C**hain-**R**eaction

Abstract

In this thesis, the understanding of the importance of memory in biological systems in close correlation with the transport of nerve impulse in neurons is our focal point. With this in mind, we first inventoried the different manifestations of memory, as well as all the biological systems involved in this transport process. It turns out that chromatin is one of them, with a type of memory very little known in biology, namely transport memory. Next, we test the stability of this memory in the presence of certain phenomena frequently encountered in the process of neuronal transport such as toxins and fluctuations. Starting from the generalization of the Brownian motion well-known as the reaction random walk, we studied the impact of fluctuations of external origin which enter the transport process on the neuronal scale. We have shown that these fluctuations increase the nonlinearity, thus inducing biological chaos in the environment. The complexity and control inherent in chaotic systems are very important for the dynamics of gene expression and translation. Finally, by considering subdiffusive regime, we studied a diffusion reaction model describing the spread of toxins in an ecosystem. The cases studied allowed us to better understand the memory effect in prey-predator competition. It clearly shows that memory can cancel the so-called Turing structures already formed, just as it can create new ones. However, no case studied has led to the extinction of the present species.

Keywords: Memory effects; Transport memory; Reaction random walk; External fluctuations; Toxicity; Subdiffusion; Turing instability.

Résumé

Dans cette thèse, la compréhension de l'importance de la mémoire dans les systèmes biologiques en étroite correlation avec le transport de l'influx nerveux dans les neurones est notre point focal. Dans cette optique, nous avons inventori dans un premier temps les différentes manifestations de la mémoire, ainsi que certains systèmes biologiques impliqués dans ce processus de transport. Il en ressort que la chromatine en fait partie, avec un type de mémoire très peu connu en biologie, à savoir la mémoire de transport. Ensuite, nous avons test la stabilité de cette mémoire face à certains phénomènes fréquemment rencontrés dans le processus du transport neuronal tels que les toxines et les fluctuations. Partant de la généralisation du mouvement Brownien plus connue sous le nom de réaction de marche aléatoire, nous avons étudié l'impact des fluctuations d'origine externe qui entrent dans le processus de transport à l' échelle neuronale. Nous avons montré que ces fluctuations augmentent la nonlinéarité, induisant ainsi un chaos biologique dans le milieu. La complexité et le contrôle inhérent aux systèmes chaotiques sont très importants pour la dynamique de l'expression et de la translation génétique. Enfin, en considérant le régime sous diffusif, nous avons étudié un modèle de réaction diffusion décrivant la propagation des toxines dans un écosystème. Les cas étudiés nous ont permis de mieux appréhender l'effet mémoire dans la compétition proie-prédateur. Il en ressort clairement que la mémoire peut annuler les structures dites de Turing déjà formées, tout comme elle peut en créer de nouvelles. Cependant, aucun cas étudié n'a conduit à l'extinction des espèces présentes.

Mots clés: Effets de mémoire; Mémoire de transport ; Réaction Random Walk; Fluctuations externes; Toxicité; sous diffusion; instabilit de Turing.

General Introduction

An electrical signal that travels along neurons, nerve impulses transmit motor commands from the brain to motor nerves, and sensory messages from sensory organs (skin, ears, nose, eyes, taste receptors) to the brain. This transmission from neurons to neurons is ensured by neurotransmitters. Neurotransmitters are often referred to as body's chemical messengers [1, 2]. They are the molecules used by the nervous system to transmit messages between neurons, or from neurons to muscles. Communication between two neurons takes place in the synaptic cleft (the small gap between the synapses of neurons) [3, 4, 5, 6, 7]. Here, electrical signals that have travelled along the axon are briefly converted into chemical signals through the release of neurotransmitters, causing a specific response in the receiving neuron. A neurotransmitter influences a neuron in one of the three ways: excitatory, inhibitory or modulatory. An excitatory transmitter promotes the generation of an electrical signal called an action potential in the receiving neuron, while an inhibitory transmitter prevents it. Whether a neurotransmitter is excitatory or inhibitory depends on the receptor it binds to. Neuromodulators are a bit different, as they are not restricted to the synaptic cleft between two neurons, and so can affect large numbers of neurons at once. Neuromodulators therefore regulate populations of neurons, while also operating over a slower time course than excitatory and inhibitory transmitters. These chemical messengers can affect a wide variety of physical and psychological functions, including heart rate, sleep, appetite, mood, fear and lead to dynamic changes in gene expression via modifying chromatin accessibility.

The mammalian brain works appropriately only when there is a proper balance between excitation and inhibition. An imbalance in the ratio of excitatory−to−inhibitory neurons (referred to as the E/I ratio) is associated with numerous neurological abnor-

malities and deficits [8]. Increased E/I ratios, that is higher excitability, leads to prolonged neocortical circuit activity, stimulus hypersensitivity, cognitive impairments, and epilepsy [9, 10, 11]. Of equal interest and importance, decrease in the E/I ratio, or a stronger inhibitory drive, have been linked to impaired social interactions, autistic behaviors, and mental retardation [12, 13]. It is well accepted that the E/I ratio changes during neuronal development, with excitation decreasing and inhibition increasing, and that deviations in this process give rise to neurological disorders. Most notably, inhibitory and excitatory neurons compose two distinct groups on the basis of several features. They release different neurotransmitters and their synapses therefore have different functional influences (-aminobutyric acid, inhibitory vs. glutamate, excitatory). Inhibitory neurons also have aspinous dendrites and are fastspiking compared to excitatory neurons which have spiny dendrites and are regular−spiking or bursting.

With the consolidation of nonlinear science and neuroscience, more and more attention has been paid to the intricate spiking rhythms in neuronal models. Previous works have revealed the mechanism for different modes of neuronal bursting or spiking from the point of view of dynamics [14, 15, 16, 17, 18, 19, 20, 21, 22]. Among these works, one of the most striking was that of Brian et al. who analyzed the dynamics of firing rate with a range of stimulus dynamics in their neurophysiology experiment [23]. Their results showed that single rat neocortical pyramidal neurons can adapt along a time−scale that depends on the change in stimulus statistics. This multiple time−scale adaptation is consistent with fractional−order differetiation, such that the neuron's firing rate is a fractional−order derivative of slowly varying stimulus [23]. Moreover, The vestibulo-ocular reflex and other oculomotor subsystems such as pursuit and saccades are ultimately mediated in the brainstem by premotor neurons in the vestibular and prepositus nuclei that relay eye movement commands to extraocular motoneurons. The premotor neurons receive vestibular signals from canal afferents. Canal afferent frequency responses have a component that can be characterized as a fractional order differentiation [24].

In recent years, fractional calculus has allowed describing several complex problems

in the fields of mathematics, physics, biology, and engineering [26, 25]. The complexity of these problems has led researchers to develop mathematical theories to model the complexities of nature taking into account the fractional calculus. The mathematical models are powerful tools used for describing real-world problems; to develop mathematical models, differential equations and differential operators are required, which can be local or non-local. The non-local can further be divided into three types: differential operators with a power-law kernel, differential operators with exponential decay law, and finally, differential operators with Mittag-Leffler law. The operators with non-singular kernel have the following features: They do not impose artificial singularities on any model, they have at the same time Markovian and non-Markovian properties, they are at the same time power law, stretched exponential and Brownian motion, the mean square displacement is a crossover from usual diffusion to sub-diffusion, the derivative probability distribution is at the same time Gaussian and non-Gaussian, and it can cross over from Gaussian to non-Gaussian even without passing through the steady state. It means that the fractional derivatives with non-singular kernel are at the same time deterministic and stochastic.

Fractional−order differentiation/integration is a fundamental and general computation that can contribute to efficient information processing, stimulus anticipation, and assessment of frequency−independent phase shifts of oscillatory neuronal firing. It has a long history from 30 September 1965, when the derivative of oder $\alpha = 1/2$ was mentioned by Leibniz. New possibilities in mathematics and theoretical physics appear, when the order of the differential operator D_x^α or the integral operator I_x^α becomes an arbitrary parameter. The fractional calculus is a powerful tool to describe physical systems that have long−term memory and long range spatial interactions. Most of the processes associated with complex systems have nonlocal dynamics and it can be characterized by long−term memory in time. Recently, a new type of memory was observed in the transport process. It arises if the linear part of the evolution represents a process which is in part ballistic and in part diffusive, and was termed transport memory [27, 28]. In this case, the memory function or correlation function which describes the transport is,

in such cases not a δ function as in the purely diffusive case, but has a finite decay time [29]. In the last decades, fractional calculus [30, 31, 26, 32, 25] has become very useful and provides an excellent instrument for modeling the biophysical phenomena [33]. It includes the properties of tissue−electrode interface [34], viscoelastic properties of tissue [35], kinetic properties of drug delivery and absorption [36, 37], diffusion process [38, 39], computational neuron models [40, 41, 42], analysis of different neural networks [43, 44, 45] and so on. The fractional−order neuron models produce diverse firing patterns [46, 47, 48]. Although the single neurons respond to applied current stimulus on very short time period, the mean firing activities and firing rates can be considered under the dynamics of fractional differentiation. It provides a general model system for the firing−rate response to time−varying statistics. It has been observed in a wide range of neural systems, from ion channels of neuronal membrane to cognitive behavior [49]. It is also possible to have a power−law response without the frequency−independent phase property of the fractional derivative. Fractional-order dynamics has been observed in the vestibular-oculomotor system [24, 50, 51] and the fly motion of sensitive neuron H1 [52]. It may contribute to the mechanisms including neural circuit theory [50], synaptic activities between the neurons [52], geometrical properties of neural cells [24, 50].

In this thesis, the investigation of the role played by the memory on different aspects linked to the transport of nerve impulses in neurons is our main focus. Enlightened by the fact that Billions of neurotransmitter molecules which ensure transmission from between neurons work constantly to keep our brains functioning, managing everything from our breathing, heartbeat to our learning and concentration levels, We decided to focus on the role that the memory effect would actually play in all the underlying processes that would result from this transport. The thesis is structured as follows: in the first chapter, we conducted a review of the scientific literature around the theme of this thesis. It presents different ways of approaching memory effects in biology. The second chapter, is developed to present analytical tools and numerical methods used. The last chapter is devoted to the results and discussions. The thesis ends with a summary of the main results and some perspectives for future investigations.

CHAPTER I

LITERATURE REVIEW

I.1 Introduction

Neurotransmitters are endogenous substances that act as chemical messengers by transmitting signals from a neuron to a target cell across a synapse. Prior to their release into the synaptic cleft, neurotransmitters are stored in secretory vesicles (called synaptic vesicles) near the plasma membrane of the axon terminal. The release of the neurotransmitter occurs most often in response to the arrival of an action potential at the synapse. When released, the neurotransmitter crosses the synaptic gap and binds to specific receptors in the membrane of the post-synaptic neuron or cell.

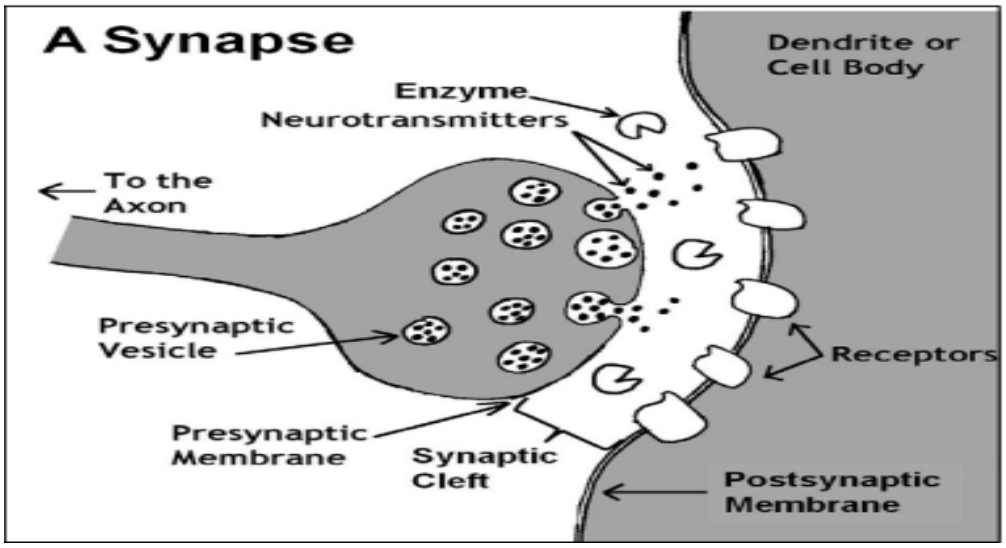

Figure 1: Chemical transmission between nerve cells

Neurotransmitters are generally classified into two main categories related to their overall activity, excitatory or inhibitory. Excitatory neurotransmitters exert excitatory effects on the neuron, thereby, increasing the likelihood that the neuron will fire an action potential. Major excitatory neurotransmitters include glutamate, epinephrine and nore-

pinephrine. Inhibitory neurotransmitters exert inhibitory effects on the neuron, thereby, decreasing the probability that the neuron will fire an action potential. Major inhibitory neurotransmitters include GABA, glycine, and serotonin. Some neurotransmitters, can exert both excitatory and inhibitory effects depending on the type of receptors that are present. In addition to excitation or inhibition, neurotransmitters can be broadly categorized into two groups defined as small molecule neurotransmitters or peptide neurotransmitters. Many peptides that exhibit neurotransmitter activity also possess hormonal activity since some cells that produce the peptide secrete it into the blood where it then can act on distant cells. Small molecule neurotransmitters include (but are not limited to) acetylcholine, GABA, amino acid neurotransmitters, ATP and nitric oxide (NO). The peptide neurotransmitters include more than 50 different peptides. As mentioned above, the transmission orchestrated by neurotransmitters affects a lot of physical and physiological function of our body. Furthermore, the discovery of memory effects in this process has facilitated the understanding of some previously unknown mechanisms, as well as the advancement of medicine. However, although the memory effect has made it possible to better understand the transport of nerve impulses in neurons, few studies have examined the influence of the memory effect on the various processes in close correlation with this transport. in this chapter, we will review the advances made in this field thanks to memory effects, after which, a presentation of the processes triggered by said transport will be made. In the next section, we will present the different manifestations of memory effects. We will end this chapter with the problematic of this thesis, the possible solutions of which will be presented in the next chapter.

I.2 Literature review on some interrelationships of the nerve impulses and some biological systems exhibiting memory effects

I.2.1 The interrelationship of nerve impulses and blood cells

Blood racing through a brain region's web of vessels is a sign that nerve cells in that locale have kicked into action. The blood rushes to active areas to supply firing neurons with the oxygen and glucose they need for energy. It is this blood flow, which can last up to a minute, that scientists track in functional magnetic resonance imaging (fMRI) to determine which brain areas are responding to different stimuli. But a new theory could pave the way for a reinterpretation of fMRI images, elevating their measurements to the evaluation of actual neuronal processing rather than the subsequent blood flow that indirectly indicates it, and thereby enhancing the fMRI's usefulness in diagnosing neurological problems.

C. Moore, an assistant neuroscience professor at the Massachusetts Institute of Technology's McGovern Institute for Brain Research, detailed his hypothesis in an article [53]. In essence, it suggests blood's role in the cortex (a key brain processing center), specifically, is more than just bringing nutrients to the cell, it can also alter the activity of local neuronal circuits. For instance, in experiments in his lab, Moore has seen that there is more blood flow can arrive in an area that processes information from a presented stimulus to a certain sense (e.g. touch, visual, auditory) prior to the appearance of the stimulus, implying that the flow can prime a circuit for activity, as well. Moore concluded that, blood should be factored into any model of neuronal processing, how nerve cells in the brain are activated, how impulses are transmitted between them, how long activity lasts, and how it is terminated. In addition to changing what fMRI is actually measuring, such models could potentially provide new clues to causes of enigmatic disorders such as Alzheimer's disease, multiple sclerosis and schizophre-

nia, potentially paving the way for treatments that involve correcting blood flow as well as (or rather than) chemical deficiencies. According to Moore, the vasculature thus directly or indirectly (via astrocytes) influences neurons. He notes that substances in blood may modulate neuron activity. The most likely candidate, he says, is nitric oxide (NO), which easily crosses the bloodbrain barrier and has been shown both in brain slices and in animal models to excite (and in some cases dampen) neuronal action. Blood vessels also affect neurons via thermal and mechanical stress. Increased blood flow can alter the local temperature in a brain region. For instance, a decrease of just one degree Celsius can lead to suppressed firing rates, in some circumstances. As a rule, blood flow changes increase the temperature in outer brain areas, while decreasing the temperature of more central regions. Pressure and volume, meanwhile, within the blood vessels can change the amount that the vessels physically impact the membranes of brain cells. If pressure or volume were to increase, a vessel could bulge, blocking receptors or ion channels and thereby causing a decrease in a neuron's electrical activity. A change in blood flow could also trigger astrocytes to release certain hormones or neurotransmitters. "If anything is going on in the blood vessel," Moore says, "the glia (astrocytes and other non-neuronal nerve cells) is in a great position to sense it." For instance, astrocytes might secrete the excitatory neurotransmitter glutamate, which binds to neurons and allows ion exchanges that cause cells to fire.

As we can see, the link between blood cells and nerve impulses is therefore clearly established. however, the human red blood cells can be deformed by external forces but returns to the biconcave resting shape after removal of the forces [54]. The shape memory was probed by an experiment called go-and-stop. In this experiment, the cells were first sheared to induce a tank-tread motion. Then the flow was stopped, and a subsequent motion of the red cell was taken as an evidence of a shape memory. It was found that virtually all cells tested showed a shape memory and that this memory was not eliminated even by continuous shearing of the red cells for four hours. Preliminary results of the go-and-stop experiment were presented as an abstract [55].

This paragraph briefly shows the close relationship that exists between nerve im-

pulses and blood vessels on the one hand, and between blood vessels and memory effects on the other. However, it should be noted that apart from blood vessels, other biological systems with similar interconnections exist.

I.2.2 The interrelationship of nerve impulses and DNA

DNA is the fundamental molecule by which information is stored and utilized to produce life. DNA is a high-density storage medium [56, 57, 58] that can be quickly copied by exponential PCR amplification and stably preserved for decades to millennia [59]. Biological information encoded in DNA can be directly converted into actionable cellular responses through gene regulation and expression. Although DNA is often thought of as a long-term information-bearing molecule, there are many examples of biological information storage and access through DNA within a single life cycle of an organism. Examples include phase variation [60], CRISPR-mediated immunity [61], mammalian adaptive immune systems [62], diversity-generating retroelements [63] and programmed genome rearrangements [64, 65]. Advances in next-generation sequencing (NGS) [66] and nucleic acid synthesis [67] have ushered in a new era of rapid and inexpensive DNA reading and writing, which has further elevated the relevance of DNA as a meaningful information storage medium. Recently, a simple molecular memory, named the ”hairpin-DNA memory”, has been developed (see Fig. 2) [68]. The memory employs the temperature-controlled conformational transition of hairpin-DNA strands in memory writing and erasing and allows parallel addressing of a very large memory space without physical wiring. Experiments on repetitive memory writing and erasing demonstrated that the molecular addressing was highly selective and parallel.

It is now ubiquitous that DNA is the memory storage molecule of all living things. It is two chains of nucleotides that coil around each other to form a double helix. The interactions between the nucleotides of each chain are so strong that scientists can fold DNA in very specific ways at a nanoscale. Like blood cells, DNA has a strong influence on nerve impulses. Indeed, Johns Hopkins scientists led by Hongjun Song, Ph.D., a pro-

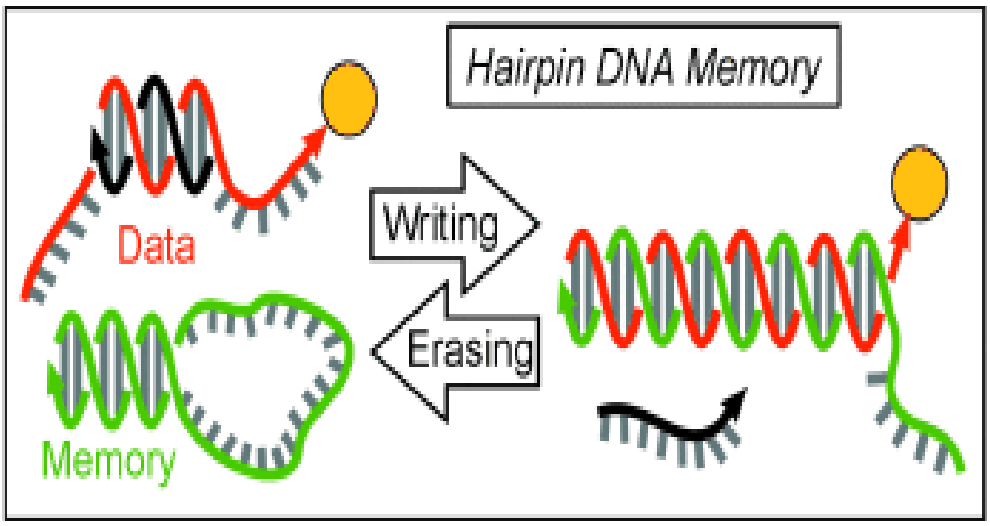

Figure 2: Mechanism of the writing and erasing of the hairpin-DNA memory.

fessor of neurology and neuroscience in that university, have discovered that neurons are risk takers: They use minor "DNA surgeries" to toggle their activity levels all day, every day. The main job of neurons is to communicate with other neurons through connections called synapses. At each synapse, an initiating neuron releases chemical messengers, which are intercepted by receptor proteins on the receiving neuron. Neurons can toggle the "volume" of this communication by adjusting the activity level of their genes to change the number of their messengers or receptors on the surface of the neuron. When Song's team added various drugs to neurons taken from mouse brains, their synaptic activity, the volume of their communication went up and down accordingly. When it was up, so was the activity of the Tet3 gene, which kicks off DNA demethylation. When it was down, Tet3 was down too [69]. Then, they flipped the experiment around and manipulated the levels of Tet3 in the cells. Surprisingly, when Tet3 levels were up, synaptic activity was down; when Tet3 levels were down, synaptic activity was up. So do Tet3 levels depend on synaptic activity, or is it the other way around? Another series of experiments showed them that one of the changes occurring in neurons in response to low levels of Tet3 was an increase in the protein GluR1 at their synapses. Since GluR1 is a receptor for chemical messengers, its abundance at synapses is one of the ways neurons can toggle their synaptic activity. The scientists say they have dis-

covered another mechanism used by neurons to maintain relatively consistent levels of synaptic activity so that neurons can remain responsive to the signaling around them. If synaptic activity increases, Tet3 activity and base excision of tagged cytosines increases. This causes the levels of GluR1 at synapses to decrease, in turn, which decreases their overall strength, bringing the synapses back to their previous activity level. The opposite can also happen, resulting in increasing synaptic activity in response to an initial decrease. So Tet3 levels respond to synaptic activity levels, and synaptic activity levels respond to Tet3 levels. This result enlighted the close correlation between the DNA and nerve impulses.

I.2.3 The interrelationship of nerve impulses and chromatin

How transient activation of mature neuronal circuits leads to changes in gene expression and properties in neurons over the short- and long- term is a fundamental question in neurobiology and has significant implications for understanding neuronal plasticity, learning and memory, and brain disorders [70]. Epigenetic mechanisms play a crucial role in regulating neuronal gene expression, and neuronal activity is known to alter epigenetic landmarks, such as DNA methylation and histone modifications [71, 72, 73, 74]. These epigenetic changes not only regulate gene activation and suppression, but also modify the dynamics of gene expression [75]. Regulation of chromatin opening is an important regulatory mechanism for the precise control of gene expression patterns. Global changes in chromatin accessibility occur during cell differentiation when cells with the same genome establish their identities through distinct gene expression patterns. Previous genome-wide studies of different tissues and cell types, including those in the nervous system, have revealed tissue-and cell-type-specific landscapes of chromatin accessibility [76]. It results that widespread chromatin accessibility changes induced by neuronal activation[77]. Moreover, It has recently been shown [78] that chromatin moves coherently across micronscale regions [79], and incoherently until segregation ends [80]. This passage of the character of the motion from coherent to incoherent

is a general feature of all physical systems with memory effects [28, 29]

I.2.4 The interrelationship of nerve impulses and RNA

Chromatin structure is influenced by multiples factors, such as pH, temperature, nature and concentration of counterions, post-translational modifications of histones and binding of structural non-histone proteins. RNA is also known to contribute to the regulation of chromatin structure as chromatin-induced gene silencing was shown to depend on the RNAi machinery in S. pombe, plants and Drosophila [81]. Moreover, in the universe of science, two worlds have recently collided those of RNA and chromatin. The intersection of these two fields has been impending, but evidence for such a meaningful collision has only recently become apparent [82]. Since chromatin is highly influenced by neuronal activation, it is, therefore, reasonable to expect that RNA also is influenced by neuronal activation. Regarding memory effects, they were highlighted for the very first time by Katchalsky et al. [83] who found that RNA in solution exhibits hysteresis phenomena with respect to changes in pH. Hysteresis cycles are independent of time but dependent on the history of the system. Indeed, RNA folding potential energy surfaces are rugged and full of kinetic traps, which can prevent the formation of the native structure and result in persistent differences in behavior between molecules, termed folding memory effects. The study of memory effects is closely linked to the development and application of single-molecule fluorescence methods, which were instrumental in the dissection of RNAs into discrete subpopulations with different dynamic properties. The ability to interconvert subpopulations confirms that memory effects are an intrinsic property of RNA folding and enables their thermodynamic and kinetic characterization [84].

In this section, it has been shown that memory effects are not limited only to the neuron, but that they are present in many processes in close correlation with the transport of nerve impulses. This tends to confirm the hypothesis that the mechanism of memory coding in the brain is similar to that in the immune system so that the permanence

of memories in the nervous system is ensured at the genomic level by a somatic recombination mechanism [85]. However, we have noticed that memory effects manifest themselves differently, depending on whether one is in a biological system or another. in the next section, we will review the different modeling of memory effects existing in the literature.

I.3 Review studies on memory effects

Memory, in a more strict sense, can be defined as the capacity to store information that can be recalled again with high distinction to steer the function correlated with the new information. It is not visible, however, depending on the environment and circumstances, its effects are identifiable, and can be modeled mathematically. The different approaches most used in the physical literature are the following:

I.3.1 Delayed differential equation approach

A retarded functional differential equation (RFDE) describes a system where the rate of change of state is determined by the present and the past states of the system. If the rate of change of the state depends on its own values as well, the system is called a neutral functional differential equations (NFDEs). When only discrete values of the past have influence on the present rate of change of state, the corresponding mathematical model is either delay differential equation (DDE) or neutral delay differential equation (NDDE). The theory of RFDEs is of both theoretical and practical interest, as they provide a powerful model of many phenomena in applied sciences such as physics, biology, economics, control theory and so on. They play an important role in explaining many different behaviors. The works reported in [86, 87, 88, 89, 90, 91, 92, 93, 94, 95] indicate the scope for applications of RFDEs in bioscience. The authors remark, therein, how delay differential equations have, prospectively, more interesting dynamics than equations that lack memory effects; in consequence they provide potentially more flexible tools for modelling.

In many applications in the life sciences a delay is introduced when there are some hidden variables and processes, which are not well understood but are known to cause a time-lag [96]. Thus, a delay may in fact represent a reaction chain or a transport process. A well-known example is Cheyne-Stokes respiration (or periodic breathing), discovered in the 19th century: some people show, under constant conditions, periodic oscillations of breathing frequency [97]. This strange phenomenon is apparently due to a delay caused by cardiac insufficiency in the physiological circuit controlling the carbon dioxide level in the blood. Delays also occur naturally in the chemostat (a laboratory device for controlling the supply of nutrient to a growing population). The use of ODEs to model the chemostat carries the implication that changes occur instantaneously. This is a potential deficiency of the ODE model. There are two sources of delays in the chemostat model: delays due to the possibility that the organizm stores the nutrient (so that the free nutrient concentration does not reflect the nutrient available for growth); and delays due to the cell cycle; see [90, 92, 98].

In immunology, the response of an immune system cannot be represented correctly without the hereditary phenomena being taken into account: cell division, differentiation, etc. (the time needed for immune cells to divide, mature, or die). The simple mathematical model of immune response employed by Marchuk [99] describes the interaction of viruses, $V(t)$; antibodies, $F(t)$; plasma cells, $C(t)$; and the relative characteristic of the affected organ, $m(t)$, of a person infected by a viral disease. This model is formulated as a system of four nonlinear DDEs:

$$\begin{aligned} V'(t) &= (p_1 - p_2 F(t))V(t), \\ C'(t) &= \xi(m) p_3 F(t-\tau)V(t-\tau) - p_5(C(t) - C^*), \\ F'(t) &= p_4(C(t) - F(t)) - p_8 F(t)V(t), \\ m'(t) &= p_6 V(t) - p_7 m(t), \end{aligned} \tag{1}$$

with $t \geq 0$, and $\xi(m)$ is defined by

$$\xi(m) = \begin{cases} 1 \quad if\ m \leq 0.1 \\ \frac{10}{9}(1-m) \quad if\ 0.1 \leq m \leq 1 \end{cases} \tag{2}$$

The first equation describes the change in the number of antigen in an organizm (it is a Volterra-Lotka like predator-prey equation). The second equation describes the creation of new plasma cells with time-lag due to infection (in the absence of infection, the second term creates an equilibrium at $C(t) = C^*$). The third equation models the balance of the number of antibody reacting with antigens: the generation of antibodies from plasma cells is described by $p_4C(t)$ and their decrease due to aging are described by $(p_4F(t))$ and binding with antigens by $(p_8F(t)V(t))$. The relative characteristic $m(t)$ of damaging organizm is given by the fourth equation of which the first term expresses the degree of damage to an organ and the second term describes the recuperation due to the recovery activity of the organizm. Finally, the definition of (m) expresses the fact that the creation of plasma cells slows down when the organizm is damaged by the viral infection.

The great potential of simple DDEs for capturing complex dynamics observed in physiological systems, was shown in a series of related works [97, 100]. Delay differential equations were used to model unstable patterns of (i) the human respiratory system and regulation of blood concentration of CO_2 (periodic breathing and prediction of low- and large-amplitude oscillations), (ii) the production of blood cells (periodic and chaotic regimes), and (iii) hormone regulation in the endocrine system (period doubling bifurcations and chaotic solutions). The following model is concerned with the regulation of hematopoiesis, the formation of blood cell elements in the body. For example white and red blood cells, platelets and so on are produced in the bone marrow from where they enter the blood stream. When the level of oxygen in the blood decreases this leads to a release of a substance which in turn cause an increase in the release of the blood elements from the marrow. There is thus a feedback from the blood to the bone marrow. As an illustrative example, let $c(t)$ be the concentration of cells (the population species)

in the circulating blood. We assume that the cells are lost (die) at a rate proportional to their concentration, that is like $\gamma c(t)$, where the parameter γ has dimensions $(day)^{-1}$. After the reduction in cells in the blood stream there is about a 6 day delay before the marrow release further cells to replenish the deficiency [97]. We thus assume that the flux λ of cells into the blood stream depends on the cell concentration at an earlier time, namely, $c(t-\tau)$, where τ is the delay. Such assumptions suggest a model equation of the form

$$\frac{dc(t)}{dt} = \lambda c(t-\tau) - \gamma c(t). \tag{3}$$

a possible replacement in the form of the non-linear delay differential equation of (3) was proposed in [101]

$$\begin{aligned} &\frac{dc(t)}{dt} = \frac{\lambda a^m c(t-\tau)}{a^m + c^m(t-\tau)} - \gamma c(t), \quad t \geq 0, \\ &c(t) = \alpha, \quad t \leq 0, \end{aligned} \tag{4}$$

where λ, a, m, g, τ, and α are positive constants.

I.3.2 Electromagnetic induction approach

Complex electrophysiological activities can induce time-varying electromagnetic field and thus the effect of electromagnetic induction on the membrane potential should be considered. Terefore, magnetic flux is proposed to model the effect of electromagnetic induction on cell, and multiple modes of electrical activities can be detected to be consistent with the biological results. In fact, the electric activity of neurons in neuronal system is too complex and many factors should be considered as well. According to the Faraday's law of induction, the fluctuations or changes in action potentials in neurons can generate magnetic field in the media; thus, the electrical activities of neurons will be adjusted under feedback effect. That is to say, the fluctuation of membrane potentials of neurons can change the distribution of electromagnetic field inner and external of neurons; thus, the magnetic flux across membrane and electromagnetic effect should

be considered. More often, it is claimed that neuronal system can be in good memory to keep normal activities and the memory effect is often described by using time delay term in the model. Indeed, magnetic field or magnet flux storage could be associated with the memory effect. It is found that the electromagnetic radiation can excite quiescent neuron but also can suppress the electrical activities in neuron as well. Particularly, it is. important to note that multiple modes of electrical activities can emerge alternatively, and these results are consistent with biological experiments [102]. For this end, several approaches have been presented. Aggarwal et al. [103] presented an optimal design of two dimensional finite impulse response (2D FIR) filter with quadrantally even symmetric impulse response, and the presented scheme did show improved design accuracy and flexibility with varying values of FDCs. Kumar and Rawat [104] proposed the use of power function and least squares method for designing of a fractional-order digital differentiator. The input signal can be transformed into a power function by using Taylor series expansion, and the fractional-order digital differentiator was described by a finite impulse response (FIR) system that yields fractional-order derivative of the G-L type for a power function. Wang et al. [105] investigated the propagation of the firing rate and synchronous firings in a $10-$layer feedforward neuronal network and found that these abilities in information processing due to synchrony can be modulated by noise and the operating mode of neurons. Suffczynski et al. [106] developed a computational model of thalamo-cortical circuits based on relevant (patho) physiological data, and these results can provide more insight into the dynamics of the neuronal networks leading to seizure generation in a rat experimental model of absence epilepsy. Cullheim and Thams [107] investigated the role for microglia in interplay with synapses, and the development of various disorders of the central nervous system (CNS) was also discussed. To discern the complex functional role of brain, the dynamic brain network was constructed from human functional magnetic resonance imaging data based on the sliding window method, and then the eigenvalues corresponding to the network were calculated. Wang et al. [108] analyzed the global properties of eigenvalues by using eigenvalue analysis, and the local properties were measured based on the random ma-

trix theory (RMT). As an example, we will present a new four-variable Hindmarsh-Rose neuron model introduced in [109]. The dynamical equations for this improved HR neuron model are described by

$$\begin{aligned} \frac{dx}{dt} &= y - ax^3 + bx^2 - z + I_{ext} - k_1\rho(\phi)x, \\ \frac{dy}{dt} &= c - dx^2 - y, \\ \frac{dz}{dt} &= r\left[s(x + 1.6) - z\right], \\ \frac{d\phi}{dt} &= x - k_2\phi, \end{aligned} \tag{5}$$

where the variables x, y, z represent the membrane potential, slow current for recovery variable, and adaption current, respectively. I_{ext} denotes the external forcing current, and the fourth variable ϕ describes the magnetic flux across membrane. The $\rho(\phi)$ is the memory conductance of a magnetic flux-controlled memristor and here used to describe the coupling between magnetic flux and membrane potential of neuron. The memory conductance of memristor is often described by $\rho(\phi) = \alpha + 3\beta\phi^2$, and α, β are fixed parameters, k_1 and k_2 are parameters that describe the interaction between membrane potential and magnetic flux. The term $k_1\rho(\phi)x$ describes the suppression modulation on membrane potential, and it is dependent on the variation in magnetic flux by generating additive faradic current. According to the Faraday law of electromagnetic induction and description about memristor, the term $k_1\rho(\phi)x$ could be regarded as additive induction current on the membrane as follows

$$i' = \frac{dq(\phi)}{dt} = \frac{dq(\phi)}{d\phi}\frac{d\phi}{dt} = \rho(\phi)V = k_1\rho(\phi)x \tag{6}$$

In fact, a specific synapse called as autapse which the synapse connects to its body via a close loop is found in some intermediate neurons, and the effect of autapse [110, 111] on membrane potential of neuron is often described by applying a time-delayed feedback

current along the close loop. That is to say, autapse connection provides evidence for intrinsic time delay or response delay, and it is also believed that another time delay (propagation time delay) exists when signals are propagated among nodes or neurons.

I.3.3 Fractional dynamics approach

It is well known that the fractional calculus is a classical mathematical notion and a generalization of ordinary differentiation and integration to arbitrary (non-integer) order.

However, the fractional calculus did not attract much attention for a long time due to the lack of application background and its complexity. Until only very recently, the fractional calculus has gained importance in both theoretical and applied aspects of several branches of science and engineering [26, 25]. Researchers pointed out that the fractional calculus plays an important role in modeling and many systems in interdisciplinary fields, and can be elegantly described with the help of fractional derivatives, such as viscoelastic systems, dielectric polarization, electromagnetic waves, heat conduction, robotics, biological systems, finance and so on. Nowadays, studyies on fractional-order calculus has become an active research field.

Why should we border at all?

The universality: The detailed structure of the propagator $W(r,t)$, i.e., the probability density function (pdf) for the initial condition $\lim_{t\to 0^+} W(r,t) = \delta(r)$, depends, in general, on the special shape of the underlying geometry. However, the interesting part of the propagator has the asymptotic behaviour $\log W(r,t) \sim c\xi^u$ where $\xi \equiv {}^{r}\!\Big/\!_{t^{\alpha/2}} \gg 1$ which is expected to be universal. Here, $u = 1/(1-\alpha/2)$ with the anomalous diffusion exponent α defined below. The fractional equations we consider in the following are universal in this respect as we do not consider any form of quenched disorder. Our results for anomalous diffusion are equivalent to findings from random walk models on an isotropic and homogeneous support [112].

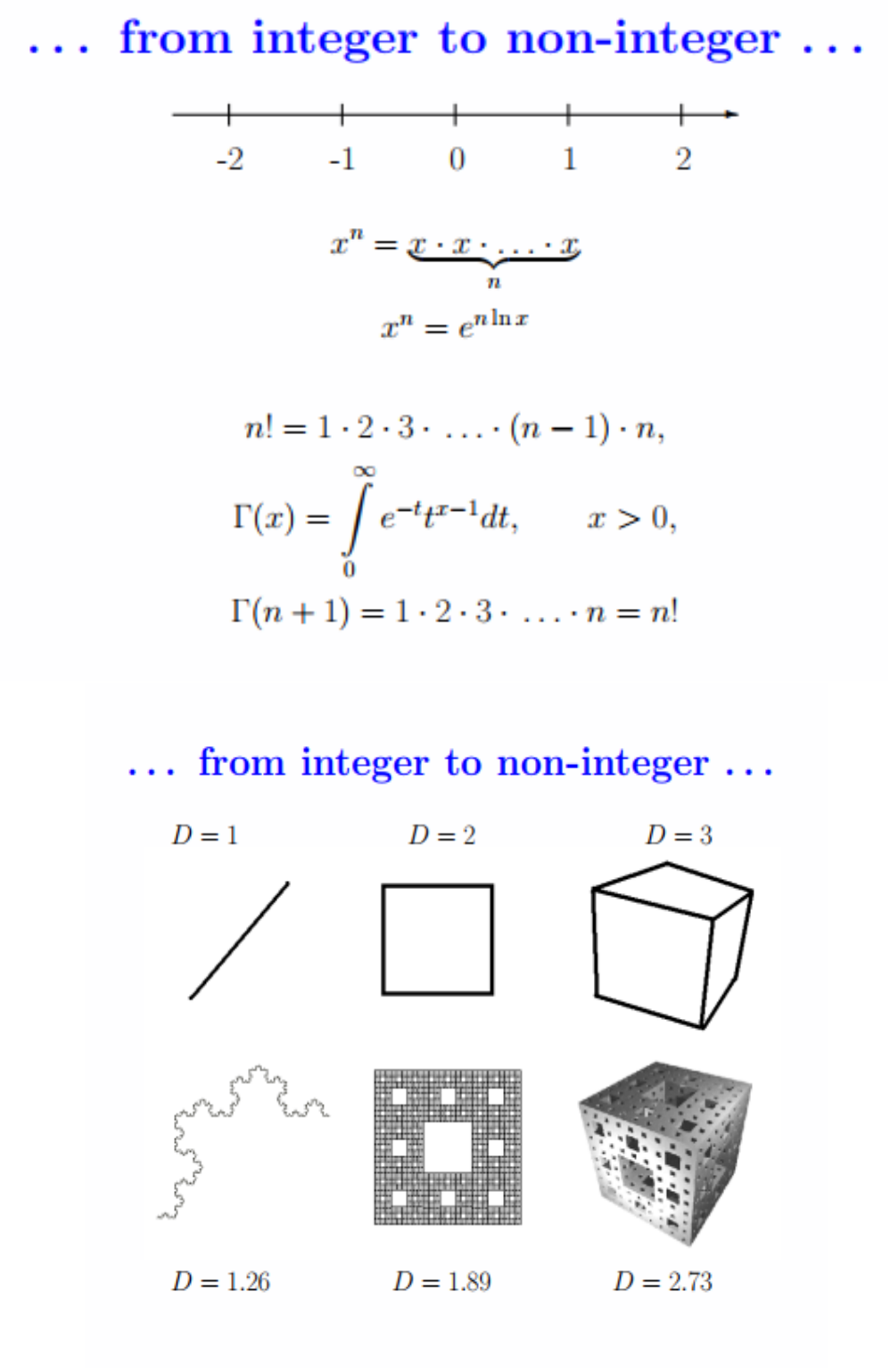

Figure 3: From integer to non-integer [26].

The non-universality: In contrast to Gaussian diffusion, fractional diffusion is non-universal in that it involves a parameter α which is the order of the fractional derivative. Obviously, nature often violates the Gaussian universality mirrored in experimental results which do not follow the Gaussian predictions. Fractional diffusion equations account for the typical "anomalous "features which are observed in many systems.

The advantage to random walk models: Within the fractional approach it is possible to include external fields in a straightforward manner. Also the consideration of transport in the phase space spanned by both position and velocity coordinate is possible within the same approach. Moreover, the calculation of boundary value problems is analogous to the procedure for the corresponding standard equations.

The comparison to other approaches: The fractional approach is in some sense equivalent to the generalised master equation approach. The advantage of the fractional model again lies in the straightforward way of including external force terms and of calculating boundary value problems. Conversely, generalised Langevin equations lead to a different description as they correspond to Fokker-Planck equations which are local in time and which contain time-dependent coefficients. In most cases of Brownian transport, the deterministic Fokker-Planck equation is employed for the description of stochastic dynamics in external fields. In analogy, the use of the fractional Fokker-Planck equation is promoted for situations where anomalous diffusion underlies the system [112].

The mathematical advantage: A very convenient issue is that standard techniques for solving partial di!erential equations or for calculating related transport moments also apply to fractional equations which is demonstrated in [112].

The relation between the fractional solution and its Brownian counterpart: There exists a transformation which maps the Brownian solution onto the corresponding fractional solution, an interesting relation which is useful for both analytic and numerical analysis. It is a simple approach: The appearance of fractional equations is very appealing due to their proximity to the analogous standard equations. It has been demonstrated recently that the fractional Fokker-Planck equation can be derived from a Langevin equation with Gaussian white noise for systems where trapping occurs. This offers some insight

into the physical mechanisms leading to fractional kinetics.

The mathematical definition of the differintegral operator of fractional order has been the subject of different approaches, the most used are the Riemann-Liouville (RL), the Grünwald-Letnikov (GL), the Caputo (C) and the Atangana-Baleanu's definitions. Although they are different in form, one can be transferred from each other under some conditions.

i- The Riemann-Liouville's approach of fractional-order derivative

As previously mentioned, The concept of non-integral order of integration can be traced back to the genesis of differential calculus itself: the philosopher and creator of modern calculus G.W. Leibniz made some remarks on the meaning and possibility of fractional derivative of order $1/2$ in the late 17^{th} century. However a rigorous investigation was first carried out by Liouville in a series of papers from $1832 - 1837$, where he defined the first outcast of an operator of fractional integration. Later investigations and further developments by among others Riemann led to the construction of the integral-based Riemann-Liouville fractional integral operator, which has been a valuable cornerstone in fractional calculus ever since. Prior to Liouville and Riemann, Euler took the first step in the study of fractional integration when he studied the simple case of fractional integrals of monomials of arbitrary real order in the heuristic fashion of the time; it has been said to have lead him to construct the Gamma function for fractional powers of the factorial [113]. An early attempt by Liouville was later purified by the Swedish mathematician Holmgren, who in 1865 made important contributions to the growing study of fractional calculus. But it was Riemann [114] who reconstructed it to fit Abel's integral equation, and thus made it vastly more useful. Today there exist many different forms of fractional integral operators, ranging from divided-difference types to infinite-sum types [115], but the Riemann-Liouville Operator is still the most frequently used when fractional integration is performed.

The classical form of fractional calculus is given by the Riemann-Liouville integral, which is essentially what has been described above. The theory for periodic functions

(therefore including the "boundary condition" of repeating after a period) is the Weyl integral. It is defined on Fourier series, and requires the constant Fourier coefficient to vanish (thus, it applies to functions on the unit circle whose integrals evaluate to 0). The Riemann-Liouville integral exists in two forms, upper and lower. Considering the interval $[a, b]$, the integrals are defined as

$$\begin{aligned} {}_aD_t^{-\alpha} f(t) &= {}_aI_t^{\alpha} f(t) = \frac{1}{\Gamma(\alpha)} \int_a^t (t-\tau)^{\alpha-1} f(\tau) d\tau, \\ {}_tD_b^{-\alpha} f(t) &= {}_tI_b^{\alpha} f(t) = \frac{1}{\Gamma(\alpha)} \int_t^b (\tau-t)^{\alpha-1} f(\tau) d\tau. \end{aligned} \tag{7}$$

The corresponding derivative is calculated using Lagrange's rule for differential operators. Computing nth order derivative over the integral of order $(n-\alpha)$, the α order derivative is obtained. It is important to remark that n is the smallest integer greater than α (that is, $n = \lceil \alpha \rceil$). Similar to the definitions for the Riemann-Liouville integral, the derivative has upper and lower variants.

$$\begin{aligned} {}_aD_t^{-\alpha} f(t) &= \frac{d^n}{dt^n} {}_aD_t^{-(n-\alpha)} f(t) = \frac{d^n}{dt^n} {}_aI_t^{n-\alpha} f(t), \\ {}_tD_b^{-\alpha} f(t) &= \frac{d^n}{dt^n} {}_tD_b^{-(n-\alpha)} f(t) = \frac{d^n}{dt^n} {}_tI_b^{n-\alpha} f(t) \end{aligned} \tag{8}$$

By contrast, the Grünwald-Letnikov derivative starts with the derivative instead of the integral.

2i- The Grünwald-Letnikov's approach of fractional-order derivative

In mathematics, the Grünwald-Letnikov derivative is a basic extension of the derivative in fractional calculus that allows one to take the derivative a non-interger number of times. It was introduced by Anton Karl Grünwald $(1838-1920)$ from Prague, in 1867, and by Aleksey Vasilievich Letnikov $(1837-1888)$ in Moscow in 1868. To constuct this

derivative, they first considered the formula

$$f'(x) = \lim_{h\to 0} \frac{f(x+h) - f(x)}{h}, \tag{9}$$

for the derivative that can be applied recursively to get higher-order derivatives. For example, the second-order derivative would be:

$$\begin{aligned} f''(x) &= \lim_{h\to 0} \frac{f'(x+h) - f'(x)}{h}, \\ &= \lim_{h_1\to 0} \frac{\lim\limits_{h_2\to 0} \dfrac{f(x+h_1+h_2) - f(x+h_2)}{h_2} - \lim\limits_{h_2\to 0} \dfrac{f(x+h_1) - f(x)}{h_2}}{h_1}, \end{aligned} \tag{10}$$

Assuming that the $h's$ converge synchronously, this simplifies to:

$$f''(x) = \lim_{h\to 0} \frac{f(x+2h) - 2f(x+h) + f(x)}{h^2}, \tag{11}$$

which can be justified rigorously by the mean value theorem. In general, we have:

$$f^{(n)}(x) = \lim_{h\to 0} \frac{\sum\limits_{0\le m\le n} (-1)^m \begin{pmatrix} n \\ m \end{pmatrix} f(x+(n-m)h)}{h^n.} \tag{12}$$

Removing the restriction that n be a positive integer, it is reasonable to define:

$$D^q f(x) = \lim_{h\to 0} \frac{1}{h^q} \sum_{0\le m\le n} (-1)^m \begin{pmatrix} q \\ m \end{pmatrix} f(x+(q-m)h). \tag{13}$$

This defines the Grünwald-Letnikov derivative.

To simplify notation, one can set:

$$\Delta_h^q f(x) = \sum_{0 \leq m \leq n} (-1)^m \begin{pmatrix} q \\ m \end{pmatrix} f(x + (q-m)h). \tag{14}$$

So the Grünwald-Letnikov derivative may be succintly written as:

$$D^q f(x) = \lim_{h \to 0} \frac{\Delta_h^q f(x)}{h^q.} \tag{15}$$

3i- The Caputo's approach of fractional-order derivative

Another option for computing fractional derivatives is the Caputo fractional derivative. It was introduced by Michele Caputo in his 1967 paper [32]. In contrast to the Riemann-Liouville fractional derivative, when solving differential equations using Caputo's definition, it is not necessary to define the fractional order initial conditions. Caputo's definition is illustrated as follows:

$${}^cD_t^\alpha f(t) = \frac{1}{\Gamma(n-\alpha)} \int_0^t \frac{f^{(n)}(\tau)d\tau}{(t-\tau)^{\alpha+1-n}}. \tag{16}$$

There is the Caputo fractional derivative defined as:

$$D^\nu f(t) = \frac{1}{\Gamma(n-\nu)} \int_0^t (t-u)^{(n-\nu-1)} f^{(n)}(u)du, \qquad (n-1) < \nu < n, \tag{17}$$

which has the advantage that is zero when $f(t)$ is constant and its Laplace Transform is expressed by means of the initial values of the function and its derivative. Moreover, there is the Caputo fractional derivative of distributed order defined as:

$${}_a^b D^\nu f(t) = \int_a^b \phi(\nu) \left[D^\nu f(t)\right] d\nu = \int_a^b \left[\frac{\phi(\nu)}{\Gamma(1-\nu)} \int_0^t (t-u)^{-\nu} f'(u)du\right], \tag{18}$$

where $\phi(\nu)$ is a weight function and which is used to represent mathematically the presence of multiple memory formalisms.

iv- The Atangana-Baleanu's approach of fractional-order derivative

Like the integral, there is also a fractional derivative using the general Mittag-Leffler function as a kernel [116]. The authors introduced two versions, the Atangana-Baleanu in Caputo sense (ABC) derivative, which is the convolution of a local derivative of a given function with the generalized Mittag-Leffler function, and the Atangana-Baleanu in Riemann-Liouville sense (ABR) derivative, which is the derivative of a convolution of a given function that is not differentiable with the generalized Mittag-Leffler function [117]. The Atangana-Baleanu fractional derivative in Caputo sense is defined as:

$$ {}_{a}^{ABC}D_{t}^{\alpha} f(t) = \frac{AB(\alpha)}{1-\alpha} \int_{a}^{t} f'(\tau) E_{\alpha}\left(-\alpha \frac{(t-\tau)^{\alpha}}{1-\alpha}\right) d\tau, \tag{19} $$

and the Atangana-Baleanu fractional derivative in Riemann-Liouville is defined as:

$$ {}_{a}^{ABR}D_{t}^{\alpha} f(t) = \frac{AB(\alpha)}{1-\alpha} \frac{d}{dt} \int_{a}^{t} f(\tau) E_{\alpha}\left(-\alpha \frac{(t-\tau)^{\alpha}}{1-\alpha}\right) d\tau. \tag{20} $$

In addition to the above-mentioned approaches, there are many others such as the Riesz derivative, the Hadamard derivative, the Marchaud derivative, the MillerRoss derivative, the Weyl derivative and so one.

I.4 Motivations

The transport of nerve impulses is of paramount importance in the majority of biological phenomena that govern human daily life, because neurons use this means of transport to communicate with each other. This transport triggers numerous genetic modifications which are still little /poorly known, and constitute the basis of the diversity of the genome in living beings. Moreover, all the informations stored during this transport,

source of various modifications is carefully saved over decades and centuries, which suggests that neurons have phenomenal dynamic memory that can store great amount of information.

The storage of information is ubiquitous in our technological society: paper, film, semiconductor memories, audio/video-tapes, magnetic/optical disks, etc., collectively contain many petabytes of information. In contrast, Nature has been frugal in its use of information storage techniques. Blueprints of life, both of plant and of animal, are stored in the DNA molecules [118, 119, 120]. Instinctive as well as learned information reside in the nervous systems of higher animals [121, 122]. The human immune system stores information about past pathogens in the form of primed lymphocytes (e.g., T-cells and B-cells), using this information to mass-produce and rapidly deploy antibodies and specialized immune cells when an old pathogen reappears [123, 124]. These instances aside, it is hard to find purposeful employment of data storage in Nature.

Despite their rarity, the natural mechanisms of information storage are extremely powerful and versatile. A complement of chromosomes not only contains the entire description of a plant or an animal, but it also carries the step-by-step instructions for building the individual from a single initial cell. The human brain can store vast amounts of information embodied in images, sounds, scents, event sequences, and abstract concepts to which an individual may be exposed through a lifetime. The brain forms automatic links among the stored data, recalls by association, and responds to external events by exploiting its reservoir of pre-programmed and learned databases.

Inspired by sophisticated tools and techniques employed by Nature for purposeful storage of information which stand in stark contrast to the primitive and relatively inefficient means used by man, efforts have been made so far to build a huge memory using DNA molecules. These efforts are targeted at increasing the size of the address space of a molecular memory and making operations on a specified word in the address space more efficient and reliable. The former issue should be solved by careful design of the base sequences of the address portions. The latter issue depends on the architecture of a molecular memory and the available memory operations. Indeed, Soon after

Adleman published his seminal work on DNA computing [125] and Lipton [126] gave a more general framework for solving nondeterministic polynomial time (NP)-complete problems using DNA, Baum wrote a technical comment in Science on building a huge memory using DNA molecules [127]. He claimed that it was possible to build an associative memory vastly larger than the brain. More concretely, he wrote that it was not completely implausible to imagine vessels storing 10^{20} words, which is comparable to standard estimates of brain capacity as 10^{14} synapses each storing a few bits. Among various proposals for constructing a molecular memory, he considered a scheme that stores DNA molecules consisting of an address portion and a data portion. In order for the scheme to work as an ordinary random access memory, each address portion should be accessible only by the sequence that is complementary to the sequence of the address portion. He even mentioned the use of an error correcting code to avoid accidental bonding due to approximate match. Through enzymatic reactions, DNA is

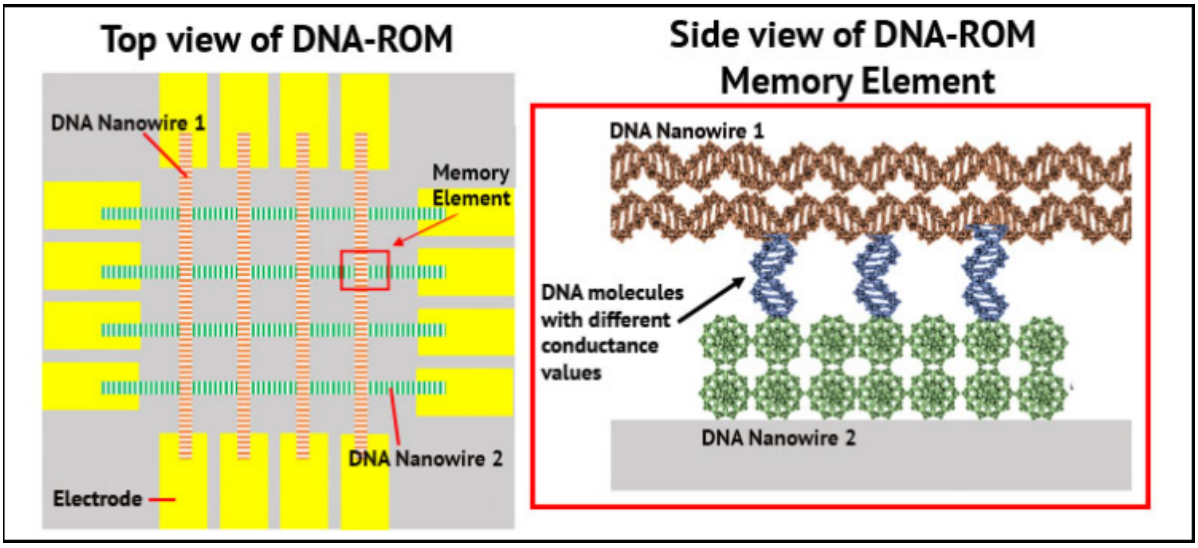

Figure 4: DNA Memory Chips proposed by Hihath.

read, written, and erased, and can store massive amounts of data. Researchers are now using the electrical properties of DNA to develop memory technologies for computational data. The main problem encountered with this promising media (DNA) which provides numerous advantages, which includes the ability to store dense information while achieving long-term stability is how the data can be retrieved from a DNA-based

archive.

Moreover, fractional dynamics are not just another way of presenting old stories. We believe that they are a powerful framework which is of use for many systems. Indeed, fractional dynamics has experienced a firm upswing during the last years, having been forged into a mature framework in the theory of stochastic processes. the occurrence of anomalous dynamics in various fields ranging from nanoscale over biological to geophysical and environmental systems is well understood by applying the fractional dynamics. The notions and concepts of anomalous dynamical properties, such as long-range spatial or temporal correlations manifested in power-laws, stretched exponentials, $1/f^{\alpha}-$noises, or non-Gaussian probability density functions (PDFs), have been predicted and observed in numerous systems from various disciplines including physics, chemistry, engineering, geology, biology, economy, meteorology, astrophysics and others. Apart from other standard tools to describe anomalous dynamics such as continuous time random walks [128, 129, 130, 131, 132], fractional dynamical equations have become increasingly popular to model anomalous transport [133, 112, 134, 135]. In the presence of an external force field, in particular, the fractional Fokker-Planck equation provides a direct extension of the classical Fokker-Planck equation, being amenable to well-known methods of solution. Moreover, fractional calculus makes it possible to clearly distinguish between super-diffusion, normal diffusion and sub-diffusion. Many studies point out the fact that nervous conduction and transmission, the main target of toxic substances are overwhelmingly dominated by subdiffusion. Subdiffusion has acquired relevance in the past decades since it has been experimentally detected in several systems such as porous media, glasses, transport through cell membranes, and other biological systems.

Now that we have a broader view of what fractional dynamics really is, and taking into account the above considerations, our motivation in this thesis comes down to:

★ Highlight the various manifestations hitherto observed of memory effects,

★ Study the biological systems linked to the transport of nerve impulses in order to see which ones can be used as palliators in the view to circumvent the problem related

to the reading of DNA memory,

★ Study the stability of memory under the influence of phenomena frequently encountered during the transport of nerve impulses such as fluctuations and toxicity.

I.5 Conclusion

In this chapter, we have briefly explained the concept of the transport of nerve impulses in neurons. We have evoked some biological processes in close correlation with this one. We have shown that memory is ubiquitous in all these processes, even if it manifests itself differently from one process to another. The different mathematical approaches to memory were presented; therefore, it became clear that the fractional derivative is more indicated for the case of neurons in general, and in particular for the transport of nerve impulses in neurons, since this can be used not only to model the memory effects, the effects of nonlocality very often created by toxins, but also to describe the anomalous diffusion phenomena encountered in the biological processes linked to the transport of nerve impulses in neurons. with regard to toxins, their presence in neurons can come from several origins (drugs, food, etc.). Their influence on memory, as well as the transport memory effects observed in chromatin dynamics will be studied in the next chapter.

CHAPTER II

MODEL AND METHODOLOGY

II.1 Introduction

In the previous chapter, we reviewed different manifestations of memory effects that come into play during the transport of nerve impulses. We have also made a description of the various techniques hitherto used to analyze these effects. We did not fail to emphasize the interest aroused by memory effects, especially for technological applications, which led us to focus our attention on the stability of said memory in the presence of phenomena frequently encountered in neurons such as fluctuations and toxins for example, and which are of paramount importance for example in the cellular dynamics, or in the dynamics of genetic populations. In this chapter, we will present analytical tools and numerical methods allowing to provide an element of response to the above-mentioned problems.

II.2 Mathematical modeling

In this section, we mathematically describe the effect of transport memory that we have used and presented in the previous chapter, as well as the influence of fluctuations and toxins on some biological systems linked to the transport of nerve impulses.

II.2.1 Mathematical description of the effect of transport memory

The model under consideration consists of a chain of particles of identical masses M, interacting with its two nearest neighbors through harmonic coupling, where A is

the harmonic coupling coefficient. The particles are under the influence of an on−site, double−well potential [136, 137] given by:

$$V(u_n) = \frac{1}{4}u_n - \frac{1+a}{3}u_n^3 + \frac{a}{2}u_n^2, \tag{21}$$

where u_n is the position of the particle n and $a \in (0, 1)$ is a so−called "detuning"parameter [138].

Since we are dealing with a dissipative chain, we need a Lagrangian description which involves dissipation. This is achieved by extending the Lagrangian formalism to include the Rayleigh dissipative function, where ξ is the dissipative coefficient. We get the equation governing the motion of the n^{th} particle

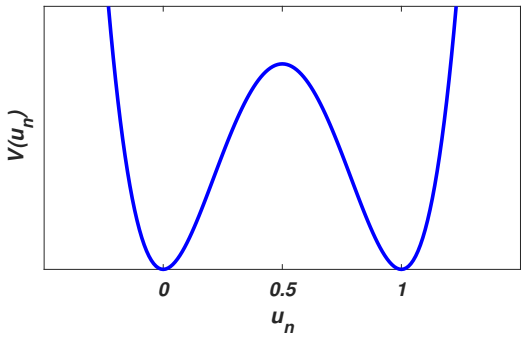

Figure 5: Double well potential with $a = 0.5$.

$$M\frac{d^2u_n}{dt^2} + \xi\frac{du_n}{dt} = A(u_{n+1} - 2u_n + u_{n-1}) - u_n^3 + (1+a)u_n^2 - au_n. \tag{22}$$

In the continuum limit, i.e., when the lattice spacing is much less than the wavelength of the excitations propagating along the chain (this is also referred to as displacive regime [139] and [140]), the dynamics of the model can be described in dimensionless units, by the following partial differential equation:

$$\frac{\partial^2 u}{\partial t^2} + \mu\frac{\partial u}{\partial t} = D\frac{\partial^2 u}{\partial x^2} + \frac{1}{M}f(u), \tag{23}$$

where $\mu = \dfrac{\xi}{M}$ is the rescaled dissipation coefficient, $D = \dfrac{A}{M}$ is the diffusion coefficient

and $f(u) = -u^3 + (1+a)u^2 - au$, is the well known Nagumo reaction term. Now, let us reduce the number of parameters by introducing the change of variables $t \to M\mu t$, $x \to \sqrt{MD}x$. Our initial model, Eq. (23) then reduces to

$$\epsilon \frac{\partial^2 u}{\partial t^2} + \frac{\partial u}{\partial t} = \frac{\partial^2 u}{\partial x^2} + f(u), \tag{24}$$

with the appearance of a new parameter (the "mass"), $\epsilon = (M\mu^2)^{-1}$ [141]. The parabolic or overdamped limit is obtained by letting $\epsilon \to 0$, which leads to

$$\frac{\partial u}{\partial t} = \frac{\partial^2 u}{\partial x^2} + f(u). \tag{25}$$

It is straightforward to show that the steady states of our function are $u_1 = 0$, $u_2 = a$ and $u_3 = 1$. We are interested in those solutions which are front-like (kinks) connecting the (unstable) state $u_1 = 0$, with the globally (stable) state $u_3 = 1$. Consequently, we supplement equations (24) and (25) with boundary conditions $u(-\infty, t) = u_1$, $u(\infty, t) = u_3$ (see Fig. 5).

Now, consider the replacement of the diffusion equation (25) by its nonlocal (in time) counterpart

$$\frac{\partial u}{\partial t} = \int_0^t \Phi(t-\tau)\frac{\partial^2 u}{\partial x^2} d\tau + kf(u), \tag{26}$$

where $u(x,t)$ is the dynamics of the field, k is the quadratic growth rate, $\Phi(t) = \alpha e^{-\alpha t}$ is the memory function which describes the finiteness of the correlation or scattering time $\frac{1}{\alpha}$.

Following the general rules of the calculus, we transform (26) into a differential equation that can easily be used to look for traveling wave solutions

$$\frac{\partial^2 u}{\partial t^2} + \left[\alpha - kf'(u)\right]\frac{\partial u}{\partial t} = v^2 \frac{\partial^2 u}{\partial x^2} + \alpha k f(u), \tag{27}$$

where, just like in [28], $v^2 = \alpha$, the physical meaning of v being the speed dictated by

the medium in the absence of scattering.

The Nagumo reaction term here represents neuronal activation, but it can also be used to model population genetics [142]. In this case, the evolution equation (25) must possess certain properties to be an acceptable description of reacting and dispersing systems. A density u cannot be negative, and evolution equations for densities must preserve positivity, i.e., $u(r,0) \geq 0$ for all r, at time $t = 0$ implies $u(r,t) > 0$ for all r for all times $t > 0$. It is well−known that the diffusion equation

$$\frac{\partial u}{\partial t} = D\Delta u, \tag{28}$$

possesses this required feature. The rate equation

$$\frac{\partial u}{\partial t} = f(u) = b(u) - d(u)u, \tag{29}$$

and the reaction-diffusion equation

$$\frac{\partial u}{\partial t} = D\Delta u + f(u), \tag{30}$$

will preserve positivity if $f(0) \geq 0$.

The diffusion equation has, however, the unrealistic feature of infinitely fast propagation. The fundamental solution of Eq. (28) with a point source at $r = 0$ and $t = 0$ is given by

$$u(r,t) = \frac{1}{\sqrt{4\pi Dt}} \exp\left[-\frac{r^2}{4Dt}\right], \quad t > 0. \tag{31}$$

No matter how small t and how large r, the density u will be nonzero, though exponentially small. This pathology can be traced back to the lack of inertia of Brownian particles; their direction of motion in successive time intervals is uncorrelated. This lack of correlation has two consequences: (i) The particles move with infinite velocity. There is some probability, though exponentially small, that a dispersing individual will travel an infinite distance from its current position in a small but nonzero period of time.

Clearly, this cannot be true for molecules or organisms. (ii) The motion of the dispersing individuals is unpredictable even on the smallest time scales. Again, this cannot be true, either for molecules or organisms. It is therefore desirable to adopt a model for dispersion that leads to more predictable motion with finite speed at smaller time scales and approaches diffusive motion on larger time scales. The natural choice is a persistent random walk, also known as a correlated random walk [143].

At the scales where particles have a well-defined finite velocity, persistent random walk (PRW) or correlated random walk provides a better description for spatial spread in population dynamics than Brownian motion, or the diffusion equation [144, 145]. In fact, PRW has several advantages from a theoretical viewpoint: (i) PRW is a generalization of Brownian motion; it contains the latter as limiting case [143]. (ii) The PRW fulfills the physical requirement of bounded velocity. (iii) The PRW provides a unified treatment that covers the whole range of transport from diffusive limit to the ballistic limit.

When the particles move according to a PRW, interact or react with each other, the evolution equations for the densities read [143]:

$$\begin{aligned} \frac{\partial u^+}{\partial t} + \gamma \frac{\partial u^+}{\partial r} &= \mu(u^- - u^+) + \frac{1}{2} b(u) - d(u)u^+, \\ \frac{\partial u^-}{\partial t} - \gamma \frac{\partial u^-}{\partial r} &= \mu(u^+ - u^-) + \frac{1}{2} b(u) - d(u)u^-, \end{aligned} \tag{32}$$

where $b(u)$ is the production or birth term and captures the processes that increase the chemical concentration or population density, and $d(u)$ is the loss or death term and captures the processes that decrease the concentration or density. $u^+(r,t)$ and $u^-(r,t)$ are the densities of particles going to the right and to the left, respectively, and $u(r,t) = u^+(r,t) + u^-(r,t)$ is the total density of the dispersing individuals. With these kinetics, PRW is called direction−independent reaction walk (DIRW). The particles travel with speed $\gamma > 0$ and turn with frequency $\mu > 0$.

Considering the advantages of PRW, we adopted it as an approach to study the effect

of fluctuations on the dynamics of genetic populations.

II.2.2 External fluctuations in front propagation in reaction random walks with direction−independent kinetics

We now consider the common case that the rate terms is of the form $f(u,v) = f_1(u,v) + r_1 h_1(u,v)$ and $g(u,v) = g_1(u,v) + r_2 h_2(u,v)$, where the external control parameters r_1 and r_2 describe the influence of the surroundings on the system. We limit ourselves to the case where r_1 and r_2 are scalar, which is true for all systems considered here. Fluctuations in the environment result in fluctuations of r_i, $i = 1, 2$, and we write

$$r_i = r_i + \varepsilon^{1/2}\eta(x,t), \quad i = 1, 2. \tag{33}$$

with $\eta(x,t)$ being a Gaussian white noise of zero mean and correlation given by

$$\langle \eta(x,t)\eta(x',t')\rangle = 2C(\frac{|x-x'|}{\xi})\delta(t-t'), \tag{34}$$

where the parameter ξ is the characteristic length of the spatial correlation of the noise, ε measures the strength of the noise and $C(x)$ is a correlation function which is a well-behaved, short-ranged and even function of space. The function $C(x)$ verifies that in the limit $\xi \to 0$, the spatial white noise case is recovered [146], and δ is the Dirac delta function. Since these fluctuations are external, they do not verify a fluctuation−dissipation relation, and the system is no longer at equilibrium.

Following the normalization procedure of $C(\frac{|x|}{\xi})$ given in Ref. [147], Eq. (34) can be approximated by the noise correlation of the Gaussian white spectrum

$$\langle \eta(x,t)\eta(x',t')\rangle = 2\delta(x-x')\delta(t-t'). \tag{35}$$

Incorporating the fluctuations in this way, system (32) transforms into a stochastic par-

tial differential equation (SPDE)

$$\begin{aligned}\frac{\partial u^+}{\partial t}+\gamma\frac{\partial u^+}{\partial r}&=\mu(u^- - u^+)+\frac{1}{2}b(u^-,u^+)-d(u)u^+ + \\ &\varepsilon^{\frac{1}{2}}h_1(u^+,u^-)\eta(x,t),\\ \frac{\partial u^-}{\partial t}-\gamma\frac{\partial u^-}{\partial r}&=\mu(u^+ - u^-)+\frac{1}{2}b(u)-d(u^-,u^+)u^- + \\ &\varepsilon^{\frac{1}{2}}h_2(u^+,u^-)\eta(x,t),\end{aligned} \tag{36}$$

where, for simplicity we have written

$$\begin{aligned}f(u^-,u^+,r_1)&=f_1(u^-,u^+)+r_1h_1(u^-,u^+)=\frac{1}{2}b(u^-,u^+)-d(u^-,u^+)u^+,\\ g(u^-,u^+,r_2)&=g_1(u^-,u^+)+r_2h_2(u^-,u^+)=\frac{1}{2}b(u^-,u^+)-d(u^-,u^+)u^-,\end{aligned} \tag{37}$$

$$\begin{aligned}f_1(u^-,u^+)&=\mu(u^- - u^+)+\frac{1}{2}b(u^-,u^+)-d(u^-,u^+)u^+,\\ g_1(u^-,u^+)&=\mu(u^+ - u^-)+\frac{1}{2}b(u^-,u^+)-d(u^-,u^+)u^-.\end{aligned} \tag{38}$$

Since the coupling functions, h_1 and h_2 are non constant, we have a nonvanishing mean value. This means that systematic contributions to the field dynamics will appear.

Let us begin by evaluating the mean value of the noisy terms with the help of the spatially extended version of Furutsu−Novikov−Donsker's theorem

$$\left\langle h_1(u^-,u^+)\eta(x,t)\right\rangle=\int_0^t dt'\int dx\,\langle\eta(x,t)\eta(x',t')\rangle\left\langle\frac{\delta h_1(u^-,u^+)}{\delta\eta(x',t')}\right\rangle, \tag{39}$$

with

$$\frac{\delta h_1(u^-,u^+)}{\delta\eta(x',t')}=\frac{\delta h_1(u^-,u^+)}{\delta u^-}\frac{\delta u^-}{\delta\eta(x',t')}+\frac{\delta h_1(u^-,u^+)}{\delta u^+}\frac{\delta u^+}{\delta\eta(x',t')}. \tag{40}$$

Formal time integration of $\dfrac{\delta u^-}{\delta\eta(x',t')}$ and $\dfrac{\delta u^+}{\delta\eta(x',t')}$ in Eq. (36) allows the evaluation of

the response function.

$$\begin{aligned} u^+(t) &= u^+(0) + \int_0^t dt' f(u^-, u^+) + \int_0^t dt' h_1(u^-, u^+)\eta(x,t), \\ u^-(t) &= u^-(0) + \int_0^t dt' g(u^-, u^+) + \int_0^t dt' h_2(u^-, u^+)\eta(x,t), \end{aligned} \tag{41}$$

so that the response function at equal time is

$$\begin{aligned} \frac{\delta u^+}{\delta \eta(x',t')} &= \varepsilon^{\frac{1}{2}} h_1(u^-, u^+)\delta(x-x'), \\ \frac{\delta u^-}{\delta \eta(x',t')} &= \varepsilon^{\frac{1}{2}} h_2(u^-, u^+)\delta(x-x'). \end{aligned} \tag{42}$$

And one finally obtains

$$\left\langle h_1(u^-, u^+)\eta(x,t)\right\rangle = \varepsilon^{1/2} C(0) \left\langle h_2(u^-, u^+)\frac{\delta h_1(u^-, u^+)}{\delta u^-} + h_1(u^-, u^+)\frac{\delta h_1(u^-, u^+)}{\delta u^+}\right\rangle \tag{43}$$

By following a similar reasoning, we obtain the mean value of the second noisy term which is given as follows:

$$\left\langle h_2(u^-, u^+)\eta(x,t)\right\rangle = \varepsilon^{1/2} C(0) \left\langle h_1(u^-, u^+)\frac{\delta h_2(u^-, u^+)}{\delta u^+} + h_2(u^-, u^+)\frac{\delta h_2(u^-, u^+)}{\delta u^-}\right\rangle \tag{44}$$

According to this result, Eq. (36) can be rewritten in a more useful form,

$$\begin{aligned} \frac{\partial u^+}{\partial t} + \gamma\frac{\partial u^+}{\partial r} &= v_1(u^+, u^-) + \varepsilon^{1/2} R_1(u^+, u^-, r, t) \\ \frac{\partial u^-}{\partial t} - \gamma\frac{\partial u^-}{\partial r} &= v_2(u^+, u^-) + \varepsilon^{1/2} R_2(u^+, u^-, r, t), \end{aligned} \tag{45}$$

where the systematic reaction terms are now given by

$$v_1(u^+,u^-) = f(u^+,u^-) + \varepsilon C(0)\left[h_2(u^-,u^+)\frac{\delta h_1(u^-,u^+)}{\delta u^-} + h_1(u^-,u^+)\frac{\delta h_1(u^-,u^+)}{\delta u^+}\right],$$

$$v_2(u^+,u^-) = g(u^+,u^-) + \varepsilon C(0)\left[h_1(u^-,u^+)\frac{\delta h_2(u^-,u^+)}{\delta u^+} + h_2(u^-,u^+)\frac{\delta h_2(u^-,u^+)}{\delta u^-}\right], \tag{46}$$

and a new noise terms of zero mean have been defined,

$$R_1(u^+,u^-,r,t) = h_1(u^-,u^+)\eta(x,t)$$

$$-\varepsilon^{1/2}C(0)\left[h_2(u^-,u^+)\frac{\delta h_1(u^-,u^+)}{\delta u^-} + h_1(u^-,u^+)\frac{\delta h_1(u^-,u^+)}{\delta u^+}\right], \tag{47}$$

$$R_2(u^+,u^-,r,t) = h_2(u^-,u^+)\eta(x,t)$$

$$-\varepsilon^{1/2}C(0)\left[h_1(u^-,u^+)\frac{\delta h_2(u^-,u^+)}{\delta u^+} + h_2(u^-,u^+)\frac{\delta h_2(u^-,u^+)}{\delta u^-}\right].$$

Now that we have been able to separate the systematic contribution from the stochastic one, the standard small-noise-expansion can be applied. The lowest order of the field obeys the equations

$$\frac{\partial u_0^+}{\partial t} + \gamma\frac{\partial u_0^+}{\partial r} = v_1(u_0^+,u_0^-),$$

$$\frac{\partial u_0^-}{\partial t} - \gamma\frac{\partial u_0^-}{\partial r} = v_2(u_0^+,u_0^-). \tag{48}$$

This way of rearranging the noise term has allowed us to separate the systematic contributions of the noise (those with nonzero mean value) from the fluctuating ones (those with zero mean value). This distinction, and its consequences, will appear more clearly in the application of this procedure to the study of front propagation dynamics under multiplicative noise. For this end, the point of departure of the present analysis is Eq. (48).

II.2.3 Dynamics and pattern formation of a diffusive predator−prey model in the subdiffusive regime in the presence of toxicity

Recently, Biologists have discovered that bacteria, often viewed as lowly, solitary creatures are actually quite sophisticated in their social interactions and communicate with one another through similar electrical signaling mechanisms as neurons in the human brain. Indeed, In a study recently published in this week's advance online publication of Nature, the scientists detail the manner by which bacteria living in communities communicate with one another electrically through proteins called "ion channels". "Our discovery not only changes the way we think about bacteria, but also how we think about our brain," said Gürol Süel, an associate professor of molecular biology at UC San Diego who headed the research project [149]. "All of our senses, behavior and intelligence emerge from electrical communications among neurons in the brain mediated by ion channels. Now we find that bacteria use similar ion channels to communicate and resolve metabolic stress. Our discovery suggests that neurological disorders that are triggered by metabolic stress may have ancient bacterial origins, and could thus provide a new perspective on how to treat such conditions."

"Much of our understanding of electrical signaling in our brains is based on structural studies of bacterial ion channels" said Süel. But how bacteria use those ion channels remained a mystery until Süel and his colleagues embarked on an effort to examine long-range communication within biofilms organized communities containing millions of densely packed bacterial cells. These communities of bacteria can form thin structures on surfaces such as the tartar that develops on teeth that are highly resistant to chemicals and antibiotics.

The scientists' interest in studying long-range signals grew out of a previous study, published recently [149], which found that biofilms are able to resolve social conflicts within their community of bacterial cells just like human societies. When a biofilm composed of hundreds of thousands of Bacillus subtilis bacterial cells grows to a certain size, the researchers discovered, the protective outer edge of cells, with unrestricted ac-

cess to nutrients, periodically stopped growing to allow nutrients specifically glutamate, to flow to the sheltered center of the biofilm. In this way, the protected bacteria in the colony center were kept alive and could survive attacks by chemicals and antibiotics. Mostly, those chemicals are considered as toxins.

During evolution, venomous animals have produced a panoply of peptide toxins, formidable defense's weapons against predators or for the captures of prey. The targets of these toxins are proteins involved in conduction and nervous transmission, mainly ion channels. These venoms constitute an invaluable source of very specific pharmacological agents for characterization of ion channel and receptor subtypes membranes. By their efficiency and selectivity of action, they offer significant therapeutic potential as evidenced by toxins whose effectiveness in neurological disorders is now being tested in therapeutic trials.

Based on the above discussions, we consider a prey-predator model to investigate the influence of toxicity in the neuronal communication in subdiffusive regime. It is assumed that prey produces a substance that is toxic to predators. For such an ecosystem, the model is as follows:

$$\begin{aligned} \frac{{}^{c}\partial^{\alpha}u}{\partial t^{\alpha}} &= d_1\Delta u + ru(1-\tfrac{u}{K}) - \frac{muv}{a+u}, \\ \frac{{}^{c}\partial^{\alpha}v}{\partial t^{\alpha}} &= d_2\Delta v + sv(1-\frac{hv}{u}) - \beta uv^2. \end{aligned} \tag{49}$$

The reaction terms in Eq. (49) were first proposed by Zhang and Zhao to describe an ecosystem where prey produces substances that are toxic to predators [150]. The term βuv^2 denotes the effect of toxic substances and β represents the efficiency of toxicity. u and v denote the sizes of the prey population and predator population, respectively. r, K, m, a, s, h, and β are all positive constants, $\alpha \leq 1$. Note that in this form, the evolution of the uniform state is controlled by subdiffusion, even if the spatial term is not present.

II.3 Nonlinear analysis

In this section, we will make a summary presentation of all the analytical steps which allowed the resolution of our different models.

II.3.1 Case of the transport memory effects

The method that will be employed to solve Eq. (27) is known as the factorization method. It is a method that seeks traveling wave solutions for a particular class of partial differential equations (PDE) that are associated with having a polynomial nonlinearity. For this purpose, we introduce a traveling wave ansatz of the form

$$u(x,t) = U(z), \tag{50}$$

where $z = x - ct$, $c \geq 0$ is the velocity of the wave. Substituting this transformation into Eq. (27) and rearranging yields,

$$\frac{d^2U}{dz^2} + \frac{c}{(v^2 - c^2)}[\alpha - kf^{'}(U)]\frac{dU}{dz} + \frac{\alpha k}{(v^2 - c^2)}f(U) = 0. \tag{51}$$

By replacing $f^{'}(U)$ and $f(U)$ by their expressions in Eq. (51), we obtain

$$\frac{d^2U}{dz^2} + \frac{c}{(v^2 - c^2)}\left[\alpha + 3kU^2 - 2k(1+a)U + ka\right]\frac{dU}{dz} + \frac{\alpha k}{(v^2 - c^2)}U(U-a)(1-U) = 0. \tag{52}$$

Let

$$G(U) = \frac{c}{(v^2 - c^2)}[\alpha + 3kU^2 - 2k(1+a)U + ka], \tag{53}$$

and

$$F(U) = \frac{\alpha k}{(v^2 - c^2)}U(U-a)(1-U). \tag{54}$$

Thus, rearranging Eq. (52) yields

$$\frac{d^2U}{dz^2} + G(U)\frac{dU}{dz} + F(U) = 0. \tag{55}$$

We aim to factorize Eq. (55) into a form given by

$$[D_z - f_2(U)]\,[D_z - f_1(U)]\,U = 0, \tag{56}$$

where $D_z = \dfrac{d}{dz}$, and the functions f_1 and f_2 relate to $F(U)$ implicitly.

We start by expanding Eq. (56) to get

$$D_z{}^2U - D_z f_1 U - f_2 D_z U + f_1 f_2 U = 0, \tag{57}$$

which leads to

$$\frac{d^2U}{dz^2} - f_1\frac{dU}{dz} - \frac{df_1}{dU}\frac{dU}{dz}U - f_2\frac{dU}{dz} + f_1 f_2 U = 0. \tag{58}$$

At this level, it is required that we factorize the expression in Eq. (58) by grouping terms. We will use the Rosu and Cornejo−Perez grouping technique [151], which is given by

$$\frac{d^2U}{dz^2} - \left(\frac{df_1}{dU}U + f_1 + f_2\right)\frac{dU}{dz} + f_1 f_2 U = 0. \tag{59}$$

Comparing Eq. (59) and Eq. (55), we obtain

$$\frac{df_1}{dU}U + f_1 + f_2 = -G(U), \tag{60}$$

and,

$$f_1 f_2 = \frac{F(U)}{U}, \tag{61}$$

where f_1 and f_2 are set to be

$$f_1 = \alpha(1 - U), \tag{62}$$

and

$$f_2 = \frac{k}{v^2 - c^2}(U - a). \tag{63}$$

We now substitute the expressions of f_1, f_2 and $G(U)$ into Eq. (60), it yields

$$-\alpha U + \alpha(1-U) + \frac{k}{v^2-c^2}(U-a) = -G(U). \tag{64}$$

After grouping terms according to the power of U, we obtain

$$3cU^2 + \eta(c,a)U + \beta(c,a) = 0, \tag{65}$$

where $\eta(c,a) = (1+2(1+a)c)k + 2(c^2-v^2)v^2$, and

$\beta(c,a) = -a(1+c)k + v^2(-c-c^2+v^2)$.

It has been shown that for $a{>}1/2$, the only traveling solution is $U = 0$ [152], which corresponds to the extinction option. For $0{<}a \leq 1/2$, and for each set of parameters of Eq. (27), there are two possibles front velocities for which there are continuous solutions that represent a transition between the stationary states.

We now implement the Rosu and Cornejo−Perez grouping technique defined in Eq. (59) to obtain

$$\frac{d^2U}{dz^2} - (-\alpha U + \alpha(1-U) + \frac{k}{v^2-c^2}(U-a))\frac{dU}{dz} + f_1 f_2 U = 0. \tag{66}$$

As stated previously, this structure allows us to get

$$\left[D_z - \frac{k}{v^2-c^2}(U-a)\right]\left[D_z - \alpha(1-U)\right]U = 0. \tag{67}$$

Eq. (67) will be related to one of the following ordinary differential equation (ODE)

$$\frac{dU}{dz} - \alpha(1-U)U = 0. \tag{68}$$

or

$$\frac{dU}{dz} - \frac{k}{v^2-c^2}(U-a)U = 0. \tag{69}$$

If we consider Eq. (68), we have

$$\int \frac{dU}{(1-U)U} = \int \alpha dz. \tag{70}$$

By integrating Eq. (70), we get

$$-ln(|1-U|) + ln(|U|) = \alpha z + c_r, \tag{71}$$

where c_r is the constant of integration. After small algebra, Eq. (71) gives

$$U = \frac{exp(\alpha z + c_r)}{1 + exp(\alpha z + c_r)}. \tag{72}$$

The constant c_r relates to an initial shift of the wave, if desired. Eq. (72) can be reduced to

$$U = 1 - \frac{1}{1 + exp(\alpha z + c_r)}. \tag{73}$$

We can now use the inverse transformation of $U(z) = u(x - ct)$, with $z = x - ct$ to get

$$U = 1 - \frac{1}{1 + exp(\alpha(x - ct) + c_r)}. \tag{74}$$

Let us now consider Eq. (69), we have

$$\int \frac{dU}{(a-U)U} = \int -bdz. \tag{75}$$

By integrating (75), we get

$$-ln(|a-U|) + ln(|U|) = -bz + c_l, \tag{76}$$

where c_l is the constant of integration. In order to avoid discontinuity, we have to make sure that $0<U<a$. Using the exponential function, and rearranging for U, Eq. (75) gives,

$$U = \frac{aexp(-bz + c_l)}{1 + exp(-bz + c_l)}. \tag{77}$$

After reduction for clarity purposes, Eq. (77) can be written in a simpler form given by

$$U = a\left[1 - \frac{1}{1 + exp(-bz + c_l)}\right]. \tag{78}$$

We now implement the inverse transformation of $U(z) = u(x - ct)$, with $z = x - ct$, to get

$$U = a\left[1 - \frac{1}{1 + exp(-b(x - ct) + c_l)}\right], \tag{79}$$

where $b = \dfrac{k}{v^2 - c^2}$, and the constant c_l relates to an initial shift of the wave, if desired.

II.3.2 Case of the front dynamics with external fluctuations in reaction random walk with direction-independent kinetics

The mean front shape of Eq. (36) is now given by the ensemble average $u_0^+(x,t) = \langle u^+(x,t)\rangle$, and $u_0^-(x,t) = \langle u^-(x,t)\rangle$. Taking the ensemble average of system (36), and using the Furutsu−Novikov−Donsker theorem [153, 154, 155, 156] for the noise term, we can get an equation of the motion for $\langle u^+(x,t)\rangle$ and $\langle u^-(x,t)\rangle$ as

$$\begin{aligned}
\frac{\partial u_0^+}{\partial t} + \gamma\frac{\partial u_0^+}{\partial r} &= v_1(u_0^-, u_0^+) + \varepsilon^{\frac{1}{2}} R_1(u_0^-, u_0^+),\\
\frac{\partial u_0^-}{\partial t} - \gamma\frac{\partial u_0^-}{\partial r} &= v_2(u_0^-, u_0^+) + \varepsilon^{\frac{1}{2}} R_2(u_0^-, u_0^+),
\end{aligned} \tag{80}$$

where

$$
\begin{aligned}
v_1(u_0^+, u_0^-) &= \mu(u_0^- - u_0^+) + \frac{1}{2}b(u_0) - d(u_0)u_0^+ \\
&\quad + \varepsilon C(0)\Big[h_1({u_0}^+, {u_0}^-)\frac{\delta h_1({u_0}^+, {u_0}^-)}{\delta {u_0}^+} \\
&\quad + h_2({u_0}^+, {u_0}^-)\frac{\delta h_1({u_0}^+, {u_0}^-)}{\delta {u_0}^-}\Big], \\
v_2(u_0^+, u_0^-) &= \mu(u_0^+ - u_0^-) + \frac{1}{2}b(u_0) - d(u_0)u_0^- \\
&\quad + \varepsilon C(0)\Big[h_1({u_0}^+, {u_0}^-)\frac{\delta h_2({u_0}^+, {u_0}^-)}{\delta {u_0}^+} \\
&\quad + h_2({u_0}^+, {u_0}^-)\frac{\delta h_2({u_0}^+, {u_0}^-)}{\delta {u_0}^-}\Big],
\end{aligned}
\tag{81}
$$

$$
\begin{aligned}
R_1({u_0}^+, {u_0}^-) &= h_1({u_0}^+, {u_0}^-)\xi(x,t) \\
&\quad - \varepsilon^{\frac{1}{2}} C(0)\Big[h_1({u_0}^+, {u_0}^-)\frac{\delta h_1({u_0}^+, {u_0}^-)}{\delta {u_0}^+} \\
&\quad + h_2({u_0}^+, {u_0}^-)\frac{\delta h_1({u_0}^+, {u_0}^-)}{\delta {u_0}^-}\Big], \\
R_2({u_0}^+, {u_0}^-) &= h_1({u_0}^+, {u_0}^-)\xi(x,t) \\
&\quad - \varepsilon^{\frac{1}{2}} C(0)\Big[h_1({u_0}^+, {u_0}^-)\frac{\delta h_2({u_0}^+, {u_0}^-)}{\delta {u_0}^+} \\
&\quad + h_2({u_0}^+, {u_0}^-)\frac{\delta h_2({u_0}^+, {u_0}^-)}{\delta {u_0}^-}\Big].
\end{aligned}
\tag{82}
$$

This rearrangement allows us to separate a systematic contribution from the noise term and a residual stochastic one.

Higher order moments can be decoupled considering that the profile functions $u^+(x,t)$

and $u^-(x,t)$ can be written as

$$u^+(x,t) = u_0^+(x,t) + \delta u^+(x,t),$$
$$u^-(x,t) = u_0^-(x,t) + \delta u^-(x,t). \tag{83}$$

The quantities $\delta u^+(x,t)$ and $\delta u^-(x,t)$ are small and fast [148] and are responsible for the systematic change of both the mean front shape and the mean front velocity, respectively. The lowest order of the density of the particle going to the right $\delta u^+(x,t)$ and to the left $\delta u^-(x,t)$, respectively, obey the equations

$$\frac{\partial u_0^+}{\partial t} + \gamma \frac{\partial u_0^+}{\partial r} = \mu(u_0^- - u_0^+) + \frac{1}{2} b^{'}(u_0) - d^{'}(u_0) u_0^+,$$
$$\frac{\partial u_0^-}{\partial t} - \gamma \frac{\partial u_0^-}{\partial r} = \mu(u_0^+ - u_0^-) + \frac{1}{2} b^{'}(u_0) - d^{'}(u_0) u_0^-, \tag{84}$$

where $b'(u_0)$ and $d'(u_0)$ are two functions to be determined according to the model used.

II.3.3 Case of the system with toxic substances in a subdiffusive regime

i- Effect of toxic substances on the dynamics properties of the fractional−order ODE system

In this work, we investigate the following parabolic activator-inhibitor model with sub-diffusion consisting of two variables:

$$\frac{{}^c\partial^\eta u}{\partial t^\eta} = d_1 \Delta u + ru(1 - \tfrac{u}{K}) - \frac{muv}{a+u},$$
$$\frac{{}^c\partial^\eta v}{\partial t^\eta} = d_2 \Delta v + sv(1 - \frac{hv}{u}) - \beta u v^2. \tag{85}$$

The reaction terms in Eq. (85) were first proposed by Zhang and Zhao to describe an ecosystem where prey produces substances that are toxic to predators [150]. The term $\beta u v^2$ denotes the effect of toxic substances and β represents the efficiency of toxicity. u

and v denote the sizes of the prey population and predator population, respectively. r, K, m, a, s, h, and β are all positive constants, $\eta \leq 1$. Note that in this form, the evolution of the uniform state is controlled by subdiffusion, even if the spatial term is not present.

We first examine the stability and Hopf bifurcation of the ODE version of the system (85). Omitting the diffusion terms in the system (85), the following ODE system arises

$$\begin{aligned} \frac{{}^c d^\eta u}{dt^\eta} &= ru(1-\frac{u}{K}) - \frac{muv}{a+u}, \\ \frac{{}^c d^\eta v}{dt^\eta} &= sv(1-\frac{hv}{u}) - \beta uv^2. \end{aligned} \tag{86}$$

An obvious steady state of the system (86) is $E_1 = (K, 0)$, the predator−free equilibrium. Assuming that the other equilibrium $E^* = (u^*, v^*)$ of the system (86) satisfies

$$\begin{cases} r(1-\dfrac{u^*}{K}) - \dfrac{mv^*}{a+u^*} = 0, \\ \\ s(1-\dfrac{hv^*}{u^*}) - \beta u^* v^* = 0. \end{cases} \tag{87}$$

Eliminating v yields

$$\begin{aligned} &\beta r u^{*4} + \beta r(a-K)u^{*3} + r(hs - Ka\beta)u^{*2} \\ &+s(Km + ahr - Khr)u^* - Kahrs = 0. \end{aligned} \tag{88}$$

The number and the signs of the roots can easy be predicted from Eq. (88), according to Descartes' rule of signs. So to say, system (88) admits one or three positive roots $u = u^*$ if one of the following inequalities hold

$$a < K, \quad hs < Ka\beta, \quad Km + ahr < Khr. \tag{89}$$

$$a < K, \quad hs > Ka\beta, \quad Km + ahr < Khr, \tag{90}$$

According to inequality (89), if $\beta > \dfrac{hs}{Ka}$, Eq. (88) has exactly one positive root. While inequality (90) states that if $\dfrac{h^2rs}{K^2(hr-m)} < \beta < \dfrac{hs}{Ka}$, Eq. (88) has at least one positive root, and can go up to three positive roots. this result is in perfect agreement with the numerical result found by Zhang et $al.$ [150]. Substituting u^*, we obtain

$$v^* = \frac{su^*}{sh + \beta u^{*2}}. \tag{91}$$

Once we know already the number of equilibria, a word should be said about their stability. The stability of the steady states is determined by the eigenvalues of the Jacobian matrix

$$J = \begin{pmatrix} r(1 - \dfrac{2u^*}{K}) - \dfrac{mav^*}{(a+u^*)^2} & -\dfrac{mu^*}{a+u^*} \\ \\ (\dfrac{sh}{u^{*2}} - \beta)v^{*2} & s(1 - \dfrac{2hv^*}{u^*}) - 2u^*v^*\beta \end{pmatrix}. \tag{92}$$

And the associated characteistic equation is

$$\lambda^2 - T\lambda + \Delta = 0, \tag{93}$$

where

$$T = a_{11} + a_{22}, \tag{94}$$

and

$$\Delta = a_{11}a_{22} - a_{12}a_{21}, \tag{95}$$

$$
\begin{aligned}
a_{11} &= r - \frac{2ru^*}{K} - \frac{mav^*}{(a+u^*)^2}, \\
a_{12} &= -\frac{mu^*}{a+u^*}, \\
a_{21} &= \frac{shv^{*2}}{u^{*2}} - \beta v^{*2}, \\
a_{22} &= s - \frac{2shv^*}{u^*} - 2\beta u^* v^*.
\end{aligned}
\tag{96}
$$

If the trace T of the Jacobian matrix is negative, and Δ, its determinant being positive, then the steady state is stable. While looking at the sign of T and Δ, respectively, we should not forget to distinguish the case of a single positive root from the one of three positive roots.

Then, taking into account conditions (89), for $\eta = 1$, the steady state E^* will be stable if

$$
\beta > \max\{\alpha_1, \alpha_2, \alpha_3\}, \tag{97}
$$

where

$$
\begin{aligned}
\alpha_1 &= \frac{hs}{Ka}, \\
\alpha_2 &= \frac{1}{2u^*v^*}\left[a_{11} + s\left(1 - \frac{2hv^*}{u^*}\right)\right], \\
\alpha_3 &= \frac{s}{2u^*v^*\left(a_{12} - a_{11}\right)}\left[\frac{hv^*}{u^*}\left(2a_{11} - a_{12}\frac{v^*}{u^*}\right) - a_{11}\right],
\end{aligned}
\tag{98}
$$

With $\beta_H = \alpha_2$ being a Hopf bifurcation for the system (86). If, on the other hand we consider conditions (90), steady states will be stable if β is bounded as follows:

$$
\max\{\alpha_2, \alpha_3\} < \beta < \alpha_1. \tag{99}
$$

However, for $\eta \in (0, 1)$, the stability of E^* is more complex and depends on the inequal-

ity

$$|\arg \lambda| > \frac{\eta\pi}{2}, \tag{100}$$

for the roots λ in the Eq. (93).

In order to really appreciate the validity of our predictions, it would be wise to assign some values to the constitutive parameters of the Eq. (88). Indeed, we choose parameters as follows: $K = 4, r = 0.7, m = 1\, a = 0.4, s = 0.25, h = 1$. With this set of parameters, $\alpha_1 = 0.15625$, $\alpha_2 = -0.059731$ and $\alpha_3 = -0.0117744$, yielding $\max\{\alpha_1, \alpha_2, \alpha_3\} = \alpha_1$.

Let us first consider the inequality (89). We choose $\beta = 0.17$, which is in agreement with (97). With this value of β, we have one positive and stable root for $\eta = 1$, as well as for $\eta \in (0, 1)$.

If we consider instead the inequality (90), and we choose $\beta = 0.09$ as in [150], we will have three positive equilibrium points E_1^*, E_2^* and E_3^*. The first equilibrium point is stable for $\eta = 1$, and for $\eta \in (0, 1)$.

For the second equilibrium point, if $\eta = 1$, $\Delta < 0$, the discriminant is always positive, $T^2 - 4\Delta > 0$, and both eigenvalues are real. However, one is positive and the other is negative. Trajectories approach the steady state along the eigenvector corresponding to the negative eigenvalue, but move away along the eigenvector corresponding to the positive eigenvalue. The steady state has one stable and one unstable direction. It is therefore unstable and called a saddle [157]. When $\eta \in (0, 1)$, this equilibrium point is stable, according to inequality (100). Regarding the third equilibrium point, its stability is guaranteed for both $\eta = 1$ and $\eta \in (0, 1)$. While remaining in inequality (90), according to Descartes' rule of signs, it is possible to have a unique positive root. So, taking $\beta = 0.03$, for $\eta = 1$, the equlibrium point E_4^* has complex conjugate eigenvalues with a positive real part, $\lambda = T/2$. The steady state is unstable. Due to the presence of a nonzero imaginary part, perturbations grow in an oscillatory manner and spiral away from the steady state. The steady state is an unstable focus. If $\eta \in (0, 1)$, E_4^* is found to be unstable, according to Eq. (100). These results confirm the paramount role that the toxic coefficient plays on the stability of the system. In addition, it would be interesting

to note that this stability, depending on the system parameters, can either be modified or maintained.

ii- Analysis of a system with toxic substances in a subdiffusive regime

We now proceed to analyze the case we are interested in, namely the modifications of Turing pattern induced by toxic substances in the presence of strong memory effects in the transport process. In order to appreciate these modifications, it is convenient to use the approach developped by Hernández et $al.$ [158] because it can help us to see every new results that will emerge. For this purpose, we start by linearizing around the fixed points, writting Eq. (85) as follows:

$$\begin{aligned} \frac{{}^{c}\partial^{\eta} u}{\partial t^{\eta}} &= d_1 \Delta u + a_{11} u + a_{12} v, \\ \frac{{}^{c}\partial^{\eta} v}{\partial t^{\eta}} &= d_2 \Delta v + a_{21} u + a_{22} v, \end{aligned} \tag{101}$$

where a_{ij} are the elements of the Jacobian matrix given by Eq. (96). Applying Fourier and Laplace transforms to Eq.(101) yields

$$\begin{aligned} s^{\eta} U - s^{\eta-1} U(k,0) &= -d_1 k^2 U + a_{11} U + a_{12} V, \\ s^{\eta} V - s^{\eta-1} V(k,0) &= -d_2 k^2 V + a_{21} U + a_{22} V, \end{aligned} \tag{102}$$

where U and V are given by

$$\begin{aligned} U &= \int_{-\infty}^{\infty} \int_{-\infty}^{\infty} e^{ikx} e^{-st} u(x,t) dt dx = \mathcal{F}(\mathcal{L}(u)), \\ V &= \int_{-\infty}^{\infty} \int_{-\infty}^{\infty} e^{ikx} e^{-st} v(x,t) dt dx = \mathcal{F}(\mathcal{L}(v)). \end{aligned} \tag{103}$$

Resolution of the sytem of Eqs. (102) yields

$$U(k,s) = \frac{(s^{\eta} + d_1 k^2 - a_{22}) s^{\eta-1} U(k,0) + s^{\eta-1} a_{12} V(k,0)}{S(k,s)},$$
$$V(k,s) = \frac{(s^{\eta} + d_2 k^2 - a_{11}) s^{\eta-1} V(k,0) + s^{\eta-1} a_{21} U(k,0)}{S(k,s)}. \tag{104}$$

The time evolution of $u(k,t) = \mathcal{L}^{-1}(U(k,s))$ is given by the singularities of Eq. (104) which is the zeros of the function

$$S(k,s) = s^{\eta+\alpha} + s^{\eta}(d_2 k^2 - a_{22}) + s^{\alpha}(d_1 k^2 - a_{11})$$
$$+ d_1 d_2 k^4 + (a_{11} a_{22} - a_{12} a_{21}) - k^2 (a_{22} d_1 + a_{11} d_2). \tag{105}$$

Solving the equation

$$S(k, s_0) = 0, \tag{106}$$

we can analyze the instability of the system near the fixed points. $s_0(k)$ will be studied numerically for different values of the toxic coefficient to determine when instabilities should appear in the system of Eq. (101), and if it is influenced by toxicity. In particular, the conditions for a Turing instability are

$$Re[s_0(k=0)] < 0, \tag{107}$$

and

$$Re[s_0(k)] > 0. \tag{108}$$

Now, let us use the approach proposed by Hernández et $al.$ [158] to have a Turing instability in the case where $\alpha = \eta < 1$. For this purpose, we start with the Fourier transform

of Eq. (101),

$$\frac{{}^{c}\partial^{\eta}}{\partial t^{\eta}}\begin{pmatrix}\widetilde{u}\\ \\ \widetilde{v}\end{pmatrix} = \begin{pmatrix}-d_1k^2+a_{11} & a_{21}\\ \\ a_{12} & -d_2k^2+a_{22}\end{pmatrix}\begin{pmatrix}\widetilde{u}\\ \\ \widetilde{v}\end{pmatrix} = A(k)\begin{pmatrix}\widetilde{u}\\ \\ \widetilde{v}\end{pmatrix}$$

The eigenvalues of the stability matrix $[A(k)]$ are given by

$$\begin{aligned}\lambda_1 &= \frac{TrA(k)}{2} + \frac{([TrA(k)]^2 - 4h(k))^{1/2}}{2},\\ \lambda_2 &= \frac{TrA(k)}{2} - \frac{([TrA(k)]^2 - 4h(k))^{1/2}}{2},\end{aligned} \tag{109}$$

where

$$\begin{aligned}TrA(k) &= -(d_1+d_2)k^2 + (a_{11}+a_{22}),\\ h(k) &= d_1d_2k^4 - (a_{11}d_2 + a_{22}d_1)k^2 + a_{11}a_{22} - a_{12}a_{21}\end{aligned} \tag{110}$$

The stability of the system is completely determined by the nature of the eigenvalues. Real and negative eigenvalues yield a stable system, meaning that no Turing instabilities are possible. Meanwhile if both are real and one of them is positive (the other being negative), then the system will no longer be stable, and the condition for this are exactly the sames as for the case $\eta = 1$. However, complex roots goes with a critical value of η. This critical value η_c only exists if $TrA(k) > 0$, and it is given by

$$\eta_c(k) = \frac{2}{\pi} arctan\left(\sqrt{\frac{4h(k)}{[TrA(k)]^2} - 1}\right). \tag{111}$$

η_c is a critical value of the anomalous exponent or bifurcation parameter that separates a regime of stationary Turing patterns from an oscillatory cellular instability, commonly known as a Hopf−Turing bifurcation [159]. The Turing conditions are fullfiled when

the stationary homogeneous state $(k = 0)$ is stable, and the system becomes unstable under perturbations with finite wavelength. So to say, when reactions take place in the presence of subdiffusion, the condition (107) can be satisfied in two ways, either

$$\beta > max\{\alpha_2, \alpha_3\}, \tag{112}$$

or

$$\beta < \alpha_2,$$

$$4u^{*2}v^{*2}\beta^2 + \alpha_4\beta + \alpha_5 < 0, \tag{113}$$

$$\eta_c(0) > \eta,$$

where

$$\alpha_4 = 4v^* \left(-a_{11}u^* - a_{12}v^* + su^* \left(1 - \frac{2hv^*}{u^*}\right)\right),$$

$$\alpha_5 = a_{11}^2 - 2a_{11}s \left(1 - \frac{2hv^*}{u^*}\right) + \frac{4a_{12}shv^{*2}}{u^{*2}} + \tag{114}$$

$$s^2 \left(1 - \frac{2hv^*}{u^*}\right)^2.$$

Condition (113) cannot be fullfiled for the classical diffusion.

To fulfill the condition in Eq. (108), it is necessary that

$$\beta > \frac{1}{2Du^*v^*} \left[a_{11} + Ds \left(1 - \frac{2hv^*}{u^*}\right)\right], \tag{115}$$

where $D \neq 1$ is the ratio of diffusion coefficients, and either

$$a_{11} > 0, \qquad \beta > \frac{s}{2u^*v^*}(1 - \frac{2hv^*}{u^*}), \tag{116}$$

or

$$a_{11} < 0, \qquad \beta < \frac{s}{2u^*v^*}(1 - \frac{2hv^*}{u^*}), \tag{117}$$

II.4 Numerical methods and iterative schemes for computational analysis

In this section, we present some numerical methods in order to solve different equations we have used in this thesis. It should be noted that several numerical approaches were used in the context of this thesis. However, we will dwell on only two, because not only do these two approaches encompass all the others, but also they deal with the fundamental problems raised by this thesis, namely the influence of spatio-temporal external multiplicative fluctuations frequently encountered in the neuronal processes, and the incorporation of strong memory effects in the neuronal transport process through fractional dynamics.

II.4.1 Numerical algorithm for spatio-temporal external multiplicative noise

Consider the following model equation for the one-dimensional infinite case, with x being real:

$$\frac{\partial n}{\partial t} = f(n) + \frac{\partial^2 n}{\partial x^2} + \sqrt{2H}g(n)\varepsilon(x,t),$$

$$\langle \varepsilon(x,t) \rangle = 0, \tag{118}$$

$$\left\langle \varepsilon(x^{'},t^{'})\varepsilon(x,t) \right\rangle = R(x^{'}-x)T(t^{'}-t).$$

for more details on this model, one can refer to [160]. This model contains two essentials: multiplicative fluctuations and the possibility of kink propagation. The nonlinear reaction term $f(n)$ is assumed to be bistable, with two stable stationary states n_1 and n_3, and one unstable stae n_2, with the boundary conditions $n(-\infty) = n_1$; $n(\infty) = n_3$. To obtain

an algorithm for the space-time discrete system, we have to integrate Eq. (118) first, over the time interval $[0, \Delta t]$, and to average after that over the box length $[-\Delta x/2, \Delta x/2]$. That leads

$$n(0,\Delta t) - n(0,0) = \int\limits_{-\Delta x/2}^{\Delta x/2} \frac{dx'}{\Delta x} \int\limits_{0}^{\Delta t} \left[f(x',t') + \frac{\partial^2 n}{\partial x^2}(x',t') + \sqrt{2H} g(x',t')\varepsilon(x,t) \right] \tag{119}$$

For the calculation of the stochastic integral, we make use of the Stratonovich calculus, which is

$$S - \int\limits_{0}^{\Delta t} dt' \phi(n(t'))\varepsilon(t') = \int dt' \left[\phi(0) + \phi'(0)(n(t') - n(0))\right]\varepsilon(t'). \tag{120}$$

The expansion in $\Delta n(x',t') = n(x',t') - n(0,0)$ of Eq. (119) leads to

$$\begin{aligned} n(0,\Delta t) - n(0,0) = f(0,0)\Delta t + \frac{\Delta t}{\Delta x^2}(n(\Delta x,0) + n(-\Delta x,0) - 2n(0,0)) + \\ \left[\frac{2H\Delta t}{\Delta x}\right]^{1/2} g(0,0)E(0,0) + o(\Delta n^2). \end{aligned} \tag{121}$$

Inserting Δn into the expanded integrands again and collecting all terms of $o(\kappa) = \{\Delta t, \Delta t/\delta x^2, H\Delta t/\delta x\}$, $(\kappa \ll 1)$, we obtain only one relevant term from the corrections. This is

$$\begin{aligned} &\sqrt{2H} g(0,0) \int\limits_{-\Delta x/2}^{\Delta x/2} \tfrac{dx'}{\Delta x} \int\limits_{0}^{\Delta t} dt' \left[\int\limits_{x'-\Delta x/2}^{x'+\Delta x/2} \tfrac{dx''}{\Delta x} \int\limits_{0}^{t'} dt'' * \left(\sqrt{2H} g(x',0)\varepsilon(x'',t'') + n(x',0) - n(0,0) \right) \right] \varepsilon(x',t'), \\ &= 2Hg(0,0)g'(0,0) * \tfrac{1}{2} \left[\int\limits_{-\Delta x/2}^{\Delta x/2} dx' \int\limits_{0}^{\Delta t} dt' \varepsilon(x',t') \right]^2, \\ &= \tfrac{H\Delta t}{\Delta x} g(0,0)g'(0,0)E^2(0,0). \end{aligned} \tag{122}$$

The final result reads

$$n(i,\tau+1) = n(i,\tau) + \Delta t f(i,\tau) + \frac{\Delta t}{\Delta x^2}\left(n(i+1,\tau) + n(i-1,\tau) - 2n(i,\tau)\right) + \frac{H\Delta t}{\Delta x} g'(i,\tau) g(i,\tau) E^2(i,\tau) + \left[\frac{2H\Delta t}{\Delta x}\right]^{1/2} g(i,\tau) E(i,\tau), \tag{123}$$

with $E(i,\tau)$ being the Gaussian white noise.

II.4.2 Numerical algorithm for subdiffusive transport processes

We used the discretization of the Caputo fractional derivatives proposed by Gorenflo and Abdel-Rehim [161], namely

$$\frac{{}^c\partial^\alpha y_{ij}}{\partial t^\alpha}\Big|_{t_{n+1}} = \sum_{m=0}^{n+1} (-1)^k \begin{pmatrix} \alpha \\ m \end{pmatrix} \frac{y_{i,j}(t_{n+1-m}) - y_{i,j}(t_0)}{(\Delta t)^\alpha}, \tag{124}$$

where $y_{i,j}(t_{n+1-m})$ is the function evaluated at the point (i,j) in a two-dimensional grid, and at a discrete time t_n. The quantity Δt represents the time step, which was chosen to be 0.01. Observe that the system has a memory of $n+2$ time steps, and there is a need to store all this information in the computer memory. There is a numerical difficulty with the combinatory factors, and much attention should be put in order to avoid losing significant figures with big numbers. This problem was solved by using the recurrence relation

$$\begin{pmatrix} \alpha \\ m \end{pmatrix} = \left[1 - \frac{1+\alpha}{m}\right] \begin{pmatrix} \alpha \\ m-1 \end{pmatrix}. \tag{125}$$

Observe that for $m = 1$, the combinatory factor is α, and the coefficient for $m = 0$ is 1 in Eq. (124). In principle, the number of terms in the summation grows with time, and the calculation becomes rapidly unmanageable. Therefore, in practice, we only retain terms whose coefficients are larger than 10^7. In the worse of cases, the number of terms needed

in the memory was 800. It was found that more terms are needed when the anomalous exponents are smaller.

II.5 Conclusion

In this chapter, we have presented the different analytical approaches allowing to provide answers to the content of this thesis. On the basis of these analytical approaches, we have presented two numerical approaches for the two phenomena which encompass the main part of our results, namely the fluctuations resulting from multiplicative spatio-temporal noise of external origin, as well as the transport processes in the subdiffusive regime. These methods will be used to obtain the results presented in Chapter III.

CHAPTER III

RESULTS AND DISCUSSION

III.1 Introduction

In this chapter, we present and discuss the results of our thesis using both analytical and numerical methods presented in chapter II. This chapter is organized as follows: In the second section, the importance of the transport memory effects in the bistable systems is presented. Furthermore, we highlight the effects of noise through the reaction random walk in population genetics. Finally, we present the effects of strong memory in the neuronal transport process in presence of toxicity, considering a subdiffusive regime.

III.2 Importance of the transport memory effects in the bistable systems

In the previous chapter, we derived the analytical expression for the front solution connecting two equilibrium states $U = 0$ to the state $U = 1$, and the state $U = 1$ to the state $U = 0$ in Eqs. (74) and (79), respectively. In order to observe the behavior of these solutions under the influence of memory effects, we plot the traces for several values of the memory function. Figure 6 (a) represents a solution connecting the equilibrium $U = 0$ to the equilibrium $U = 1$. These trajectories correspond to fronts of state 0 invading the state 1, for different values of the memory function at very short times. When α increases, the width of the front wave decreases, it means that the memory effects increase the speed of the front wave. Figure 6 (b) corresponds to the left propagating front that connects the front state $U = 1$ with the front state ($U = 0$). We have an overdamped trajectory, since negative solutions are not allowed [28]. In this case, when the memory

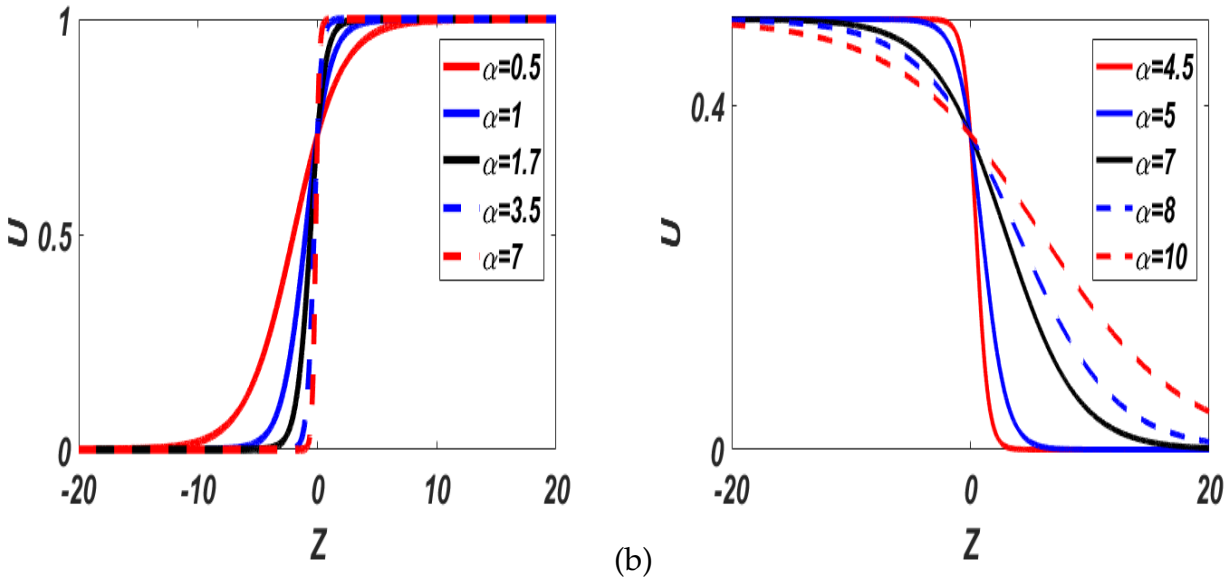

(a) (b)

Figure 6: (a): Right propagating front. (b): left propagating front..

effects increase, the width of the front wave decreases, it means that the memory acts like a damping coefficient.

In order to really appreciate the effect of transport memory, we carry out a piecewise linearization of Eq. (51). Indeed, explicit solutions corresponding to the front waves described above cannot be found in the fully nonlinear situation.

III.2.1 Piecewise linearization

Another way to treat the Nagumo's reaction term is to replace the nonlinear function by its piecewise linear approximation. Following Elmer [162], we rewrite the reaction function as

$$f(U) = \begin{cases} -U & U < \dfrac{a}{2}, \\ U - a & \dfrac{a}{2} \leq U \leq \dfrac{a+1}{2}, \\ 1 - U & \dfrac{a+1}{2} < U. \end{cases} \tag{126}$$

Denoting differentiation with respect to z by primes and by using Eq. (50), we reduce the PDE (27) to an ODE, which describes a damped harmonic oscillator:

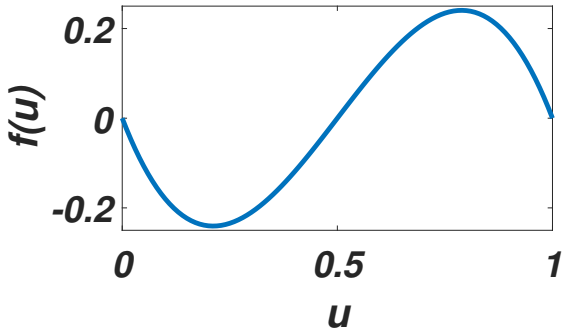

Figure 7: The Nagumo's function with $a = 0.5$.

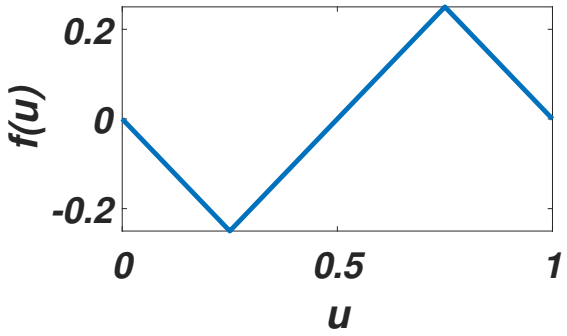

Figure 8: The piecewise linear approximation.

$$\begin{aligned} &mU'' + 2\gamma_1 U' - \omega^2 U = 0,\ U \leq \frac{a}{2}, \\ &mU'' + 2\gamma_2 U' + \omega^2 (U - a) = 0,\ \frac{a}{2} \leq U \leq \frac{a+1}{2}, \\ &mU'' + 2\gamma_3 U' + \omega^2 (1 - U) = 0,\ U > \frac{a+1}{2}. \end{aligned} \tag{127}$$

Here, we used the notation of Manne et *al*. [28], $m = v^2 - c^2$ to emphasize the formal similarity between Eq. (27), where we have inserted Eq. (50) and the equation of motion of a damped oscillator of mass m subject to a nonlinear force $-\alpha k U(U - a)(1 - U)$. Parameters are as follows:

$$\gamma_1 = \gamma_3 = \frac{c}{2}(\alpha + k), \gamma_2 = \frac{c}{2}(\alpha - k), \omega = \sqrt{\alpha k}. \tag{128}$$

It is clear that eq. (127) is the equation of motion of three damped harmonic oscillators, which is in agreement with the results obtained by Zhao et *al*. [163] showing that chromatin behaves like a set of synchronized oscillators either by the coupling of

an electromagnetic field generated by a longitudinal oscillation of the nucleosomes, or by the physical interactions of the DNA-protein complexes. These results are in agreement with [164] showing that the telegraph−type equations do not take into account the mechanical and thermodynamic effects. Solutions for wave amplitude as a coordinate function $x - ct$ can be obtained for each region $U<\frac{a}{2}$, $\frac{a}{2}<U<\frac{a+1}{2}$ and $U>\frac{a+1}{2}$.

In the region $U<\frac{a}{2}$, depending on the values of m, solutions are given as follows:

If $m = 0$, we have

$$U(z) = Be^{\frac{\omega^2}{2\gamma_1}z}. \tag{129}$$

and,

If $m \neq 0$, we obtain

$$U(z) = B_+e^{r_+z} + B_-e^{r_-z}, \tag{130}$$

with

$$r_\pm = \frac{-\gamma_1 \pm \sqrt{\gamma_1^2 + m\omega^2}}{m}. \tag{131}$$

In the region $\frac{a}{2} \leq U \leq \frac{a+1}{2}$, depending again on the values of m, we obtain the following solutions:

if $m = 0$, we get

$$U(z) = a + Ce^{-\frac{\omega^2}{2\gamma_2}z} \tag{132}$$

and,

if $m \neq 0$, we have

$$U(z) = \begin{cases} a + C_+e^{R_+z} + C_-e^{R_-z} & R_+ \neq R_-, \\ a + C_0e^{Rz} + C_1ze^{Rz}, & R_+ = R_- = R, \end{cases} \tag{133}$$

with

$$R_\pm = \frac{-\gamma_2 \pm \sqrt{\gamma_2^2 - m\omega^2}}{m}. \tag{134}$$

In the region $U>\frac{a+1}{2}$,

if $m=0$, it leads

$$U(z)=1-De^{\frac{\omega^2}{2\gamma_3}z}, \tag{135}$$

and,

if $m\neq 0$, we obtain

$$U(z)=\begin{cases} 1-D_+e^{\mu_+ z}-D_-e^{\mu_- z} & \mu_+\neq\mu_-, \\ 1-D_0e^{\mu z}+D_1ze^{\mu z}, & \mu_+=\mu_-=\mu, \end{cases} \tag{136}$$

where

$$\mu_\pm=\frac{-\gamma_3\pm\sqrt{\gamma_3^2-m\omega^2}}{m}. \tag{137}$$

We define the following variables U_L, U_{R1} and U_{R2} following Ref. [28]

$$\begin{aligned} &U_L(-z)=U(z), \quad z\geq 0, \\ &U_{R1}(z)=a+U(z), \quad z\geq 0, \\ &U_{R2}(z)=1-U(z), \quad z\geq 0, \end{aligned} \tag{138}$$

and we have

$$\begin{aligned} &mU_L^{''}+2\gamma_1U_L^{'}-\omega^2U_L=0,\ z<0, \\ &mU_{R1}^{''}+2\gamma_2U_{R1}^{'}+\omega^2U_{R1}=0,\ 0<z<z_1, \\ &mU_{R2}^{''}+2\gamma_3U_{R2}^{'}+\omega^2U_{R2}=0,\ z>z_1. \end{aligned} \tag{139}$$

We obtain a system of differential equations describing the three damped harmonic oscillators, one of which has a negative mass, and the other two having positive masses. The negative mass of the first oscillator is biologically explained by the fact that many biological systems are very repressive. They trigger a response that tends to oppose the solicitation. The first oscillator thus appears clearly as a low−pass filter, since it allows only signals whose wave velocity is lower than that imposed on it, and the rest is rejected.

We are interested in non−negative solutions, because U is assumed to be a concentration or density [29]. It follows that the damped oscillator U_L representing the shape of the front of the wave must be critically damped to prevent this concentration from oscillating and ending up with negative values. The role of the first oscillator is thus to avoid that one finds itself in a situation where the speed imposed by the stress is superior to that dictated by the medium. Therefore, the condition that this oscillator should be critically damped is verified.

Let us consider the case of the oscillators U_{R1} and U_{R2}. They can be slightly damped, since there is no problem if the concentration oscillates around a positive value. The condition for U_{R1} to be critically damped is: $\gamma_2 = \sqrt{m}\omega$, and the corresponding velocity is given by

$$c_{thr1} = v\frac{1}{\sqrt{1+\frac{1}{4}(y-\frac{1}{y})^2}}, \tag{140}$$

where $y = \sqrt{\frac{\alpha}{k}}$. If $c<c_{thr1}$, the wave front shape exhibits spatial oscillations.

The condition for U_{R2} to be critically damped is $\gamma_3 = \sqrt{m}\omega$, and the corresponding velocity is given by

$$c_{thr2} = v\frac{1}{\sqrt{1+\frac{1}{4}(y+\frac{1}{y})^2}}. \tag{141}$$

Fig 9 shows a comparative study between v, c, c_{thr1} and c_{thr2}, and we see that $c_{thr2} \leq c_{thr1} \leq v$. Using this graph, we can determine explicit solutions of the following regions $c \leq c_{thr2}$, $c_{thr2} \leq c \leq c_{thr1}$ and $c \leq v$.

In the first region, $c \leq c_{thr2}$, depending on each of the three regions $z<0$, $0<z<z_1$ and $z>z_1$, solutions are given by

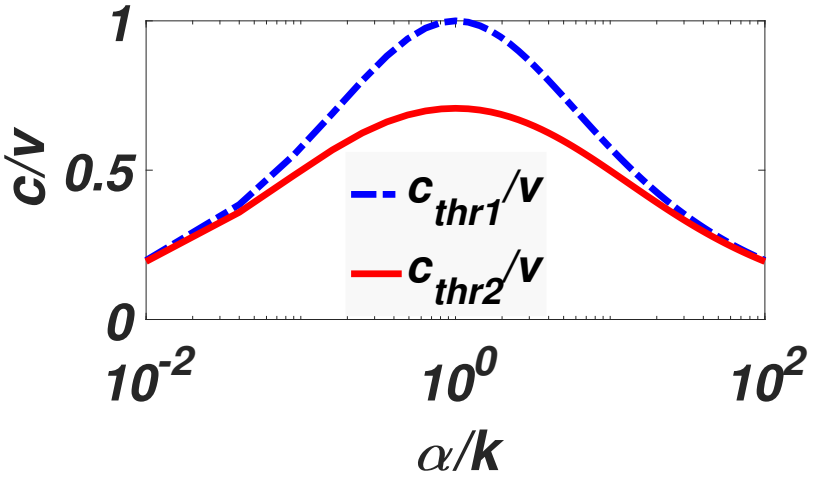

Figure 9: The dependence of the respective ratios of c_{thr1} and c_{thr2} to the speed v dictated by medium on the damping−nonlinearity parameter ratio α/k.

$$U(z) = \begin{cases} \frac{a}{2}e^{r_+ z} & z<0, \\ a(1 - D_1 cos(\frac{2\pi}{\lambda_1}z - \delta_1)) & 0 \leq z \leq z_1, \\ 1 - D_2 e^{\mu z} cos(\frac{2\pi}{\lambda_2}z - \delta_2) & z>z_1, \end{cases} \tag{142}$$

where

$$D_1 = \frac{1}{2cos\delta_1}e^{Rz}, \tag{143}$$

$$D_2 = \frac{1 - a + \frac{a}{2cos\delta_1}cos(\frac{2\pi}{\lambda_1}z_1 - \delta_1)}{e^{\mu z_1}cos(\frac{2\pi}{\lambda_2}z_1 - \delta_2)}, \tag{144}$$

$$\delta_1 = -tan^{-1}\left(\frac{\lambda_1}{2\pi}(r_+ + R)\right), \tag{145}$$

$$\lambda_1 = \frac{2\pi m}{\sqrt{m\omega^2 - \gamma_2^2}}, \tag{146}$$

$$\lambda_2 = \frac{2\pi m}{\sqrt{m\omega^2 - \gamma_1^2}}, \tag{147}$$

$$R_{\pm} = R \pm i\frac{\lambda}{2\pi}, \tag{148}$$

$$\delta_2 = \frac{2\pi}{\lambda_2} - tan^{-1}\left[\frac{\lambda_1}{2\pi}\left(\mu + \frac{\delta_N}{\delta_D}\right)\right], \tag{149}$$

$$\begin{aligned}\delta_N = a(-\frac{R}{2}cos(\frac{2\pi}{\lambda_1}z_1 - \delta_1) + \\ \frac{\pi}{\lambda}sin(\frac{2\pi}{\lambda_1}z_1 - \delta_1))e^{Rz_1},\end{aligned} \tag{150}$$

$$\delta_D = (1 - a[1 - \frac{1}{2cos\delta_1}cos(\frac{2\pi}{\lambda_1}z_1 - \delta_1)])cos\delta_1. \tag{151}$$

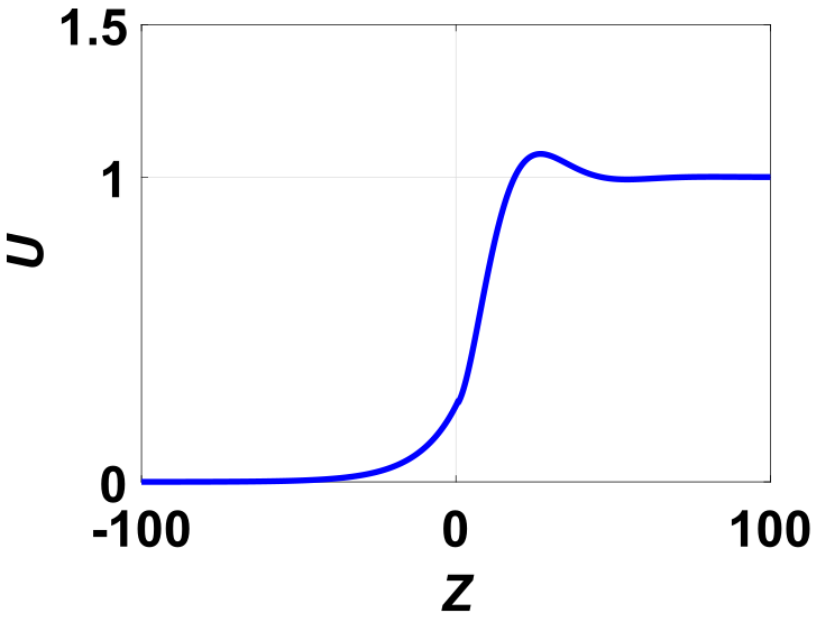

Figure 10: Wave front shape with oscillations (142), using $\alpha = 3$, $a = 0.5$, $k = 1$, $c = 5$, $v = 10$ and $z_1 = \dfrac{a+1}{2}$.

We have an oscillating wave front in space, which proves that there is a supply of energy from the outside environment in this region. If we consider this region as a sink, biophysically, this energy may come from locally ingested nutrients, drugs, or information transmitted into the region considered. This energy can be considered as a source [165]. The sink in this case can be mechanical coupling imposing a coherent

motion to the biological system as, for instance, chromatin. With this coherent motion, chromatin cannot undergo a segregation which is essential before any cell division. The source will therefore break this mechanical coupling, so that the motion of the chromatin becomes incoherent, and therefore, it can be subjected to free diffusion that will allow it to undergo segregation, and give rise to cell division (see Fig. 10).

In the second region , $c_{thr2} \leq c \leq c_{thr1}$, m is positive, and we obtain

$$U(z) = \begin{cases} \frac{a}{2}e^{r+z}, \quad z<0, \\ a(1 - \frac{1}{2cos\delta}e^{Rz}cos(\frac{2\pi}{\lambda}z - \delta)), \quad 0 \leq z \leq z_1, \\ 1 - D_-e^{\mu - z} \quad z>z_1, \end{cases} \tag{152}$$

where

$$\lambda = \frac{2\pi m}{\sqrt{m\omega^2 - \gamma_2^2}}, \tag{153}$$

$$\delta = -tan^{-1}(\frac{\lambda(r_p + R_p)}{2\pi}), \tag{154}$$

$$C = -\frac{a}{2cos\delta}, \tag{155}$$

$$D_- = (1 - a - Ce^{Rz_1}cos(\frac{2\pi z_1}{\lambda} - \delta))e^{-\mu - z_1}. \tag{156}$$

The second region corresponds to a transition zone towards a state of no oscillations, which means that the mechanical coupling has been removed, and the energy used to break this coupling will initiate free diffusion processes in the second region (see Fig. 11).

In the third region, $c \leq v$, m is still positive, the solution is given by:

$$U(z) = \begin{cases} \frac{a}{2}e^{r+z} \quad z<0, \\ a + C_+e^{R+z} + C_-e^{R-z} \quad 0 \leq z \leq z_1, \\ 1 - D_-e^{\mu - z} \quad z>z_1, \end{cases} \tag{157}$$

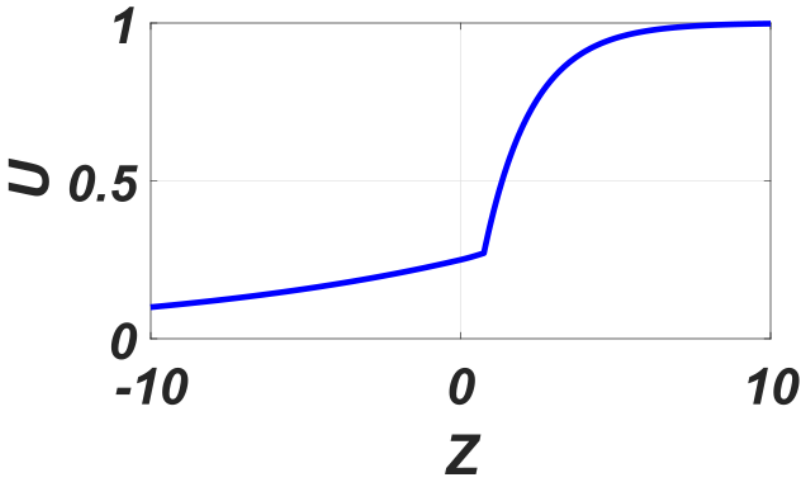

Figure 11: Wave front shape with transition to no oscillations regime (152), with $\alpha = 3$, $a = 0.5$, $k = 1$, $c = 7$, $v = 10$ and $z_1 = \dfrac{a+1}{2}$.

where

$$C_+ = \frac{a(r_+ + R_+)}{2(R_- - R_+)}, \tag{158}$$

$$C_- = \frac{a(r_+ + R_-)}{2(R_+ - R_-)}, \tag{159}$$

$$D_- = \frac{1 - a - C_+ e^{R_+ z_1} - C_- e^{R_- z_1}}{e^{\mu_- z_1}}. \tag{160}$$

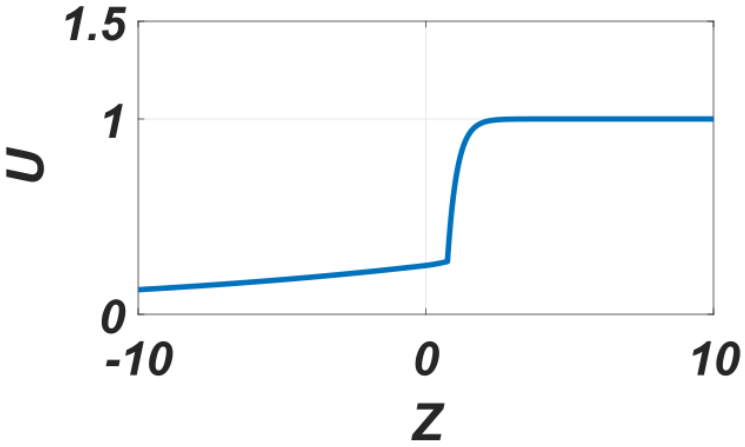

Figure 12: Wave front shape without oscillations (157), for $\alpha = 3$, $a = 0.5$, $k = 1$, $c = 9.5$, $v = 10$ and $z_1 = \dfrac{a+1}{2}$.

Here, we realize that all oscillations have disappeared completely. It means that the process was successfully completed, and another cycle is on his way to start (see Fig. 12).

III.3 Effects of noise through the reaction random walk in population genetics

As mentioned in the previous chapter, $b'(u_0)$ and $d'(u_0)$ are closely related to the model. In this part, we will use the Nagumo equation which is a simple nonlinear reaction-diffusion equation, which has important applications in neuroscience, biological electricity as well as population genetics. The choice made on this model was prompted by these applications, all of which are closely correlated with the transport of nerve impulses. Mathematically, it is given by

$$f(u) = u(u-a)(1-u), \tag{161}$$

where a is the detuning or control parameter. In other words, if $a > 0$, the state $(0,0)$ is stable, and

$$\begin{aligned} b(u) &= (1+a)u^2, \\ d(u) &= u^2 + a. \end{aligned} \tag{162}$$

In this case, the front connects two stable states and is said to be propagating into a metastable state. On the other hand, if $a < 0$, the state $(0,0)$ is unstable, and

$$\begin{aligned} b(u) &= (1+a)u^2 - au, \\ d(u) &= u^2, \end{aligned} \tag{163}$$

the front is said to be propagating into the unstable state.

i-Propagating front into a metastable state

Considering Eq. (162), we can easily determine $b'(u_0)$ and $d'(u_0)$, which are given by

$$\begin{aligned} b'(u_0) &= \varepsilon C(0){u_0}^3 + (1 + a - \varepsilon C(0)){u_0}^2, \\ d'(u_0) &= {u_0}^2 - 2\varepsilon C(0)u_0 - 1 + a. \end{aligned} \tag{164}$$

In this situation, Eq. (84) becomes

$$\begin{aligned} &\frac{\partial u_0^+}{\partial t} + \gamma\frac{\partial u_0^+}{\partial r} = \mu(u_0^- - u_0^+) + \frac{1}{2}(\varepsilon C(0){u_0}^3 + (1 + a - \varepsilon C(0)){u_0}^2) - \\ &({u_0}^2 - 2\varepsilon C(0)u_0 - 1 + a)u_0^+, \\ &\frac{\partial u_0^-}{\partial t} - \gamma\frac{\partial u_0^-}{\partial r} = \mu(u_0^+ - u_0^-) + \frac{1}{2}(\varepsilon C(0){u_0}^3 + (1 + a - \varepsilon C(0)){u_0}^2) - \\ &({u_0}^2 - 2\varepsilon C(0)u_0 - 1 + a)u_0^-, \end{aligned} \tag{165}$$

Before moving forward, it will be wise to look at the behaviour of the parameters of Eq. (36) in the moving frame. This could help us to choose the appropriate parameters while looking at the solutions which are acceptable physically.

Figure Fig. 13 depicts the solution of Eq. (36). It clearly appears that for certain value of parameter a, convergent solutions can be found. In order to see more clearly, we made other plots, in particular that of the speed, the densities as well as the location of a front defined by

$$\begin{aligned} z^+ &= \frac{1}{u_{st}^+}\int_{r_0}^{\infty} dr u^+(r,t), \\ z^- &= \frac{1}{u_{st}^-}\int_{r_0}^{\infty} dr u^-(r,t), \end{aligned} \tag{166}$$

from which the instantaneous velocity for a particular realization were obtained accord-

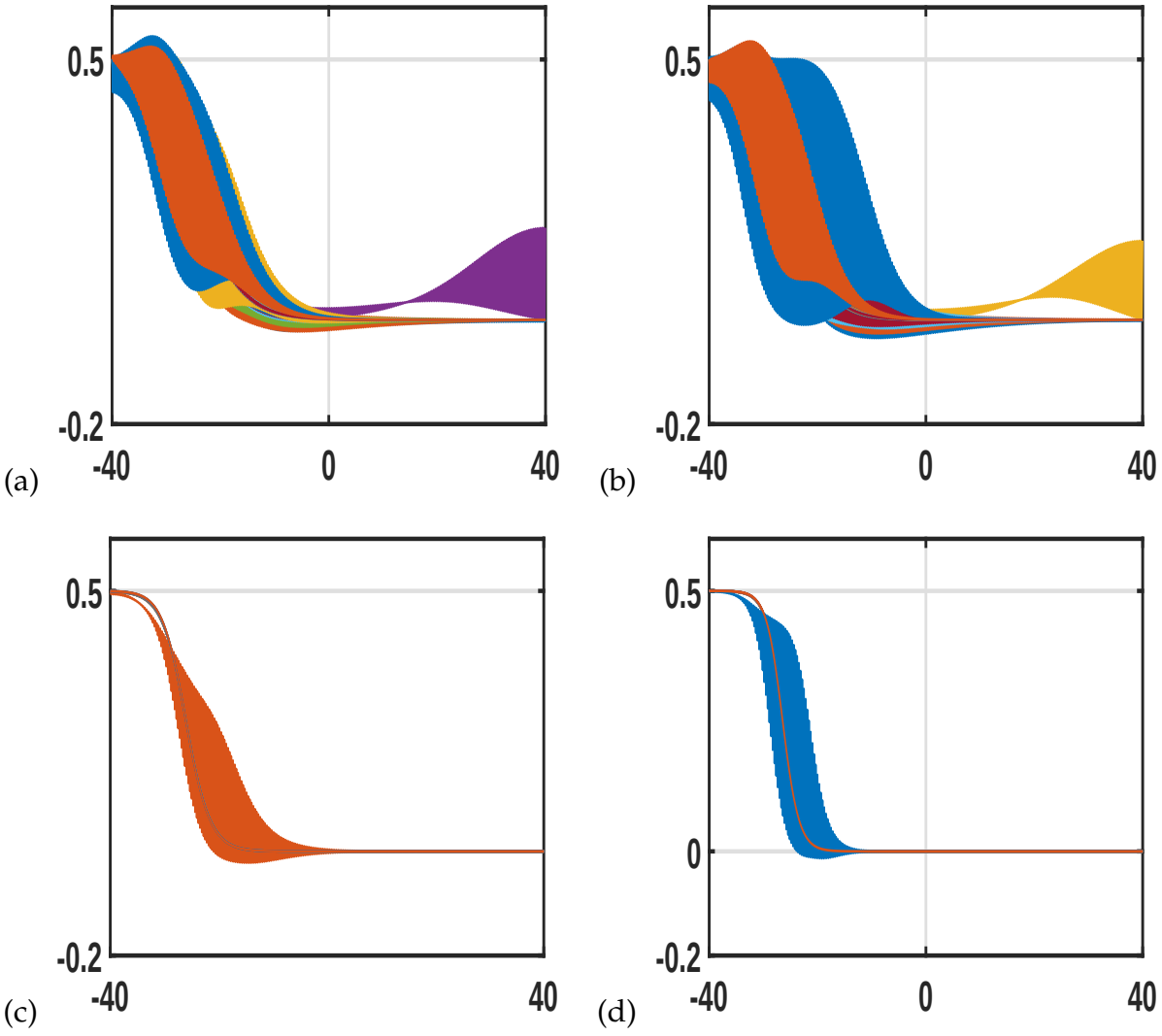

Figure 13: Front solutions obtained for differents values of the detuning parameter a in differents regimes, with $0 \leq a \leq 0.5$. (a) $\mu = 0.35$, (b) $\mu = 0.56$, (c) $\mu = 1.7$, (d) $\mu = 4.0$

ing to the relations

$$v^+ = \frac{du^+}{dt} = \dot{z}^+,$$
$$v^- = \frac{du^-}{dt} = \dot{z}^-. \tag{167}$$

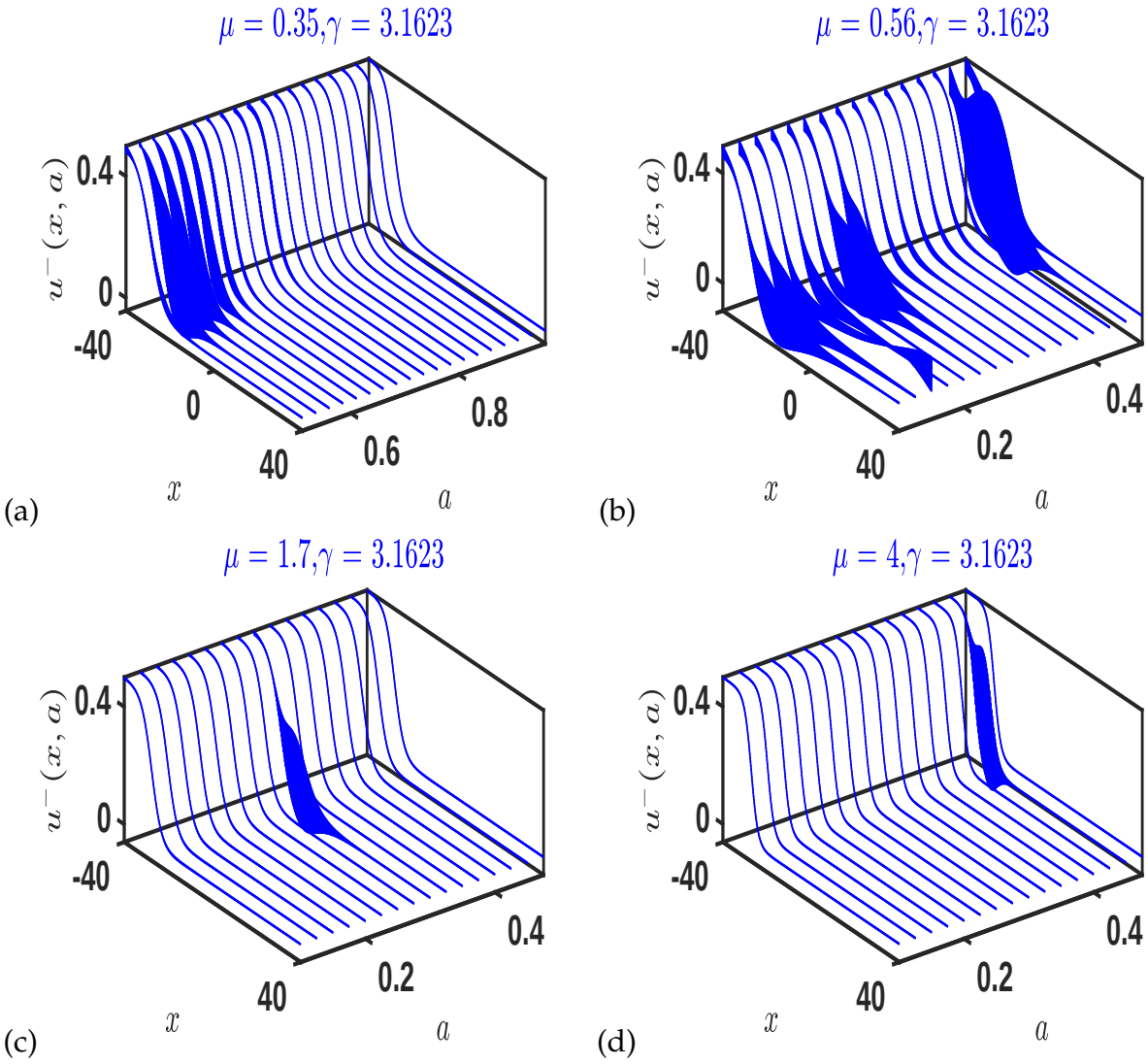

Figure 14: Stables and unstables front profile for left moving particles a in differents regimes, with $0 \leq a \leq 0.5$. (a) $\mu = 0.35$, (b) $\mu = 0.56$, (c) $\mu = 1.7$, (d) $\mu = 4$

These results allow us to illustrate the influence of the parameter a on the dynamics of our system. Indeed, the stability and the convergence of this system are strongly linked to this parameter, because when $a = 0.35$ (ballistic regime), we observe that the wave fronts obtained are very divergent, and oscillate around the fixed points $u^{\pm} = 0.5$ (see Fig. 13). When $\mu = 0.56$, one is already in diffusive mode, but taking into account

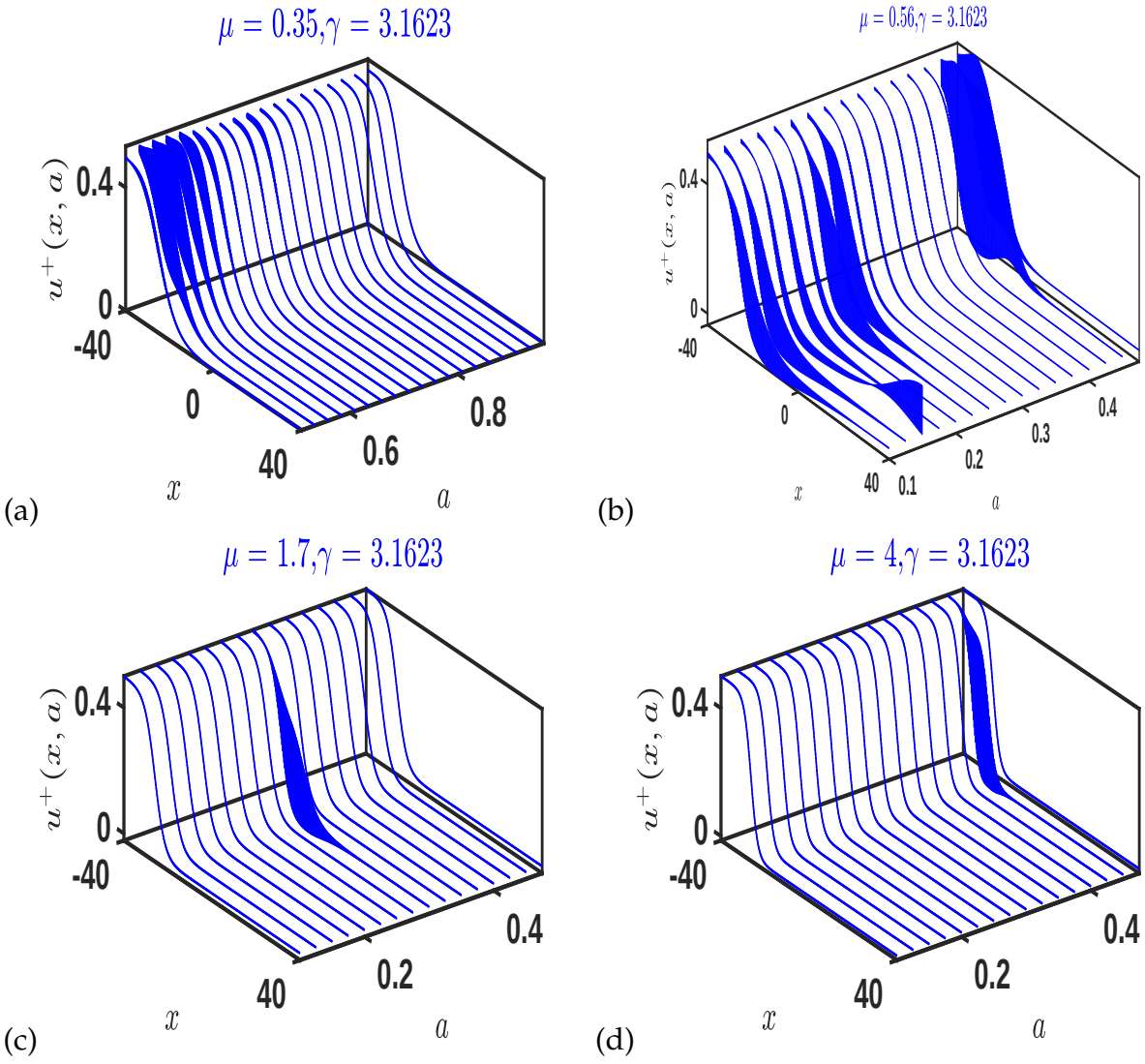

Figure 15: Stables and unstables front profile for right moving particles a in differents regimes, with $0 \leq a \leq 0.5$. (a) $\mu = 0.35$, (b) $\mu = 0.56$, (c) $\mu = 1.7$, (d) $\mu = 4$

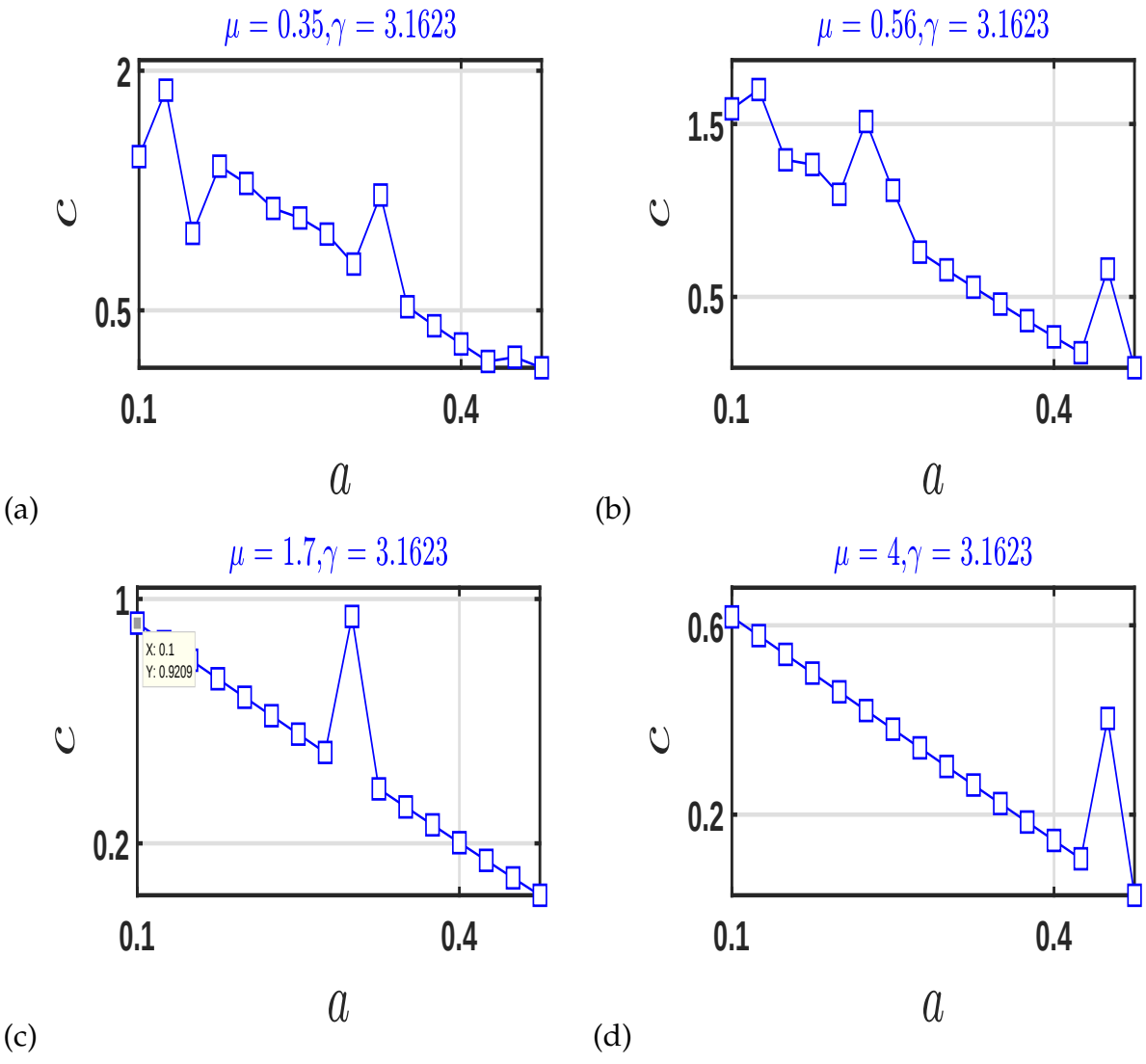

Figure 16: Front speeds for left and right moving particles for different regimes, with $0 \leq a \leq 0.5$. (a) $\mu = 0.35$, (b) $\mu = 0.56$, (c) $\mu = 1.7$, (d) $\mu = 4$

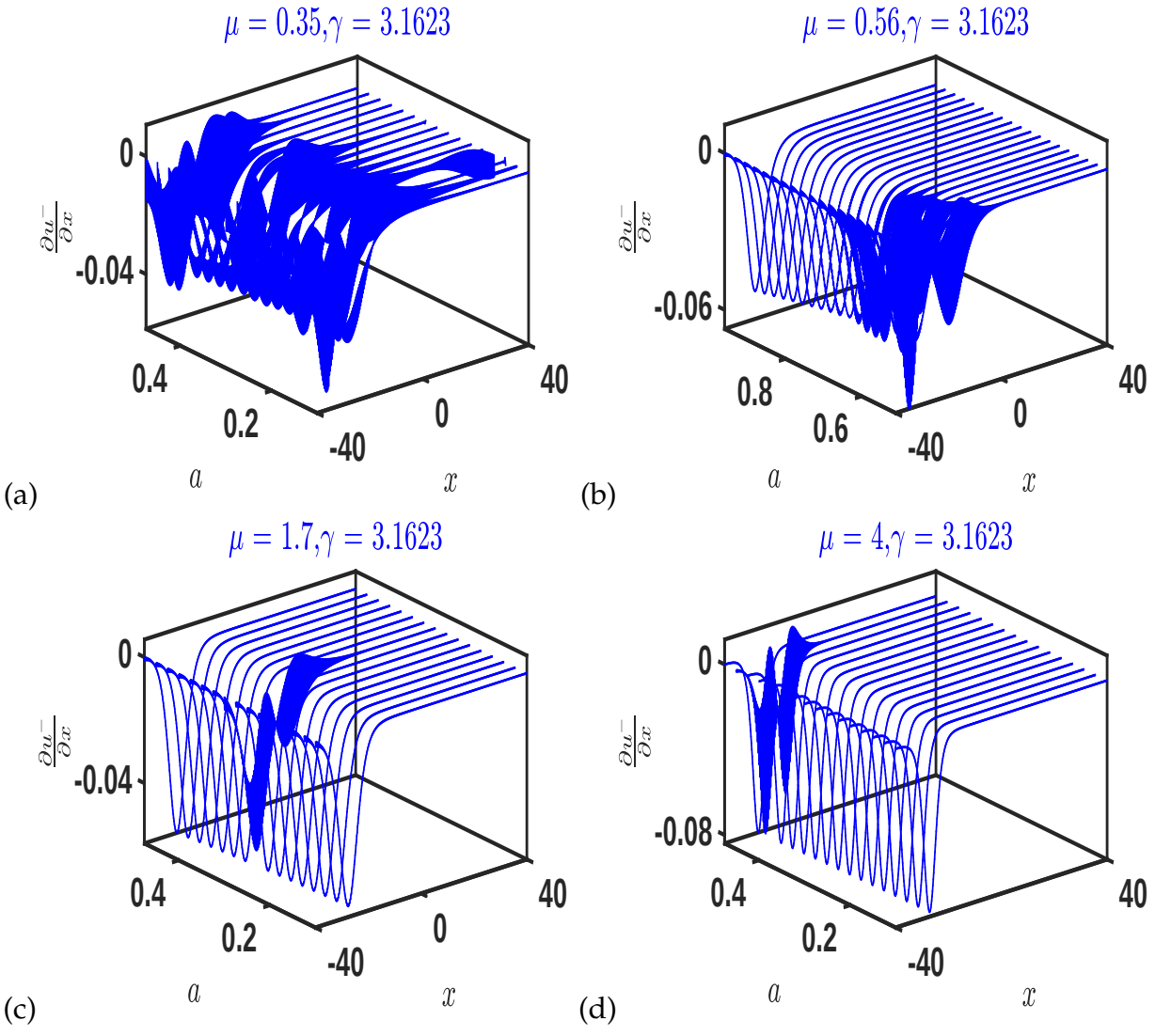

Figure 17: Instantaneous velocity of left moving particles a in differents regimes, with $0 \leq a \leq 0.5$. (a) $\mu = 0.35$, (b) $\mu = 0.56$, (c) $\mu = 1.7$, (d) $\mu = 4$

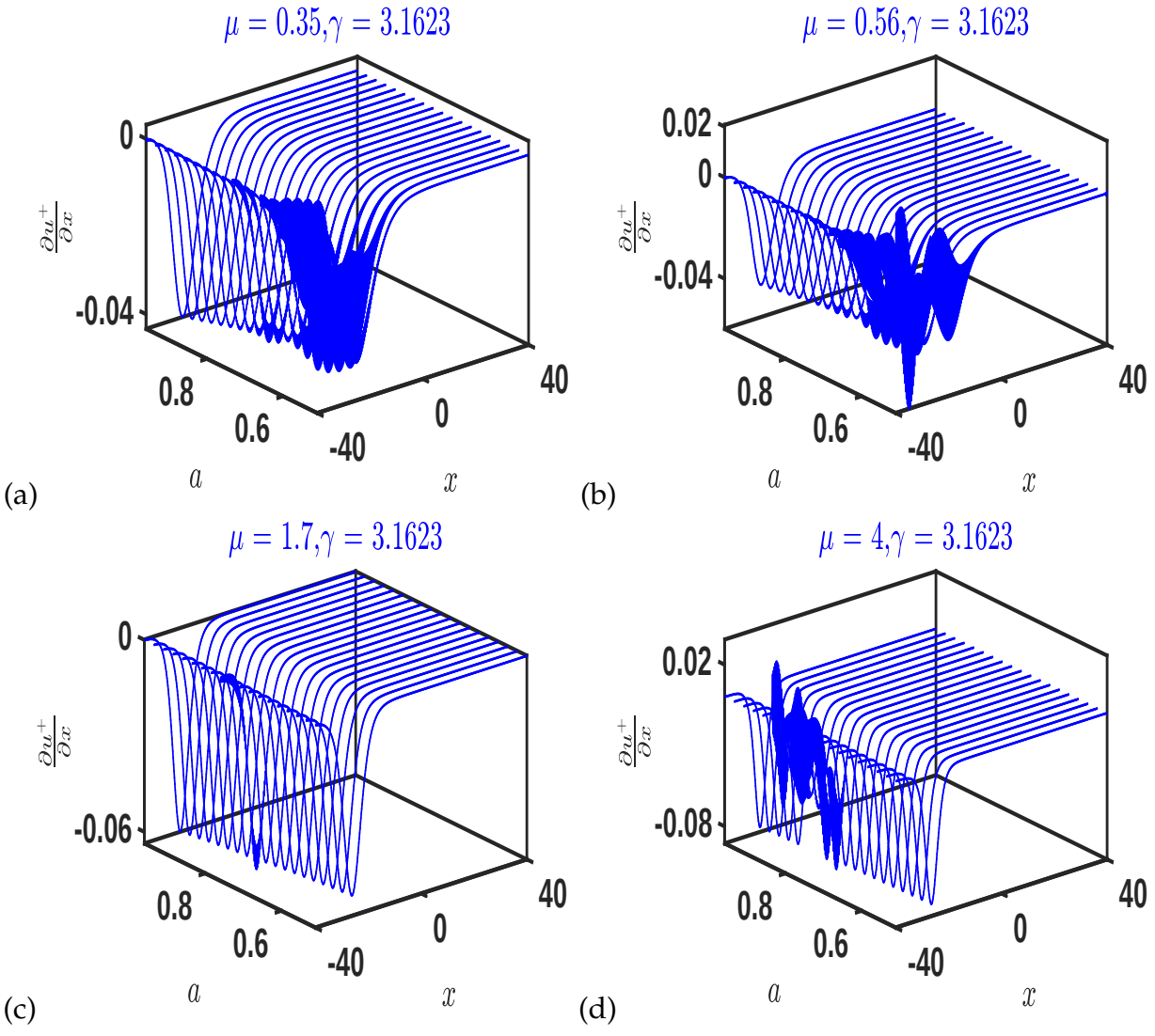

Figure 18: Instantaneous velocity of right moving particles a in differents regimes, with $0 \leq a \leq 0.5$. (a) $\mu = 0.35$, (b) $\mu = 0.56$, (c) $\mu = 1.7$, (d) $\mu = 4$

the proximity with the ballistic mode, one observes a kind of transition, because the fronts seem more unstable (see Fig. 13-b). As one moves away in the diffusive regime, these instabilities move towards the large values of a as illustrated by Figs. 14 and 15,respectively. It would nevertheless be judicious to notice that the particles moving towards the right converge faster than those moving to the left. These results are corroborated by the plot of the instantaneous speeds (see Figs. 17, 18 and 16)

ii- Propagating front into a unstable state

Within the propagation into the unstable state, Eq. (84) becomes

$$\frac{\partial u_0^+}{\partial t} + \gamma\frac{\partial u_0^+}{\partial r} = \mu(u_0^- - u_0^+) + \frac{1}{2}(8\varepsilon C(0){u_0}^3 + (1 + a - 12\varepsilon C(0)){u_0}^2 + 4\varepsilon C(0)u_0) - d(u_0)u_0^+,$$

$$\frac{\partial u_0^-}{\partial t} - \gamma\frac{\partial u_0^-}{\partial r} = \mu(u_0^+ - u_0^-) + \frac{1}{2}(8\varepsilon C(0){u_0}^3 + (1 + a - 12\varepsilon C(0)){u_0}^2 + 4\varepsilon C(0)u_0) - d(u_0)u_0^-, \quad (168)$$

whith $d^{'}(u_0) = d(u_0)$.

It is then clear that in the presence of noise, nonlinearity increases both in the front propagating in the unstable and metastable states, respectively. Indeed, it has become fashionable to emphasis the importance of nonlinearity in ecological model, as well as in population dynamics, and there are situations notably those involving competitions in fluctuating environments, where fundamentally nonlinear phenomena are critical to critical ecological understanding. Moreover, it has been found that insect population trends were highly nonlinear (74%), followed by mamals (58%), bony fish and birds (35%). Faster reproducing animals are more likely to have nonlinear and high-dimensional dynamics [166]. Recently, it has been shown that elevated nonlinearity could be used as an additional indicator to infer changes in the dynamics of populations under stress.

In the fully nonlinear situation, the analysis of the front velocity could not be performed. However, a piecewise linearization of Eq. (32) can be made. As in Refs.

[162, 78], we take the reaction function (126):

$$f(U) = \begin{cases} -U & U < \frac{a}{2}, \\ U - a & \frac{a}{2} \leq U \leq \frac{a+1}{2}, \\ 1 - U & \frac{a+1}{2} < U. \end{cases} \tag{169}$$

Whith this reaction term, the evolution Eq.(32) in the traveling wave ansatz then reduces

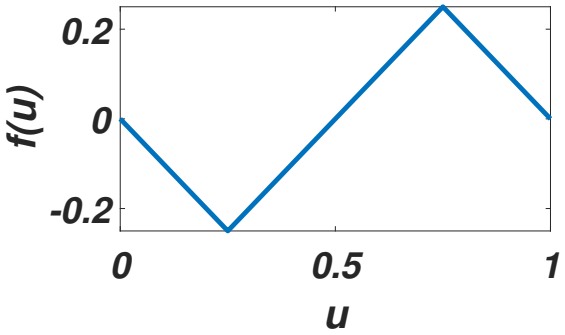

Figure 19: Piecewise linearization of the reaction term.

our nonlinear problem to a set of three regions. Each region can be reduced to a classical two−state Markovian model for the density of cells moving right, U^+, and the density of cells moving left, U^-.

The first region corresponds to a region where $U^{\pm} < z_1$, with $z_1 = \frac{a}{2}$. Within this region, death rate is constant, and there is no birth, then, extinction should be the final outcome. The density should go to zero for large times; this is referred to as the pure death process. Phase plane analysis of this region shows that in the ballistic regime ($\mu << 1$), the nullcline is a zero slope line; whereas, in the diffusive regime ($\mu > 1$), it divides the plane into two regions, the first region being the region where the vector field is going to the left and the second one, corresponding to the right motion of the vector field, for $c < \gamma$. For $c > \gamma$, the vector field points toward the nullcline. The resulting equations read

$$U^{+'} = \frac{1}{\gamma - c}[\mu(U^- - U^+) - \frac{1}{2}U^+], \quad \gamma \neq c,$$

$$0 = \mu(U^- - U^+) - \frac{1}{2}U^+, \quad \gamma = c, \tag{170}$$

$$U^{-'} = -\frac{1}{\gamma + c}[\mu(U^+ - U^-) - \frac{1}{2}U^-].$$

The second region is delimited by $z_1 \leq U^{\pm} \leq z_2$, with $z_2 = \frac{a+1}{2}$. Within this region, only birth process takes place. Phase plane analysis of this region shows that in the ballistic regime, for $c > \gamma$, the vector field is going to the left, the nullcline is a zero slope line. For $c < \gamma$, the vector field is going to the right. In the diffusive regime($\mu >> 1$), the traveling wave corresponds to a non$-$negative heteroclinic orbit connecting the point z_1 to the point z_2. For $c < \gamma$, the vector field points away from the nullcline, and a stable heteroclinic orbit does not exist. For $c > \gamma$, the vector field points towards the nullcline. The resulting equations are

$$U^{+'} = \frac{1}{\gamma - c}[\mu(U^- - U^+) + \frac{1}{2}(U^+ + U^- - a)], \quad \gamma \neq c,$$

$$0 = \mu(U^- - U^+) + \frac{1}{2}(U^+ + U^- - a), \quad \gamma = c, \tag{171}$$

$$U^{-'} = -\frac{1}{\gamma + c}[\mu(U^+ - U^-) + \frac{1}{2}(U^+ + U^- - a)].$$

The third region is the one where $U^{\pm} > z_2$. Within this region, both birth and death rates are constants, but the death rate is higher than the birth one. So, as in the first region, the final outcome should be extinction and the density should go to zero for large times. For $c < \gamma$, the nullcline separates the plane into two parts. The left part is caracterized by the fact that both reaction terms are negative, and the right one is caracterized by the fact that all the reaction terms are positive, for $c < \gamma$. For $c > \gamma$, the left part is caracterized by the fact that the first reaction term is positive, and the second one is null. In the second part, the field vector points towards nullcline, and all

the reaction terms are positive. The resulting equations are

$$U^{+'} = \frac{1}{\gamma - c}[\mu(U^- - U^+) + \frac{1}{2} - U^+], \quad \gamma \neq c,$$

$$0 = \mu(U^- - U^+) + \frac{1}{2} - U^+, \quad \gamma = c, \tag{172}$$

$$U^{-'} = -\frac{1}{\gamma + c}[\mu(U^+ - U^-) + \frac{1}{2} - U^-].$$

The dynamics of the whole system can be viewed as the movement of a particle in a potential which has one stable point, and the other one is unstable.

Now, as in the previous section, we assume that the control parameter a fluctuates locally around its mean value according to

$$a \to a(x,t) = a + \varepsilon^{\frac{1}{2}}\xi(x,t). \tag{173}$$

In this way, the noise is added to the reaction term in the second region, and the resulting equation has the general form

$$\begin{aligned} U^{+'} &= \frac{1}{\gamma - c}[\mu(U^- - U^+) - \frac{1}{2}U^+], \\ U^{-'} &= -\frac{1}{\gamma + c}[\mu(U^+ - U^-) - \frac{1}{2}U^-], \end{aligned} \tag{174}$$

$$\begin{aligned} U^{+'} &= \frac{1}{\gamma - c}[\mu(U^- - U^+) + \frac{1}{2}(U^+ + U^- - a)] - \frac{1}{2}\varepsilon^{\frac{1}{2}}\xi, \\ U^{-'} &= -\frac{1}{\gamma + c}[\mu(U^+ - U^-) + \frac{1}{2}(U^+ + U^- - a)] - \frac{1}{2}\varepsilon^{\frac{1}{2}}\xi, \end{aligned} \tag{175}$$

$$\begin{aligned} U^{+'} &= \frac{1}{\gamma - c}[\mu(U^- - U^+) + \frac{1}{2} - U^+], \\ U^{-'} &= -\frac{1}{\gamma + c}[\mu(U^+ - U^-) + \frac{1}{2} - U^-]. \end{aligned} \tag{176}$$

As discussed previously in the deterministic case, phase plane analysis revealed that the system has now two fixed points: one located at $z_{st} = z_1$, and the other at $z_{st} = z_2$.

Now, consider that the initial state of the system at $t = 0$ is $z = z_2$. Despite being

unstable because this is a fixed point, the system will remain at $z = z_2$, forever. In this situation, fluctuations play a critical role because, they will force the system to move out of the unstable fixed point and decay to the stable fixed point. As the decay is an event triggered by noise, the time is stochastic. Characterization of its statistical properties reveals that the left moving particles spread out quickly than the right moving one. This result shows that the left moving particle has less dissimilarities than the right moving one up to a certain time. After this time, left moving particles have more dissimilarities than the right moving ones (see Fig. 20).

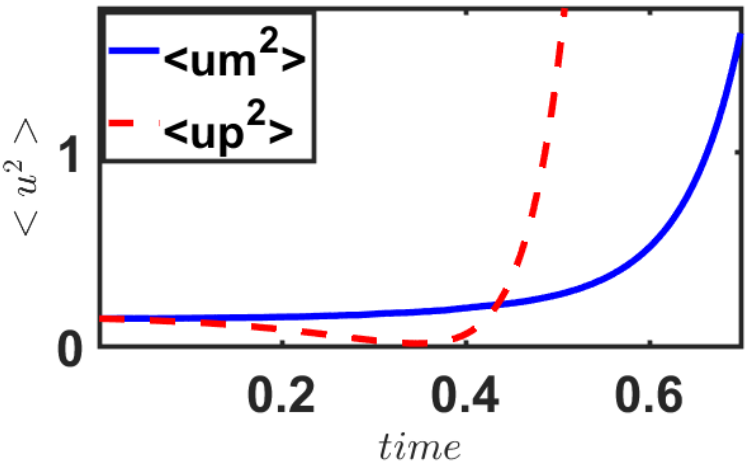

Figure 20: Variance of the stochastic time.

III.4 Effects of strong memory in the neuronal transport process in presence of toxicity

In this section, a numerical study on the formation of patterns with subdiffusion on a reaction-diffusion system (85) put forward by Zhang [150] is proposed. This system describes an ecosystem where prey produces a substance that is toxic to predators.

In Fig. 21, we depict the influence of the toxic substances on the parameter that constitute the anomalous exponent. It is clear that the slight variation of the efficiency of the toxicity modifies this parameter, yielding a modification of the anomalous exponent

itself. However, it would be premature to assert, based solely on Fig. 21, that this modification would systematically lead to a modification in the Turing instabilities. In order to decide on this, it would be necessary that one of the two relations (107), or (108) should be satisfied. If at least one of the two is verified, then the relationship between the degree of toxicity and the Turing instabilities will be clearly established, as depicted in Fig. 22 which displays clearly the efficiency of toxicity on the Turing instabilities. These results are a direct consequence of Hernandez's work [158] on subdiffusion, where the existence of Turing structures has been demonstrated. In this work, we will take a few cases to study the phenomenon of subdiffusion under the influence of toxicity.

We provide now some simulations as evidence of the analytical predictions derived in the previous sections.

$Example1$. Consider system (85) with the parameter values $r = 0.7$, $K = 2$, $s = 0.25$, $m = 1.5$, $h = 1$, $d_1 = 0.008$, $d_2 = 1$, $a = 0.1$ and $\beta = 0.1$. For this set of parameters, we first have to make sure that all the above mentioned conditions are met. This can trivially be done numerically by checking if Eq. (108) is fullfiled. Upon this, the Turing patterns obtained for this set of parameters are depicted in Fig. 23.

In this case, we observe that before taking into account the memory effect ($\eta = 1$), there are oscillations both in predators and in preys, which means that predators indiscriminately consume toxic preys. However, if the memory effect is triggered ($\eta < 1$), we observe that after a certain time, there is stabilization both in preys and predators. This stabilization can be explained in two ways. Either the predators have known how to recognize the less toxic preys, and therefore consume only those preys whose toxicity is reduced, or the predators completely abstain from ingesting the toxic preys. This behavior has been observed in European starlings which, when their body masses have been experimentally reduced become more willing to eat prey items that have been injected with quinine, which is toxic to birds in high doses [167, 168]. It is now clear that memory effects play a key role in ways in which naive predators learn to associate warningly preys with their defenses and remember to avoid them in future encounters. This field underpins an extensive body of evolutionary theory [169, 170, 171, 172, 173]. Moreover,

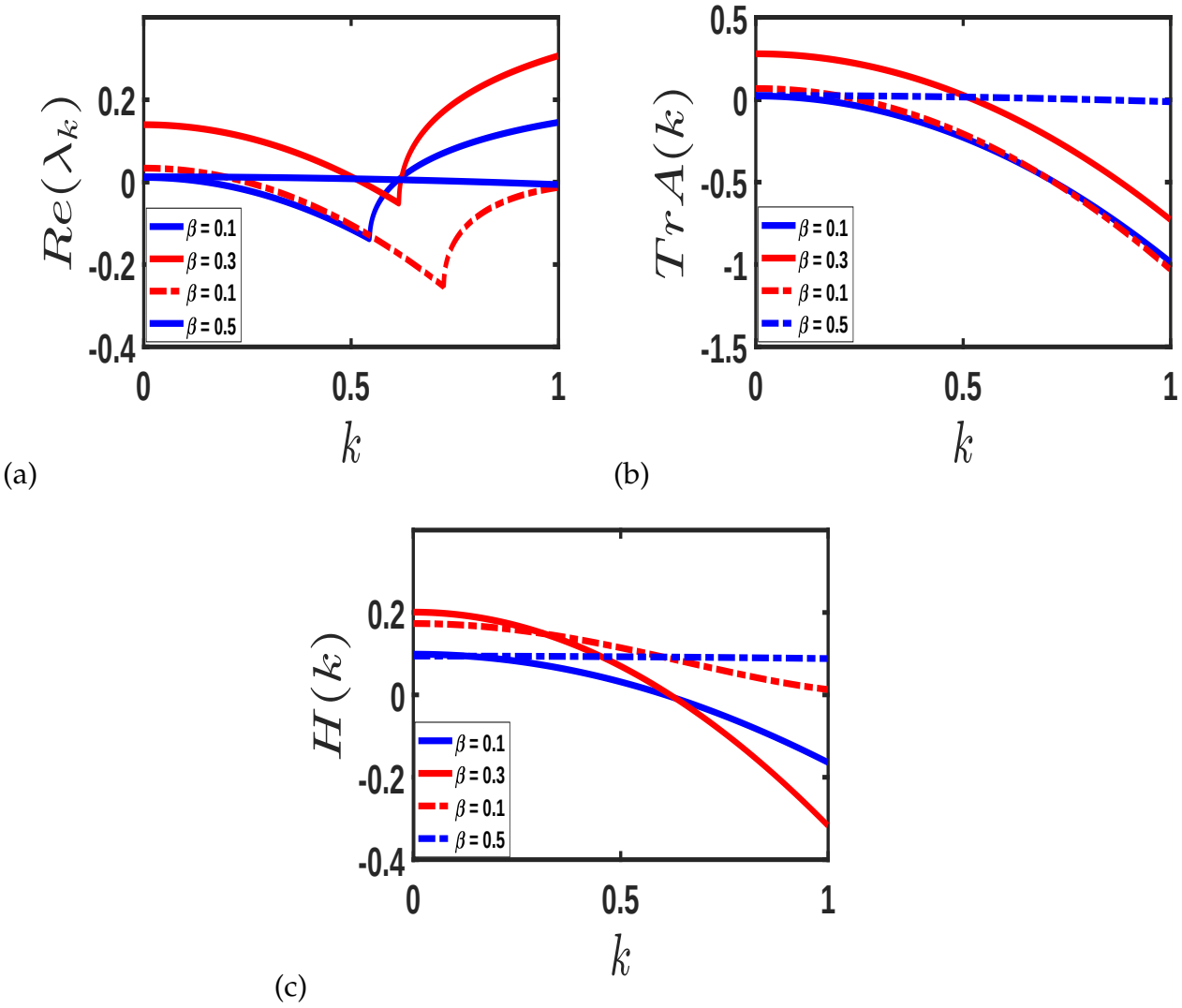

Figure 21: (a): Effect of toxicity on the real part of the eigenvalue. (b): Effect of toxicity on $TrA(k)$. (c): Effect of toxicity on $h(k)$. Efficiency of the toxic substances on system's variables. Simulations were performed with $K = 2$, $s = 0.25$ and $h = 1$, $m = 1.5$, $r = 0.7$. Continuous blue line corresponds to $a = 0.1$, $\beta = 0.1$; continuous red line corresponds to $a = 0.05$, $\beta = 0.3$ dashed blue line corresponds to $a = 0.1$, $\beta = 0.5$, $d_1 = 0.008$ and $d_2 = 0.3$ and dashed red line corresponds to $a = 0.05$, $\beta = 0.1$

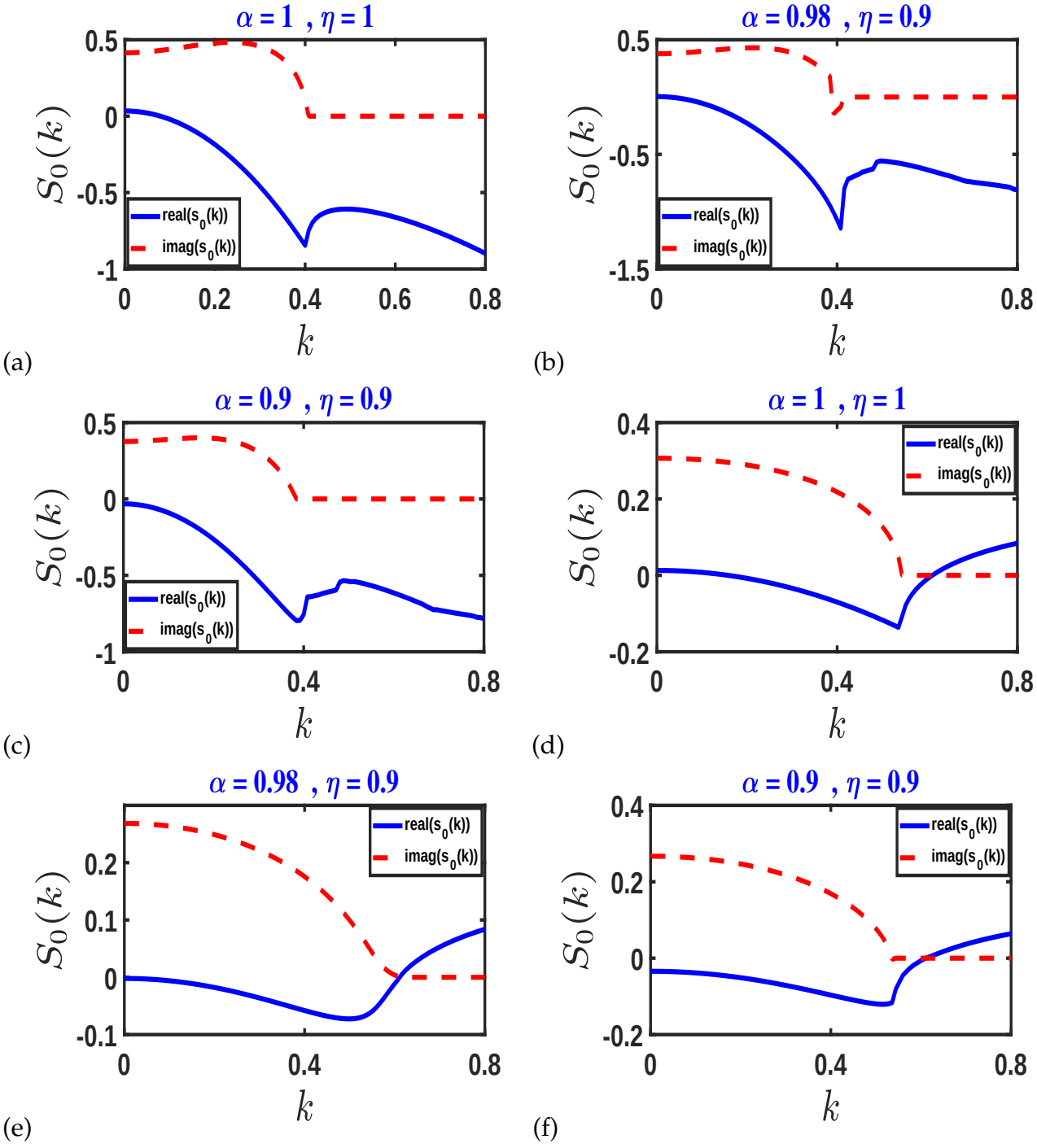

Figure 22: Conditions for the Turing instabilities mentioned in (108) for different value of the derivative order index. Simulations were performed with $K = 2$, $s = 0.25$ and $h = 1$, $m = 1.5$, $r = 0.7$, $d_1 = 0.008$. In (a), (b) and (c), $a = 0.05$, $\beta = 0.1$, with $u(x,0) = 0.4221 + 0.01cos(x)$ and $v(x,0) = 0.3654 + 0.01cos(x)$. While in (d), (e) and (f), $a = 0.1$, $\beta = 0.5$, $d_2 = 0.03$, with $u(x,0) = 0.0830 + 0.01cos(x)$, and $v(x,0) = 0.0818 + 0.01cos(x)$.

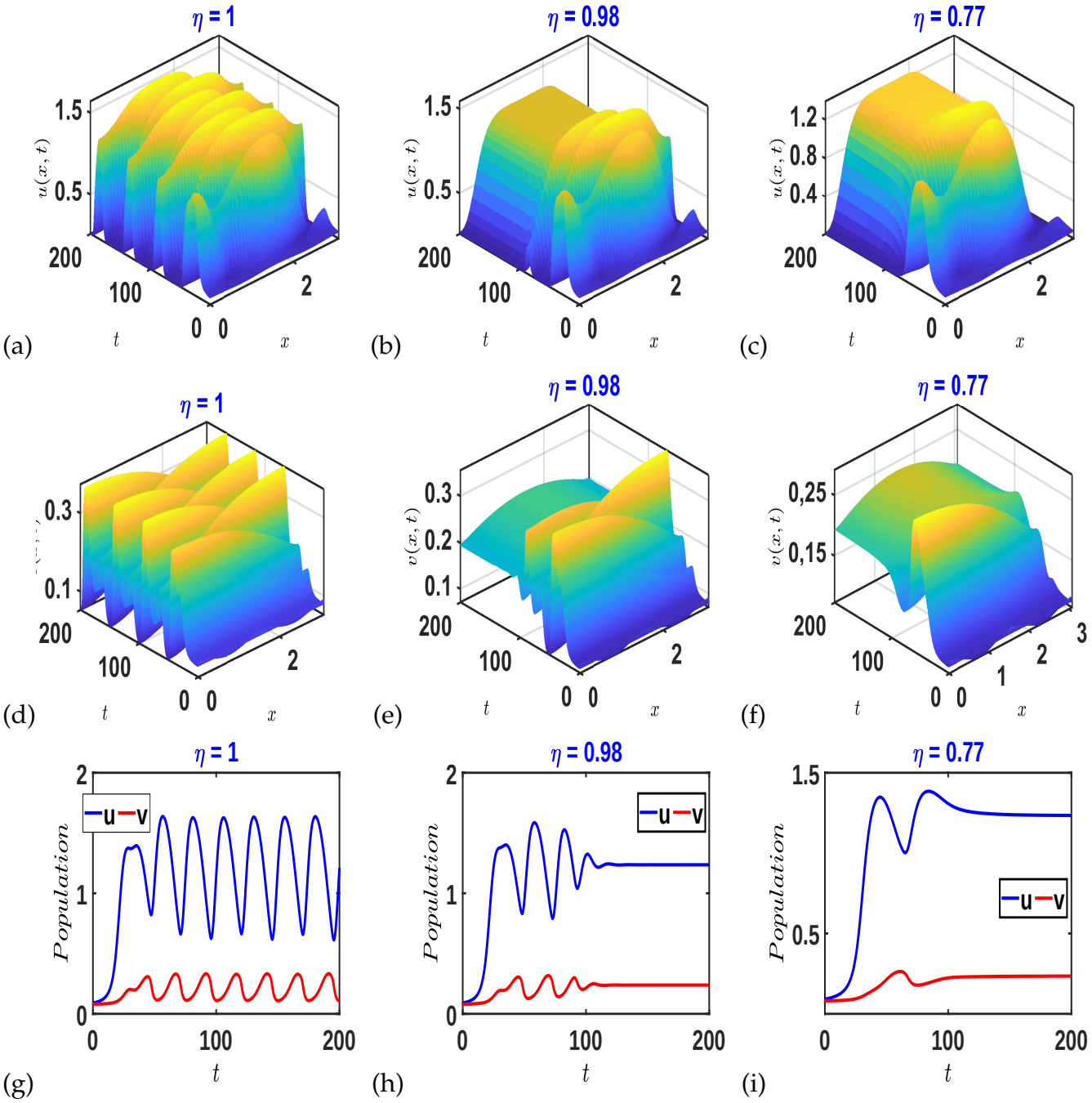

Figure 23: Efficiency of the toxic substances on prey's density. Simulations were performed with $K = 2$, $s = 0.25$ and $h = 1$, $m = 1.5$, $r = 0.7$. $a = 0.05$, $\beta = 0.1$, $d_1 = 0.008$, $d_2 = 1$. The initial values are $u(x,0) = 0.0814 + 0.01cos(4x)$, $v(x,0) = 0.0812 + 0.01cos(4x)$

it is obvious that memory effects regulate the effect of toxic substances on predators. In other word, predators are affected by toxic substances for a certain time, then, they become used to it, and the ecosystem becomes locally stable as shown in Figs. 23 (e)-(f) and (h)-(i).

$Example2$. Let $a = 0.05$, $d_1 = 0.1$, and the other parameters remain as in the first exemple. As previously, we make sure that condition (108) is satisfied. For this set of parameters, we have the structures of Fig. 24

Despite the toxicity of preys, the cohabitation between predator and prey takes place without any problems, even if the number of predators remains relatively low. However, when we take into account the memory effect, we realize that the number of preys decreases considerably, while that of predators remains relatively constant. By further reducing the fractional order of the derivative, we observe a complete stabilization of the two entities (predators and preys). Albeit the drastic fall in their respective population, no species will disappear due to the effect of fractional - order parameter or memory effect. This scenario is similar to the one described in Ref. [174] where predators deliberately choose to swallow toxic preys, choice which is a trade-off between the benefits of obtaining nutrients and the costs of ingesting toxins. This trade-off is affected by the fact that: animals will consume more toxic preys if they are food-deprived. Indeed, animals face constant decisions about what to eat and what not to eat. While some items are never worth eating, there are many cases where the decision to eat or not should depend on the environment and the individual's current state [175, 176, 177]. For example, many potential preys available to wild birds are chemically defended, and so contain toxins that will be harmful in the long term or if eaten in excess [178, 179]. However, such preys also contain valuable nutrients. In such cases, having lower energy reserves or poorer foraging prospects shifts the balance of costs and benefits in favour of consumption [177].

$Example3$. Once more, we consider system (85) with the parameter values $\beta = 0.3$, $a = 0.05$, the others ramain unchanged. In this case also, the validity of Eq. (108) is checked. The resulting structures are shown in Fig. 25. This case presents some sim-

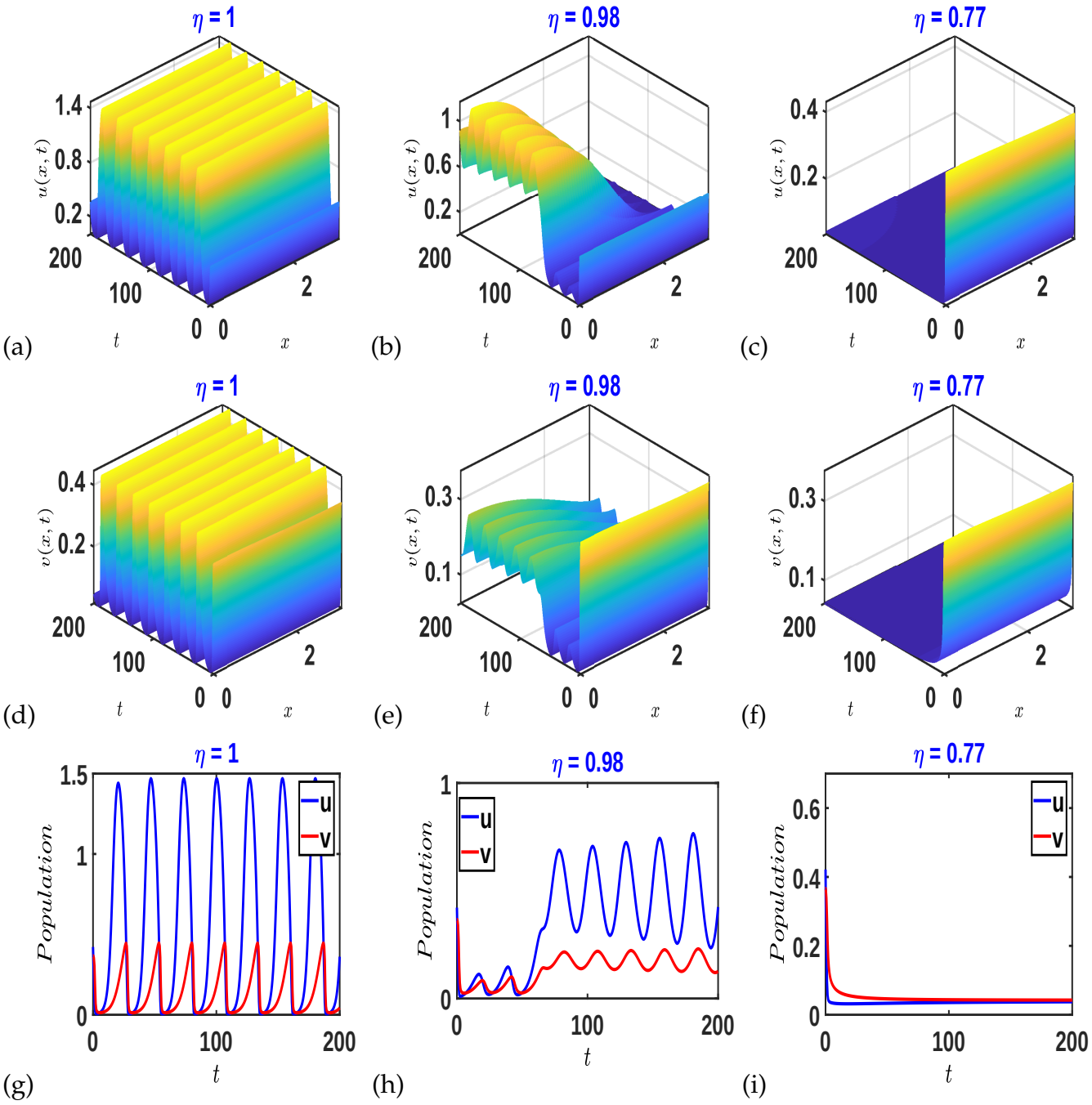

Figure 24: Efficiency of the toxic substances on prey's density. Simulations were performed with $K = 2$, $s = 0.25$ and $h = 1$, $m = 1.5$, $r = 0.7$. $a = 0.05$, $\beta = 0.1$, $d_1 = 0.008$, $d_2 = 1$, with the initial values being $u(x,0) = 0.4221 + 0.01cos(x)$, $v(x,0) = 0.3654 + 0.01cos(x)$

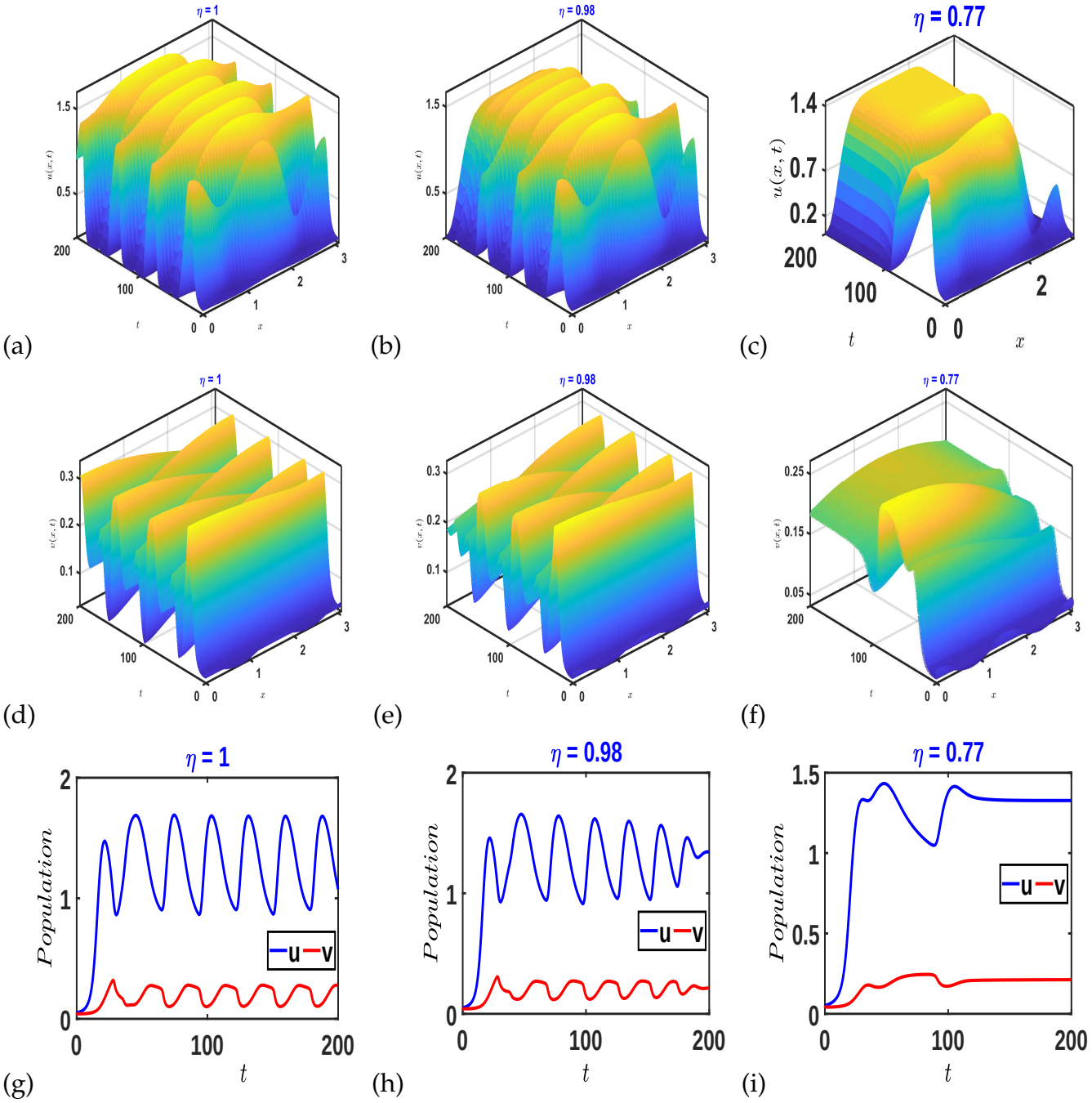

Figure 25: Efficiency of the toxic substances on prey's density. Simulations were performed with $K = 2$, $s = 0.25$ and $h = 1$, $m = 1.5$, $r = 0.7$. $a = 0.05$, $\beta = 0.3$, $d_1 = 0.08$, $d_2 = 1$, and $u(x, 0) = 0.0422 + 0.01cos(4x)$, $v(x, 0) = 0.0421 + 0.01cos(4x)$

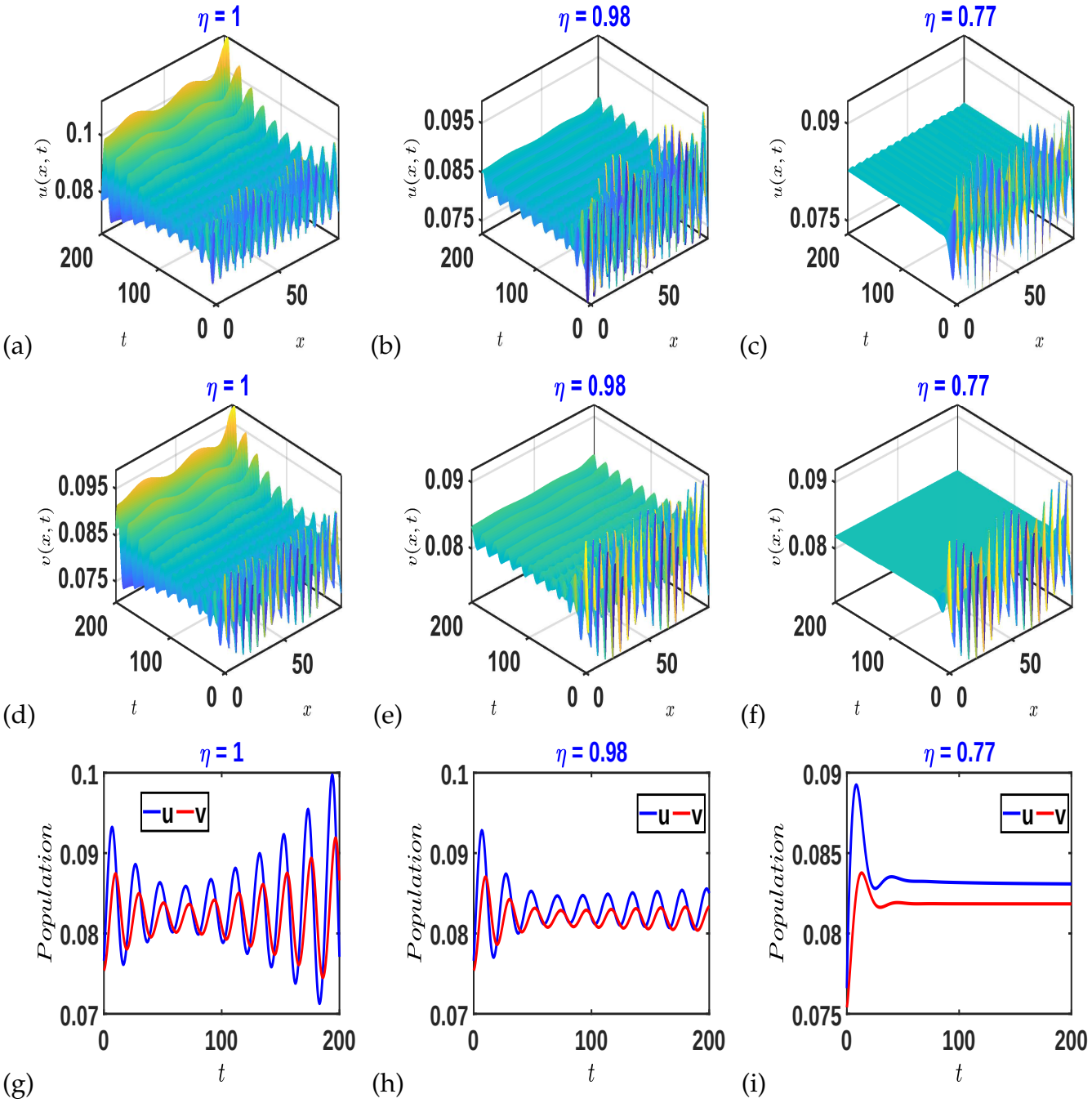

Figure 26: Efficiency of the toxic substances on prey's density. Simulations were performed with $K = 2$, $s = 0.25$ and $h = 1$, $m = 1.5$, $r = 0.7$. $a = 0.1$, $\beta = 0.5$, $d_2 = 0.03$, $d_1 = 0.1$, $u(x,0) = 0.0830 + 0.01cos(x)$, $v(x,0) = 0.0818 + 0.01cos(x)$

ilarities with the one depicted in $example\ 2$. The preys are not really affected by the predators, which is similar to the case discussed in Ref. [180] Here, the first conspicuous mutants would have to survive greater levels of predation than previously thought, because even when the learning process is complete, educated predators may still be prepared to eat aposematic prey. There may be another reason for this phenomenon. Indeed, a predator's ability to moderate and process toxins would be a key factor in limiting attack rates on chemically defended preys, and one that could have significant implications for the survival advantage of being aposematic [180].

$Example4$. The set of parameters used here is almost the same as in the previous cases, except for $a = 0.1$, $\beta = 0.5$, $d_1 = 0.1$ and $d_2 = 0.03$. For these parameter values, condition (108) is also met. The resulting structures of Fig. 26. reveal that predators and prey may be simultaneously exposed to toxins. Since the natural dispersive force of the movement of each species is weak ($\frac{d_2}{d_1} < 1$), we can conclude that this configuration corresponds to environmental toxins exposure. Indeed, if toxin came from either preys or predators, it could not be affected as much. This means that toxin comes from the environment. The impact of environmental toxins on predator-prey dynamics has recently been investigated [181]. Since mobility is reduced, we are in a situation of confinement in a toxic environment. The direct effects of toxins typically reduce organism abundance by increasing mortality or reducing fecundity. Such direct effects, therefore, alter both bottom-up food availability and top-down predatory ability. However, the indirect effects, when mediated through predator-prey interactions, may lead to counterintuitive effects. Environmental toxins also reduce population variability by preventing populations from fluctuating around a coexistence equilibrium [181] as depicted in Figs. 26 (f) and (i).

III.5 Conclusion

In this chapter, we have numerically presented the results obtained from the analytical predictions made in the previous chapter. First, we have presented the effect of

transport memory and its importance in certain phenomena observed on biological systems. Then, starting from the generalization of the Brownian movement better known under the name of reaction random walk, we studied the importance of the fluctuations in the movements of genetic population. We realized that these increase nonlinearity in the environment. Finally, the effect of toxins under the influence of memory was presented by taking a few cases. We realized that memory plays a major role in the phenomena observed in ecology. Indeed, memory can stabilize structures just as it can create new ones.

General Conclusion and Perspectives

Main results

The aim of this thesis was the understanding of the importance of memory in biological systems linked to the transport of nerve impulses and to test their stability under the influence of certain factors frequently encountered in the process of said transport such as toxicity and fluctuations. To this end, the work was divided into three. First of all, it has been shown that the transport memory exists in biological phenomena like chromatin. Then, starting from a generalization of the Brownian motion, we studied the effects of fluctuations on the dynamics of genetic populations. Finally, we examined the effect of toxicity on the dynamics of genetic populations, taking into account the strong memory effects. From these analyzes, it follows that:

♣ The effects of transport memory of the wave fronts in the bistable reaction-diffusion which arises in biological system were analyzed considering two hypotheses. Firstly, we assumed that these systems can be modeled as a chain of particles of identical masses, each one of them interacting with its two nearest neighbors through harmonic coupling, and secondly, we have considered that these systems can lead to a bistable regime. A model was proposed and nonlinear analysis was carried out. From this analysis, traveling front solution were obtained, connecting the hyperbolic points located at the two maxima of the potential, at $U = 0$ and $U = 1$, representing the invasion of one of the states by the other. We found that memory effects play an important role. When moving from the state $U = 0$ to the state $U = 1$, memory effects accelerate the speed of the traveling wave (see Fig. 6 (a)), and when moving from the state $U = 1$ to the state $U = 0$, memory effects play the role of a damping (see Fig. 6 (b)). The piecewise linear approx-

imation was carried out, and results gotten agreed with the behavior of the chromatin since it can be seen as clustered oscillators. The first oscillator behaving as a resistor, thus protecting against high wave-speeds. The other oscillators working together and which can be classified into three regions. The first one is where the mechanical coupling is located. This mechanical coupling is there to impose coherent motion to the system, the problem is that this mechanical coupling prevents segregation (in the case of chromatin). Hence, the memory effects transported by the wave fronts in the bistable reaction-diffusion play a key role as it help break down this mechanical coupling for segregation to take place. The second region corresponds to a transition zone between the wave-like behavior and the diffusive behavior. In the third region, another cycle is yet to start.

♣ With regard to fluctuations, they clearly appear to be the main source of nonlinearity in the environment. Indeed, our analytical approach clearly shows that in the presence of fluctuations, nonlinearity increases in the system. This nonlinearity can, when high, be used as an additional factor inducing changes in the dynamics of stressed biological populations. In addition, the strong nonlinearity induces chaos which can be described as "biological chaos". The importance of this biological chaos is that the variables which govern the spatial and temporal geometries of the system are reduced in a number of fractional dimension, thus allowing a control of low energy with complex deterministic consequences. The complexity of control inherent in chaotic systems is very important for the dynamics of gene expression and translation.

♣ With regard to toxins, depending on the parameters, the memory can stabilize any so-called Turing instabilities, or else generate new instabilities, creating new patterns. In this work, we considered four examples, and each time we varied the parameters, which allowed us to switch from one system configuration to another. The results obtained were in perfect agreement with the experiments carried out in ecology. This suggests that many of the phenomena that govern ecology have memories.

Perspectives

♣ Studying the effects of memory on the dynamics of genetic populations in the presence of fluctuations, according to the generalist approach of Brownian motion, is one of our future projects, because it would allow us to better understand the effects of memory in an environment close to the neuron.

♣ Study the effect of superdiffusion associated with memory according to the so-called random walk reaction approach, because superdiffusion is just as present in many transport processes occurring at the neuron level

♣ Deepen the study on a 3D model of chromatin in order to better understand the effects of transport memory

♣ Cooperative and non cooperative studies of the memory effects and fractional Brownian motion on the dynamics of genetic populations

♣ Considering bifurcations and dynamics of a predator-prey model with double-Allee effects and time delay

Bibliography

[1] J. S. Nevid Essentials of Psychology: Concepts and Applications, (Cengage Learning, Boston, 2017).

[2] S. Alters Biology: Understanding life, (Jones and Bartlett, Ontario, 1999).

[3] M. Bertuzzi, W. Chang, K. Ampatzis, "*Adult spinal motoneurons change their neurotransmitter phenotype to control locomotion*", Proc Natl Acad Sci USA (2018), https: 10.1073/pnas.1809050115.

[4] K. F. Faull, Desiderio D.M. (eds) Mass Spectrometry. Modern Analytical Chemistry, (Springer, Boston, 1992).

[5] M. F. Bear, B. W. Connors, M. A. Paradiso, Neuroscience Exploring the Brain, (Lippincott Williams & Wilkins, Philadelphia, 2006).

[6] U. HOMBERG, "*Neurotransmitters and Neuropeptides in the Brain of the Locust*", Microscopy Research and Technique, (2002).

[7] K. E. Andersson, "*Neurotransmitters: central and peripheral mechanisms*", International Journal of Impotence Research, (2000).

[8] C. Carlson, L. Harms, E. Enghofer, K. H. Kim, C. Kannemeier, S. DeLaura, T. Burke, B. Anson, A. Thompson, E. Jones, K. P. Mangan, "*Endogenously Bursting, Synchronous iPSCderived Neural Cultures Display a Seizurogenic Response to Excitatory Pharmacology*", Cellular Dynamics, (2018).

[9] R. J. Hagerman, P. J. Hagerman. "*The fragile X premutation: into the phenotypic fold*", Curr Opin Genet Dev, (2002), https: doi:10.1016/s0959-437x(02)00299-x.

[10] D. G. Gibson, L. Young, R. Y. Chuang, J. C. Venter, C. A. Hutchison 3rd, H. O. Smith, "*Enzymatic assembly of DNA molecules up to several hundred kilobases*", Nat Methods, (2009), https: doi:10.1038/nmeth.1318.

[11] Y. E. Zhang, M. D. Vibranovski, B. H. Krinsky, M. Long, "*A cautionary note for retrocopy identification: DNA-based duplication of introncontaining genes significantly contributes to the origination of single exon genes*", Bioinformatics, (1998).

[12] K. Tabuchi, J. Blundell, M. R. Etherton, et al., "*A neuroligin-3 mutation implicated in autism increases inhibitory synaptic transmission in mice*", Science, (2007), https: doi:10.1126/science.1146221.

[13] V. S. Dani, Q. Chang, A. Maffei, G. G. Turrigiano, R. Jaenisch, S. B. Nelson, "*Reduced cortical activity due to a shift in the balance between excitation and inhibition in a mouse model of Rett syndrome*", Proc Natl Acad Sci USA, (2005), https: doi:10.1073/pnas.0506071102.

[14] L. Yong, X. Yong, "*Dynamical characteristics of the fractional-order FitzHugh-Nagumo model neuron and its synchronization*", Acta Phys Sin, (2010).

[15] Z. Guang-jun, X. Jian-xue, "*Stochastic resonance induced by novel random transitions of motion of FitzHugh-Nagumo neuron model*", Chaos Solitons Fractals, (2005).

[16] M. Perc, "*Spatial coherence resonance in excitable media*", Phys. Rev. E 72, 016207 (2005)..

[17] M. Perc, M. Marhl, "*Amplification of information transfer in excitable systems that reside in a steady state near a bifurcation point to complex oscillatory behavior*", Phys Rev E 71, 026229 (2005).

[18] Z. Q. Yang, Q. S. Lu, L. Li, "*The genesis of period-adding bursting without bursting-chaos in the chay mode*", Chaos Soliton Fractals 27, 689 (2006).

[19] X. Sun, J. Lei, M. Perc, J. Kurths, G. Chen, "*Burst synchronization transitions in a neuronal network of subnetworks*", Chaos 21, 016110 (2011).

[20] M. Perc, M. Marhl, "*Noise-induced spatial dynamics in the presence of memory loss*", Phys A 375, (2007).

[21] Q. Wang, G. Chen, M. Perc, "*Synchronous bursts on scale-free neuronal networks with attractive and repulsive coupling*", Chaos 26, 033107 (2016).

[22] Y. Yamada, Y. Kashimori, "*Neural mechanism of dynamic responses of neurons in inferior temporal cortex in face perception*", Cogn Neurodyn 7(1), 23 (2013).

[23] B. N. Lundstrom, M. H. Higgs, W. J. Spain, A. L. Fairhall, "*Fractional differentiation by neocortical pyramidal neurons*", Nat Neurosci 1(11), 1335 (2008).

[24] T. J. Anastasio, "*The fractional-order dynamics of brainstem vestibulo-oculomotor neurons*", Biol. Cybern. 72, 69 (1994).

[25] R. Scherer, S. L. Kalla, Y. Tang, J. Huang, "*The Grunwald-Letnikov method for fractional differential equations*", Comput. Math. Appl. 62, 902 (2011).

[26] I. Podlubny, Fractional Differential Equations: An Introduction to Fractional Derivatives, Fractional Differential Equations, to Methods of Their Solution and Some of Their Applications, (Academic Press, Cambridge, 1998).

[27] V. M. Kenkre, P. Reineker, Exciton Dynamics in Molecular Crystals and Aggregates, (Springer, Berlin, 1982); V. M. Kenkre, Proceedings of the NATO Advance Study Institute on Energy Transfer, (Plenum, New York, 1984).

[28] K. K. Manne, A. J. Hurd, V. M. Kenkre, "*Nonlinear waves in reaction-diffusion systems: The effect of transport memory*", Phys. Rev. E 61, 4177 (2000).

[29] G. Abramson, A. R. Bishop, V. M. Kenkre, "*Effects of transport memory and nonlinear damping in a generalized Fisher's equation*",Phys. Rev. E 64, 066615 (2001).

[30] K. B. Oldham, J. Spanier, The Fractional Calculus, 17, (Academic Press, New York 1974).

[31] K. S. Miller, B. Ross, An Introduction to the Fractional Calculus and Fractional Differential Equations, (Wiley, New York 1993).

[32] M. Caputo, "*Linear models of dissipation whose Q is almost frequency independent II*", Geophys. J. Int. 13, 529 (1967).

[33] R. L. Magin, "*Fractional calculus in bioengineering Part* 1", Crit. Rev. Biomed. Eng. 32, (2004)

[34] R. L. Magin, M. Ovadia, "*Modeling the cardiac tissue electrode interface using fractional calculus*", J. Vib. Control 14, 1431 (2008).

[35] R. L. Magin, Fractional calculus models of complex dynamics in biological tissues, Comput. Math. Appl. 59, 1586 (2010).

[36] A. Dokoumetzidis, P. Macheras, "*Fractional kinetics in drug absorption and disposition processes*", J. Pharmacokinet. Pharmacodyn. 36, 165 (2009).

[37] I. Petr, R. L. Magin, "*Simulation of drug uptake in a two compartmental fractional model for a biological system*", Commun. Nonlinear Sci. Numer. Simul. 16, 4588 (2011).

[38] I. Goychuk, P. Hanggi, "*Fractional diffusion modeling of ion channel gating*", Phys. Rev. E 70, 051915 (2004).

[39] D. Sierociuk, T. Skovranek, M. Macias, I. Podlubny, I. Petras, A. Dzielinski, "*Diffusion process modeling by using fractional-order models*", Appl. Math. Comput. 257, 2 (2015).

[40] M. Armanyos, A. Radwan, "*Fractional-order FitzhughNagumo and Izhikevich neuron models*", In: 13th International Conference on Electrical Engineering/Electronics, Computer, Telecommunications and Information Technology (ECTI-CON), IEEE (2016).

[41] W. Teka, T. M. Marinov, F. Santamaria, "*Neuronal spike timing adaptation described-with afractional leaky integrateand-fire-model*", PLoS Comput. Biol. 10(3), e1003526 (2014).

[42] R. K. Upadhyay, A. Mondal, W. Teka, "*Fractional order excitable neural system with bidirectional coupling*", Nonlinear Dyn. 87, 2219 (2017).

[43] E. Kaslik, S. Sivasundaram, "*Nonlinear dynamics and chaos in fractional-order neural networks*", Neural Netw. 32, 245 (2012).

[44] L. Chen, J. Qu, Y. Chai, R. Wu, G. Qi, "*Synchronization of a class of fractional-order chaotic neural networks*", Entropy 15(8), 3265 (2013).

[45] H. Safdari, M. Z. Kamali, A. Shirazi, M. Khalighi, G. Jafari, M. Ausloos, "*Fractional dynamics of network growth constrained by aging node interactions*", PLoS ONE 11(5), e0154983 (2016).

[46] M. Shi, Z. Wang, "*Abundant bursting patterns of a fractional-order Morris-Lecar neuron model*", Commun. Nonlinear Sci. Numer. Simul. 19, 1956 (2014).

[47] R. K. Upadhyay, A. Mondal, "*Dynamics of fractional-order modified Morris-Lecar neural model*", Netw. Biol. 5(3), 113 (2015).

[48] S. H. Weinberg, "*Membrane capacitive memory alters spiking in neurons described by the fractional-order Hodgkin-Huxley model*", PLoS ONE 10, e0126629 (2015).

[49] P. J. Drew, L. F. Abbott, "*Models and properties of power-law adaptation in neural systems*", J. Neurophysiol. 96, 826 (2006).

[50] T. J. Anastasio, "*Nonuniformity in the linear network model of the oculomotor integrator produces approximately fractional-order dynamics and more realistic neuron behavior*", Biol. Cybern. 79, 377 (1998).

[51] M. G. Paulin, L. F. Hoffman, C. Assad, "*Vibrational resonance in excitable neuronal systems*", Chaos 21, 043101 (2011).

[52] A. L. Fairhall, G. D. Lewen, W. Bialek, R. de Ruyter van Steveninck, Multiple timescales of adaptation in a neural code. In: Leen, T.K., Dietterich, T.G., Tresp, V. (eds.) Advances in Neural Information Processing Systems 13, (MIT Press, Cambridge, 2001).

[53] C. I. Moore, R. Cao, "*The Hemo-Neural Hypothesis: On The Role of Blood Flow in Information Processing*", J Neurophysiol 99, 2035 (2008).

[54] T. M. Fischer, "*Shape Memory of Human Red Blood Cells*", Biophysical Journal 86, 3304 (2004).

[55] R. A. Taylor, A. White and J. A. Sherratt, "*How do variations in seasonality affect population cycles?*", Proceedings. Biological Sciences 280, 20122714, (2013).

[56] G. M. Church, Y. Gao, S. Kosuri, "*Next-generation digital information storage in DNA*", Science 337, 1628 (2012).

[57] Goldman, N. et al., "*Towards practical, high-capacity, low-maintenance information storage in synthesized DNA*", Nature 494, 77 (2013).

[58] Y. Erlich, D. Zielinski, "*DNA Fountain enables a robust and efficient storage architecture*", Science 355, 950 (2017).

[59] R. N. Grass, R. Heckel, M. Puddu, D. Paunescu, W. J. Stark, "*Robust chemical preservation of digital information on DNA in silica with error-correcting codes*", Angew. Chem. Int. Ed. 54, 2552 (2015).

[60] M. W. van der Woude, A. J. Baumler, "*Phase and antigenic variation in bacteria*", Clin. Microbiol. Rev. 17, 581 (2004).

[61] L. A. Marraffini, "*CRISPR-Cas immunity in prokaryotes*", Nature 526, 55 (2015).

[62] D. Nemazee, "*Receptor editing in lymphocyte development and central tolerance*", Nat. Rev. Immunol. 6, 728 (2006).

[63] B. Medhekar, J. F. Miller, "*Diversity-generating retroelements*", Curr. Opin. Microbiol. 10, 388 (2007).

[64] R. Haselkorn, "*Developmentally regulated gene rearrangements in prokaryotes*", Annu. Rev. Genet. 26, 113 (1992).

[65] M. Nowacki, K. Shetty, L. F. Landweber, "*RNA-mediated epigenetic programming of genome rearrangements*", Annu. Rev. Genomics Hum. Genet. 12, 367 (2011).

[66] J. Shendure, et al, "*DNA sequencing at 40: past, present and future*", Nature 550, 345 (2017).

[67] S. Kosuri, G. M. Church, "*Large-scale de novo DNA synthesis: technologies and applications*", Nat. Methods 11, 499 (2014).

[68] M. Takinoue, A. Suyama, "*Hairpin-DNA memory Using Molecular Addressing*", Small 2, 1244 2006, doi: 10.1002/smll.200600237.

[69] Y. Huimei, et al., "*Tet3 regulates synaptic transmission and homeostatic plasticity via DNA oxidation and repair*", Nature Neuroscience, (2015), https: www.DOI:10.1038/nn.4008.

[70] F. Crick, "*Memory and molecular turnover*", Nature 312, 101 (1984).

[71] J. Gräff, D. Kim, M. M. Dobbin, L. H. Tsai, "*Epigenetic regulation of gene expression in physiological and pathological brain processes*", Physiol. Rev. 91, 603 (2011).

[72] J. D. Sweatt, "*The emerging field of neuroepigenetics*", Neuron 80, 624 (2013).

[73] M. J. Meaney, A. C. Ferguson-Smith, "*Epigenetic regulation of the neural transcriptome: the meaning of the marks*", Nat. Neurosci. 13, 1313 (2010).

[74] Y. L. Weng, R. An, J. Shin, H. Song, G. L. Ming, "*DNA modifications and neurological disorders*", Neurotherapeutics 10, 556 (2013).

[75] R. Jaenisch, A. Bird, "*Epigenetic regulation of gene expression: how the genome integrates intrinsic and environmental signals*", Nat. Genet. 33 (Suppl.), 245 (2003).

[76] R. S. Schmid, et al., "*Core pathway mutations induce de-differentiation of murine astrocytes into glioblastoma stem cells that are sensitive to radiation but resistant to temozolomide*", Neuro-oncol. 18, 962 (2016).

[77] Y. Su, et al., "*Neuronal activity modifies the chromatin accessibility landscape in the adult brain*", Nature Neuroscience 20, 476 (2017), https:www.doi: 10.1038/nn.4494.

[78] D.C. Bitang A Ziem, A. Mvogo, T.C. Kofane, "*Effects of transport memory in wave fronts in a bistable reaction-diffusion system*", Physica A 517, 36 (2019).

[79] A. Zidovska, D. A. Weitz, T. J. Mitchison, "Micron-scale coherence in interphase chromatin dynamics" Proc. Natl. Acad. Sci. USA 110, 15555 (2013), https: www.doi:10.1073/pnas.1220313110.

[80] R. Dockhorn, J. U. Sommer, "*A Model for Segregation of Chromatin after Replication: Segregation of Identical Flexible Chains in Solution*", Biophys. J. 100 , (2011) 2539.

[81] A. Rodríguez-Campos, Fernando Azorín, "*RNA Is an Integral Component of Chromatin that Contributes to Its Structural Organization*", PLoS ONE 2, e1182 (2011). https:www.doi:10.1371/journal.pone.0001182.

[82] E. Bernstein, C. D. Allis, "RNA meets chromatin", GENES & DEVELOPMENT 19 , 1635 (2005).

[83] A. Katchalsky, A. Oplatka, "*Hysteresis and. Macromolecular Memory*", Neurosci. Res. Progr. Bull. 3, 15 (1965).

[84] R. Russell, Biophysics of RNA Folding, (Springer-Verlag, New York,2013).

[85] S. Penã de Ortiz, Y. I. Arshavsky, "*DNA Recombination as a Possible Mechanism in Declarative Memory: A Hypothesis*", J. of Neurscience Research 63, 72 (2001).

[86] C. T. H. Baker, G. Bocharov, E. Parmuzin, F. A. Rihan, "*Some aspects of causal & neutral equations used in modelling*", J. Comput. Appl. Math. 229, 335 (2009).

[87] C. T. H. Baker, G. Bocharov, F. A. Rihan, "*Neutral delay differential equations in the modelling of cell growth*", J. Egypt. Math. Soc. 16 (2), 13 (2008).

[88] C. T. H. Baker, G. Bocharov, C. A. H. Paul, F. A. Rihan, "*Models with delay for cell population dynamics: Identification, selection and analysis*", Appl. Num. Math. 53, 107 (2005).

[89] A. Bellen, M. Zennaro, Numerical Methods for Delay Differential Equations, (Oxford University Press, New York, 2003).

[90] G. Bocharov, F. A. Rihan, "*Numerical modelling in biosciences using delay differential equations*", J. Comput. Appl. Math. 125, 183 (2000).

[91] F. A. Rihan, "*Sensitivity analysis of dynamic systems with time lags*", J. Comput. Appl. Math. 151, 445 (2003).

[92] F. A. Rihan, *Numerical Treatment of Delay Dfferential Equation in Bioscience*, A PhD thesis submitted to the University of Manchester.

[93] A. C. Fowler, M. C. Mackey, "*Relaxation oscillations in a class of delay differential equations*", SIAM J. Appl. Math. 63, 299 (2002).

[94] N. W. Nelson, A. S. Perelson, "*Mathematical analysis of delay differential equation models of HIV-1 infection*", Math. Biosc. 179 73 (2002).

[95] H. Smith, An Introduction to Delay Differential Equations with Applications to the Life Sciences, (Springer: New York Dordrecht Heidelberg, London, 2011).

[96] K. Cooke, Z. Grossman, "*Discrete delays, distributed delays and stability switches*", J. Math. Anal. Appl. 86, 592 (1982).

[97] M. Mackey, L. Glass, "*Oscillations and chaos in physiological control systems*", Science 197, 287 (1997).

[98] E. Bertta, G. Bischi, F. Solimano, "*Stability in chemostat equations with delayed nutrient recycling*", J. Math. Biol. 28, 99 (1990).

[99] G. Marchuk, Mathematical Modelling of Immune Response in Infectious Diseases, (Springer, Netherlands, 1997).

[100] U. an der Heiden, M. Mackey, "*The dynamics of production and destruction: analytic insight into complex behaviour*", J. Math. Biol. 16, 75 (1982).

[101] L. Glass, M. Mackey, "*Pathological conditions resulting from instabilities in physiological control systems*", Ann. A.Y. Acad. Sci. 316, 214 (1979).

[102] L. Mi, J. Ma, "*Multiple modes of electrical activities in a new neuron model under electromagnetic radiation*", Neuro-computing 205,375 (2016).

[103] A. Aggarwal, M. Kumar, T. K. Rawat, etal:, "*Optimal design of 2-D FIR filters with quadrantally symmetric properties using fractional derivative constraints*", Circ. Syst. Signal Process, (2016), https: doi:10.1007/s00034-016-0283-x.

[104] M. Kumar, T. K. Rawat, "*Fractional order digital differentiator design based on power function and least-squares*", Int. J. Electron, (2016), https: doi:10.1080/00207217.2016.1138520.

[105] S. T. Wang, W. Wang, F. Liu, "*Propagation of firing rate in a feed-forward neuronal network*", Phys. Rev. Lett. 96, 018103 (2006).

[106] P. Suffczynski, S. Kalitzina, F. H. Lopes Da Silva, "*Dynamics of non-convulsive epileptic phenomena modeled by a bistable neuronal network*", Neuroscience 126, 467 (2004).

[107] S. Cullheim, S. Thams, "*The microglial networks of the brain and their role in neuronal network plasticity after lesion*", Brain Res. Rev. 55, 89 (2007).

[108] R. Wang, Z. Z. Zhang, J. Ma, "*Spectral properties of the temporal evolution of brain network structure*", Chaos 25, 123112 (2015).

[109] M. Lv, C. Wang, G. Ren, J. Ma, X. Song, "*Model of electrical activity in a neuron under magnetic flow effect*", Nonlinear Dyn. 85(3), 1479 (2016).

[110] X. L. Song, W. Y. Jin, J. Ma, "*Energy dependence on the electric activities of a neuron*", Chin. Phys. B 24, 128710 (2015).

[111] X. L. Song, C. N. Wang, J. Ma, etal:, "*Transition of electric activity of neurons induced by chemical and electric autapses*, Sci. China Technol. Sci. 58, 1007 (2015)

[112] R. Metzler, J. Klafter, "The random walk's guide to anomalous diffusion: a fractional dynamics approach", Physics Reports 339, 1 (2000), and references therein.

[113] J. L. Lavoie, T. J. Osler, R. Tremblay, "*Frational Derivatives and Special Functions*", SIAM Review, 18, 240.

[114] B. Riemann, "*Versuch einer allgemeinen Auffassung der Integration und Differentiation*", Gesammelte Werke, 62 (1876).

[115] S. G. Samko, A. A. Kilbas, O. I. Marichev, "*Fractional Integrals and Derivatives: theory and applications*", (Gordon and Breach, Amsterdam, 1993).

[116] A. Atangana, D. Baleanu, "*New Fractional Derivatives with Nonlocal and Non-Singular Kernel: Theory and Application to Heat Transfer Model*", arXiv:1602.03408, (2016).

[117] A. Atangana, I. Koca, "*Chaos in a simple nonlinear system with AtanganaBaleanu derivatives with fractional order*", Chaos, Solitons & Fractals 89, 447 (2016).

[118] E. Schrödinger, *What is Life?*, (Cambridge University Press, London, 1944).

[119] R. Dawkins, *The Selfish Gene*, (Oxford University Press London, 1976).

[120] R. Dawkins, *The Blind Watchmaker*, (W. W. Norton, New York, 1986).

[121] D. E. Wooldridge, *The Machinery of the Brain*, (McGraw-Hill, New York, 1963).

[122] F. Crick, *The Astonishing Hypothesis*, (Simon & Schuster, New York, 1994).

[123] Special Issue of Scientific American, "*Life, Death, and the Immune System*", September 1993.

[124] T. Boon, "*Teaching the Immune System to Fight Cancer*", Scientific American, 82 (1993).

[125] L. Adleman, "Molecular computation of solutions to combinatorial problems", Science 266, 1021 (1994).

[126] R. J. Lipton, "*DNA solution of hard computational problems*", Science 268, 542 (1995).

[127] E. B. Baum, "*Building an associative memory vastly larger than the brain*", Science 268, 583 (1995).

[128] A. Blumen, J. Klafter, G. Zumofen, *In Optical Spectroscopy of Glasses*, (Zschokke I, Dordrecht, 1986).

[129] J. P. Bouchaud, A. Georges, "*Anomalous diffusion in disordered media: Statistical mechanisms, models and physical applications*", Phys. Rep. 195, 127 (1990).

[130] B. D. Hughes, *Random Walks and Random Environments*, (Oxford University Press, Oxford, 1995).

[131] J. Klafter, M. F. Shlesinger, G. Zumofen, "*Beyond Brownian Motion*", Physics Today 49(2), 33 (1996).

[132] M. F. Shlesinger, G. M. Zaslavsky, J. Klafter,"*Strange kinetics*", Nature 363, 31 (1993).

[133] E. Barkai,"*Fractional Fokker-Planck equation, solution, and application*", Phys. Rev. E 63, 046118 (2001).

[134] R. Metzler, "*Anomalous Transport: Foundations and Applications*", Euro. Phys. J. B 19, 249 (2001).

[135] I. M. Sokolov, Solutions of a class of non-Markovian Fokker-Planck equations, Phys. Rev. E 66, 041101 (2002).

[136] P. Woafo, T. C. Kofane and A. S. Bokosah, "*Discreteness effects in an extended ϕ^4 chain with dissipation and external field*", Phys. Lett. A 160, 237 (1991).

[137] A. Sanchez, L. Vazquez, V. V. Konotop, "*Dynamics of a ϕ^4 kink in the presence of strong potential fluctuations, dissipation, and boundaries*",Phys. Rev. A 44, 1086 (1991).

[138] J.W. Cahn, E.S.V. Vleck, "*Traveling wave solutions for systems of odes on a twodimensional spatial lattice*", SIAM J. Appl. Math. 59, 455 (1998).

[139] S. Aubry, "*A unified approach to the interpretation of displacive and order-disorder systems. I. Thermodynamical aspect*", J. Chem. Phys. 62, 3217 (1975); S. Aubry, "*A unified approach to the interpretation of displacive and order?disorder systems. II. Displacive systems*", J. Chem. Phys. 64, 3392 (1976).

[140] J. A. Krumhansl, J. R. Schrieffer, "*Dynamics and statistical mechanics of a onedimensional model Hamiltonian for structural phase transitions*", Phys. Rev. B 11, 3535 (1975).

[141] J.M. Sancho, A. Sanchez, "*External fluctuations in front dynamics with inertia: The overdamped limit*", Eur. Phys. J. B 16, 127 (2000).

[142] B. Bradshaw-Hajek, "*Reaction-diffusion equations for population genetics*", University of Wollongong thesis collection, (2004).

[143] W. Horsthemke, "*Spatial instabilities in reaction random walks with directionindependent kinetics*", Phys. Rev. E 60, 2651 (1999).

[144] E. E. Holmes, "*Are diffusion models too simple? A comparison with telegraph models of invasion*", Am. Nat. 142, 779 (1993).

[145] T. Hillen, "*A Turing model with correlated random walk*", J. Math. Biol. 35, 49 (1996).

[146] J. García-Ojalvo, J. M. Sancho, *Noise in Spatially Extended Systems*, (Springer-Verlag, New York, 1999).

[147] J. Armero, J. M. Sancho, J. Casademunt, A. M. Lacasta, L. RamirezPiscina and F. Sagués, "*External fluctuations in front propagation*" Phys. Rev Lett. 76, 3045 (1996).

[148] J. Armero, J. Casademunt, L. RamirezPiscina and J. M. Sancho, "*Ballistic and diffusive correction to a front propagation in the presence of multiplicative noise*", Phys. Rev. E 58, 5494 (1998).

[149] A. Prindle, J. Liu, M. Asally, S. Ly, J. Garcia-Ojalvo, G. M. Süel, "*Ion channels enable electrical communication in bacterial communities*", Nature 527, 59 (2015), DOI: 10.1038/nature15709.

[150] H. Zhang, H. Zhao, "*Dynamics and patern formation of a diffusive predator-prey model in the presence of toxicity*", Nonlinear Dyn, https:www.doi.10.1007/s11071-018-4683-2 (2018).

[151] H. C. Rosu, O. Cornejo-Perez, "*Supersymmetric pairing of kinks for polynomial nonlinearities*", Phys. Rev. E 71, 046607 (2005).

[152] H. P. Jr. McKean, "*Nagumo's equation*", Advances in mathematics 4, 209 (1970).

[153] K. E. Hyland, S. McKee and M. W. Reeks, "*Derivation of a pdf kinetic equation for the transport of particles in turbulent flows*", J. Phys. A: Math. Gen. 32, 6169 (1999).

[154] K. Furutsu, "*On the statistical theory of electromagnetic waves*", J. Res. Natl Bur. Stand. D 67, 303 (1963).

[155] A. Novikov, "*Functionals and the random-force method in turbulence theory*", Sov. Phys. JETP 20, 1290 (1965).

[156] M. D. Donsker, *on functional space integrals in : Analysis in function space*, (MIT press, Cambridge MA, 1964).

[157] V. Méndez, S. Fedotov, W. Horsthemke, *ReactionTransport Systems. Mesoscopic Foundations, Fronts, and Spatial Instabilities*. (Springer, New York 2010).

[158] D. Hernández, C. Varea, R. A. Barrio, "*Dynamics of reaction-diffusion systems in a subdiffusive regime*", Phys. Rev. E 79, 026109 (2009).

[159] V. V. Gafiychuk, B. Y. Datsko, "*Stability analysis and oscillatory structures in time-fractional reaction diffusion systems*", Phys. Rev. E 75, 055201(R) (2007)

[160] L. Schimansky-Geier, C. Zülicke, "*Kink propagation induced by multiplicative noise*", Z. Phys. B- Condensed Matter 82, 157 (1991).

[161] R. Gorenflo, E. A. Abdel-Rehim, "*Convergence of the Grünwald-Letnikov scheme for time-fractional diffusion*" , J. Comput. Appl. Math. 205, 871 (2007).

[162] C.E. Elmer,"*Finding stationary fronts for a discrete Nagumo and wave equation; construction*", Physica D 218, 11 (2006).

[163] Y. Zhao, Q. Zhan, "*Ketone physics-structure, conformations, and dynamics of methyl isobutyl ketone explored by microwave spectroscopy and quantum chemical calculations*" Theor. Biol. Med. Model. 545, 9 (2012).

[164] R. Appali, U.V. Rienen, T.A. Heimburg, "*Chapter Nine-A Comparison of the Hodgkin-Huxley Model and the Soliton Theory for the Action Potential in Nerves*" Adv. Planar Lipid Bilayers Liposomes 16, 275 (2012).

[165] J.O. Indekeu, R. Smets, *Traveling wavefront solutions to nonlinear reaction-diffusion-convection eq*
J. Phys. A 50, 315601 (2017)

[166] T. J. Clark, A. D. Luis, "*Nonlinear population dynamics are ubiquitous in animals*", Nature eco. & evol., https:www.doi.10.1038/s41559-019-1052-6.

[167] C. A. Barnett, M. Bateson, C. Rowe: "*State-dependent decision making: educated predators strategically trade off the costs and benefits of consuming aposematic*", prey. Behavioral Ecology 18(4), 645 (2007). http://dx.doi.org/10.1093/beheco/arm027.

[168] Barnett, C. A., Skelhorn, J., Bateson, M., C. Rowe, "*Educated predators make strategic decisions to eat defended prey according to their toxin*", content. Behavioral Ecology 23, (2), 418-424 (2012). http://dx.doi.org/10.1093/beheco/arr206.

[169] M. P. Speed, "*Muellerian mimicry and the psychology of predation*", Anim. Behav. 45, 571 (1993).

[170] F. Müller, "*Ituna and Thyridia: a remarkable case of mimicry in butterflies*", Proc. Ent. Soc. 1879 xx (1878)

[171] M. P. Speed, "*Can receiver psychology explain the evolution of mimicry?*" Anim. Behav. 61. 205 (2001a).

[172] M. P. Speed, Batesian, "*quasi-Batesian or Muüllerian mimicry? Theory and data in mimicry*" research. Evol. Ecol. **13**, 755 (2001b).

[173] M. R. Servedio, "*The effects of predator learning, forgetting, and recognition errors on the evolution of warning coloration*", Evolution Int. J. Org. Evolution 54, 751 (2000).

[174] L. Bloxham, M. Bateson, T. Bedford, B. Brilot, D. Nettle. "*The memory of hunger: developmental plasticity of dietary selectivity in the European starling, Sturnus vulgaris*". Anim. Behav. 91, 33 (2014).

[175] H. Kokko, J. Mappes, L. Lindström, "*Alternative prey can change modelmimic dynamics between parasitism and mutualism*", Ecology Letters 6(12), 1068 (2003).

[176] A. Sih, B. Christensen, "*Optimal diet theory: when does it work, and when and why does it fail?*" Anim. Behav. 61(2), 379 (2001).

[177] D. W. Stephens, J. R. Krebs, "*Foraging theory*, (Princeton University Press, Princeton, 1986).

[178] T. Eisner, M. Eisner, Siegler, "*Secret weapons: Defences in insects, spiders, scorpions, and other many-legged creatures*", (Harvard University Press, Cambridge, 2005) Press.

[179] T. Eisner, J. Meinwald, "*Defensive secretions of arthropods*". Science 153(3742), 1341 (1966).

[180] J. Skelhorn, R. Rowe, "*Predators' Toxin Burdens Influence Their Strategic Decisions to Eat Toxic Prey*". Current Biology 17, 479 (2007).

[181] Q. Huang, H. Wang, M. A. Lewis, "*The impact of environmental toxins on predatorprey dynamics*", J. Theor. Bio. 378, 12 (2015).

List of Publications

1- **D. C. Bitang A Ziem**, A. Mvogo and T. C. Kofané. *Effects of transport memory in wave fronts in a bistable reaction-diffusion system*. Physica A **517**, 36 (2019).

2- **D. C. Bitang. A Ziem**, C. L. Gninzanlong, C. B. Tabi and T. C. Kofané. *Dynamics and pattern formation of a diffusive predator−prey model in the subdiffusive regime in the presence of toxicity*. Chaos, Solitons and Fractals **151**, 111238 (2021) .

Physica A 517 (2019) 36–46

Contents lists available at ScienceDirect

Physica A

journal homepage: www.elsevier.com/locate/physa

Effects of transport memory in wave fronts in a bistable reaction–diffusion system

D.C. Bitang A. Ziem [a,c,*], A. Mvogo [b,c], T.C. Kofané [a,c]

[a] Laboratory of Mechanics, Department of Physics, Faculty of Science, University of Yaounde I, P.O. Box 812, Yaounde, Cameroon
[b] Laboratory of Biophysics, Department of Physics, Faculty of Science, University of Yaounde I, P.O. Box 812, Yaounde, Cameroon
[c] African Center of Excellence in Information and Communication Technologies, University of Yaounde I, P.O. Box 812, Yaounde, Cameroon

ARTICLE INFO

Article history:
Received 10 July 2018
Received in revised form 13 October 2018
Available online 5 November 2018

Keywords:
Memory effects
Bistable reaction–diffusion systems

ABSTRACT

In this paper, we analyze transport memory effects in bistable reaction—diffusion systems. Traveling wave fronts are obtained for two interesting cases: (*i*)The nonlinear reaction term is treated without any approximation by factorization method. We find that transport memory effects appear to play a key role as it prevents the concentration or the amplitude from taking negative values. These memory effects enter the dynamics of the reaction diffusion systems through their influence on the speed of the traveling wave fronts. (*ii*) The nonlinear reaction term is replaced by a piecewise linear approximate form. We obtain a system of differential equations describing the three damped harmonic oscillators, one of which has a negative mass and the others positive masses.

1. Introduction

Memory effects are transported when the linear part of the evolution represents a process which is in part ballistic and in part diffusive. The memory function or correlation function which describes the transport is, in such cases, not a δ function as in the purely diffusive case, but has a finite decay time [1]. The dynamics of physical systems which behave as such has been the subject of a great amount of work during past decades [1–3]. A choice of wide applicability is the logistic reaction term whose interest resides in its relevance to chemical and population dynamics, where the reaction term models an autocatalytical "Malthusian" growth of the one—dimensional field, with a saturation due to intraspecies competition [4].

Recent progress in biology showed that biological systems like chromatin whose accessibility is modified dynamically by transient neuronal activation [5], moves coherently across micron—scale regions [6], and incoherently until segregation ends [7]. This passage of the character of the motion from coherent to incoherent is a general feature of all physical systems with memory effects [1,2]. Neuronal activation here can be represented by the well known Nagumo reaction term, which is a cubic polynomial and derive from a bistable potential.

Among reaction diffusion models, bistable biological systems with Nagumo reaction term have been extensively studied in connection with pattern formation [8,9]. The focal theme lies in the interesting traveling wavefront solutions and related issues which have been studied extensively by several authors in various recent contexts.

In this paper, we address the analysis of wave front dynamics in one component bistable reaction—diffusion model where we incorporate an exponential memory in the linear part. Traveling wave solutions obtained by analytical means is first treated by the factorization method, then a piecewise approximation of the reaction term is considered.

* Corresponding author.
E-mail addresses: danielcassidi7@gmail.com (D.C.B.A. Ziem), tckofane@yahoo.com (T.C. Kofané).

https://doi.org/10.1016/j.physa.2018.10.049
0378-4371/

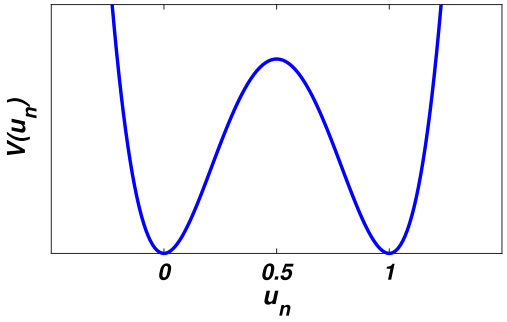

Fig. 1. Double well potential.

2. Model and nonlinear analysis

2.1. Model description

The model under consideration consists of a chain of particles of identical masses M, each one of them interacting with its two nearest neighbors through harmonic coupling, where A is the harmonic coupling coefficient. The particles are under the influence of an on−site, double well potential [10,11] given by:

$$V(u_n) = \frac{1}{4}u_n - \frac{1+a}{3}u_n^3 + \frac{a}{2}u_n^2, \tag{1}$$

where u_n is the position of the particle n and $a \in (0, 1)$ is a so−called "detuning" parameter [12].

Since we are dealing with a dissipative chain, we need a Lagrangian description which involves dissipation. This is achieved by extending the Lagrangian formalism to include the Rayleigh dissipative function, where ξ is the dissipative coefficient. We get the equation governing the motion of the nth particle.

$$M\frac{d^2u_n}{dt^2} + \xi\frac{du_n}{dt} = A(u_{n+1} - 2u_n + u_{n-1}) - u_n^3 + (1+a)u_n^2 - au_n. \tag{2}$$

In the continuum limit, i.e, when the lattice spacing is much less than the wavelength of the excitations propagating along the chain (this is also referred to as displacive regime [13,14]), the dynamics of the model can be described in dimensionless units, by the following partial differential equation:

$$\frac{\partial^2 u}{\partial t^2} + \mu\frac{\partial u}{\partial t} = D\frac{\partial^2 u}{\partial x^2} + \frac{1}{M}f(u), \tag{3}$$

where $\mu = \dfrac{\xi}{M}$ is the rescaled dissipation coefficient, $D = \dfrac{A}{M}$ is the diffusion coefficient and $f(u) = -u^3 + (1+a)u^2 - au$, is the well known Nagumo reaction term. Now, let us reduce the number of parameters by introducing the change of variables $t \to M\mu t, x \to \sqrt{MD}x$. Our initial model, Eq. (3) then reduces to

$$\epsilon\frac{\partial^2 u}{\partial t^2} + \frac{\partial u}{\partial t} = \frac{\partial^2 u}{\partial x^2} + f(u), \tag{4}$$

with the appearance of a new parameter (the "mass"), $\epsilon = (M\mu^2)^{-1}$ [15]. The parabolic or overdamped limit is obtained by letting $\epsilon \to 0$, which leads to

$$\frac{\partial u}{\partial t} = \frac{\partial^2 u}{\partial x^2} + f(u), \tag{5}$$

It is straightforward to show that the steady states of our function are $u_1 = 0$, $u_2 = a$ and $u_3 = 1$. We are interested in those solutions which are front-like (kinks) connecting the (unstable) state $u_1 = 0$ with the globally (stable) state $u_3 = 1$. Consequently, we supplement Eqs. (4) and (5) with boundary conditions $u(-\infty, t) = u_1$, $u(\infty, t) = u_3$ (see Fig. 1).

Now, consider the replacement of the diffusion equation Eq. (5) by its nonlocal (in time) counterpart

$$\frac{\partial u}{\partial t} = \int_0^t \Phi(t-\tau)\frac{\partial^2 u}{\partial x^2}d\tau + kf(u), \tag{6}$$

where $u(x, t)$ is the dynamics of the field, k is the quadratic growth rate, $\phi(t) = \alpha e^{-\alpha t}$ is the memory function which describes the finiteness of the correlation or scattering time $\dfrac{1}{\alpha}$.

Following the general rules of the calculus, we transform Eq. (6) into a differential equation that can easily be used to look for traveling wave solutions

$$\frac{\partial^2 u}{\partial t^2} + \left[\alpha - kf'(u)\right]\frac{\partial u}{\partial t} = v^2\frac{\partial^2 u}{\partial x^2} + \alpha k f(u), \tag{7}$$

where, just like in [1], $v^2 = \alpha$, the physical meaning of v being the speed dictated by the medium in the absence of scattering.

In the following section, we will analyze the nonlinear model by the factorization method.

2.2. Nonlinear analysis

The method that will be employed to solve Eq. (7) is known as the factorization method. It is a method that seeks traveling wave solutions for a particular class of partial differential equations (PDE) that are associated with having a polynomial nonlinearity. For this purpose, we introduce a traveling wave ansatz of the form

$$u(x, t) = U(z), \tag{8}$$

where $z = x - ct$, $c \geq 0$ is the velocity of the wave. Substituting this transformation into Eq. (7) and rearranging yields,

$$\frac{d^2U}{dz^2} + \frac{c}{(v^2 - c^2)}[\alpha - kf'(U)]\frac{dU}{dz} + \frac{\alpha k}{(v^2 - c^2)}f(U) = 0. \tag{9}$$

By replacing $f'(U)$ and $f(U)$ by their expressions in Eq. (9), we obtain

$$\frac{d^2U}{dz^2} + \frac{c}{(v^2 - c^2)}\left[\alpha + 3kU^2 - 2k(1 + a)U + ka\right]\frac{dU}{dz} + \frac{\alpha k}{(v^2 - c^2)}U(U - a)(1 - U) = 0. \tag{10}$$

Let

$$G(U) = \frac{c}{(v^2 - c^2)}[\alpha + 3kU^2 - 2k(1 + a)U + ka], \tag{11}$$

and

$$F(U) = \frac{\alpha k}{(v^2 - c^2)}U(U - a)(1 - U). \tag{12}$$

Thus, rearranging Eq. (10) yields

$$\frac{d^2U}{dz^2} + G(U)\frac{dU}{dz} + F(U) = 0. \tag{13}$$

We aim to factorize Eq. (13) into a form given by

$$[D_z - f_2(U)]\,[D_z - f_1(U)]\,U = 0, \tag{14}$$

where $D_z = \dfrac{d}{dz}$, and the functions f_1 and f_2 relate to $F(U)$ implicitly.

We start by expanding Eq. (14) to get

$$D_z{}^2U - D_z f_1 U - f_2 D_z U + f_1 f_2 U = 0, \tag{15}$$

which leads to

$$\frac{d^2U}{dz^2} - f_1\frac{dU}{dz} - \frac{df_1}{dU}\frac{dU}{dz}U - f_2\frac{dU}{dz} + f_1 f_2 U = 0. \tag{16}$$

At this level, it is required that we factorize the expression in Eq. (16) by grouping terms. We will use the Rosu and Cornejo–Perez grouping technique [16], which is given by

$$\frac{d^2U}{dz^2} - \left(\frac{df_1}{dU}U + f_1 + f_2\right)\frac{dU}{dz} + f_1 f_2 U = 0. \tag{17}$$

Comparing Eqs. (17) and (13), we obtain

$$\frac{df_1}{dU}U + f_1 + f_2 = -G(U), \tag{18}$$

and,

$$f_1 f_2 = \frac{F(U)}{U}, \tag{19}$$

where f_1 and f_2 are set to be

$$f_1 = \alpha(1 - U), \tag{20}$$

and

$$f_2 = \frac{k}{v^2 - c^2}(U - a). \tag{21}$$

We now substitute the expressions of f_1, f_2 and $G(U)$ into Eq. (18), it yields

$$-\alpha U + \alpha(1 - U) + \frac{k}{v^2 - c^2}(U - a) = -G(U). \tag{22}$$

After grouping terms according to the power of U, we obtain

$$3cU^2 + \eta(c, a)U + \beta(c, a) = 0, \tag{23}$$

where $\eta(c, a) = (1 + 2(1 + a)c)k + 2(c^2 - v^2)v^2$, and
$\beta(c, a) = -a(1 + c)k + v^2(-c - c^2 + v^2)$.

It has been shown that for $a > 1/2$, the only traveling solution is $U = 0$ [17], which corresponds to the extinction option. For $0 < a \leq 1/2$, and for each set of parameters of Eq. (7), there are two possibles front velocities for which there are continuous solutions that represent a transition between the stationary states.

We now implement the Rosu and Cornejo—Perez grouping technique defined in Eq. (17) to obtain

$$\frac{d^2U}{dz^2} - (-\alpha U + \alpha(1 - U) + \frac{k}{v^2 - c^2}(U - a))\frac{dU}{dz} + f_1 f_2 U = 0. \tag{24}$$

As stated previously, this structure allows us to get

$$\left[D_z - \frac{k}{v^2 - c^2}(U - a)\right][D_z - \alpha(1 - U)]\,U = 0. \tag{25}$$

Eq. (25) will be related to one of the following ordinary differential equation (ODE)

$$\frac{dU}{dz} - \alpha(1 - U)U = 0. \tag{26}$$

or

$$\frac{dU}{dz} - \frac{k}{v^2 - c^2}(U - a)U = 0. \tag{27}$$

If we consider Eq. (26), we have

$$\int \frac{dU}{(1 - U)U} = \int \alpha dz. \tag{28}$$

By integrating Eq. (28), we get

$$-\ln(|1 - U|) + \ln(|U|) = \alpha z + c_r, \tag{29}$$

where c_r is the constant of integration. After small modifications, Eq. (29) gives

$$U = \frac{exp(\alpha z + c_r)}{1 + exp(\alpha z + c_r)}. \tag{30}$$

The constant c_r relates to an initial shift of the wave, if desired. Eq. (30) can be reduced to

$$U = 1 - \frac{1}{1 + exp(\alpha z + c_r)}. \tag{31}$$

We can now use the inverse transformation of $U(z) = u(x - ct)$, with $z = x - ct$ to get

$$U = 1 - \frac{1}{1 + exp(\alpha(x - ct) + c_r)}. \tag{32}$$

This is a solution connecting the equilibrium $U = 0$ to the equilibrium $U = 1$. These trajectories correspond to fronts of state 0 invading the state 1, for different values of the memory function at very short times (see Fig. 2). When α increases, the width of the front wave decreases, it means that the memory effects increase the speed of the front wave.

Let us now consider Eq. (27), we have

$$\int \frac{dU}{(a - U)U} = \int -bdz. \tag{33}$$

By integrating Eq. (33), we get

$$-\ln(|a - U|) + \ln(|U|) = -bz + c_l, \tag{34}$$

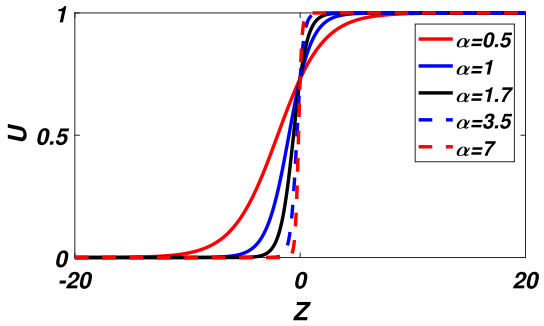

Fig. 2. Right propagating front.

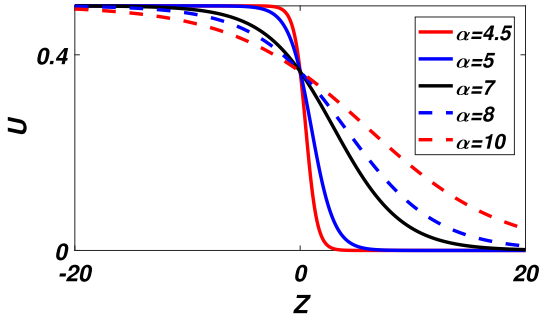

Fig. 3. Left propagating front for $k = 1$, $a = 0.5$ and $c = 2$.

where c_l is the constant of integration. In order to avoid discontinuity, we have to make sure that $0 < U < a$. Using the exponential function, and rearranging for U, Eq. (33) gives,

$$U = \frac{aexp(-bz + c_l)}{1 + exp(-bz + c_l)}. \tag{35}$$

After reduction for clarity purposes, Eq. (35) can be written in a simpler form given by

$$U = a\left[1 - \frac{1}{1 + exp(-bz + c_l)}\right]. \tag{36}$$

We now implement the inverse transformation of $U(z) = u(x - ct)$, with $z = x - ct$, to get

$$U = a\left[1 - \frac{1}{1 + exp(-b(x - ct) + c_l)}\right], \tag{37}$$

where $b = \dfrac{k}{v^2 - c^2}$, and the constant c_l relates to an initial shift of the wave, if desired.

This solution corresponds to the left propagating front that connects the front state $U = 1$ with the front state $(U = 0)$. We have an overdamped trajectory, since negative solutions are not allowed [1] (see Fig. 3). In this case, when the memory effects increase, the width of the front wave decreases, it means that the memory acts like a damping coefficient.

3. Piecewise linearization

Another way to treat the Nagumo's reaction term is to replace the nonlinear function (see Fig. 4) by its piecewise linear approximation (see Fig. 5). Following Elmer [18], we rewrite the reaction function as

$$f(U) = \begin{cases} -U & U < \dfrac{a}{2}, \\ U - a & \dfrac{a}{2} \leq U \leq \dfrac{a+1}{2}, \\ 1 - U & \dfrac{a+1}{2} < U. \end{cases} \tag{38}$$

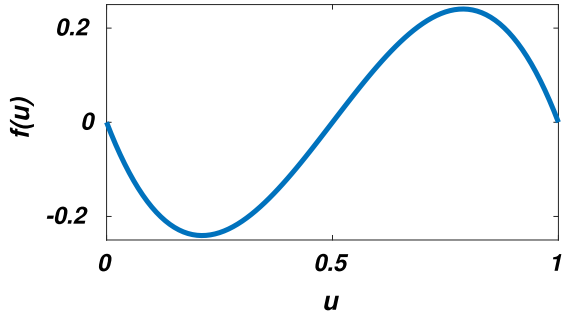

Fig. 4. The Nagumo's function with $a = 0.5$.

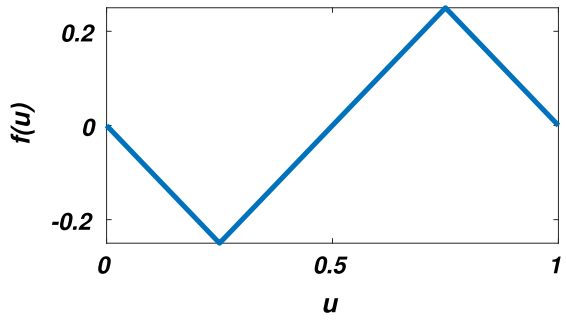

Fig. 5. The piecewise linear approximation.

Denoting differentiation with respect to z by primes and by using Eq. (8), we reduce the PDE Eq. (7) to an ODE which describes a damped harmonic oscillator

$$\begin{aligned} &mU'' + 2\gamma_1 U' - \omega^2 U = 0,\ U \le \frac{a}{2}, \\ &mU'' + 2\gamma_2 U' + \omega^2 (U - a) = 0,\ \frac{a}{2} \le U \le \frac{a+1}{2}, \\ &mU'' + 2\gamma_3 U' + \omega^2 (1 - U) = 0,\ U > \frac{a+1}{2}. \end{aligned} \tag{39}$$

Here, we used the notation of Manne et al. [1], $m = v^2 - c^2$ to emphasize the formal similarity between Eq. (7), where we have inserted Eq. (8) and the equation of motion of a damped oscillator of mass m subject to a nonlinear force $-\alpha k U(U - a)(1 - U)$. Parameters are as follows

$$\gamma_1 = \gamma_3 = \frac{c}{2}(\alpha + k),\ \gamma_2 = \frac{c}{2}(\alpha - k),\ \omega = \sqrt{\alpha k}. \tag{40}$$

It is clear that Eq. (39) is the equation of motion of three damped harmonic oscillators, which is in agreement with the results obtained by Zhao et al. [19] showing that chromatin behaves like a set of synchronized oscillators either by the coupling of an electromagnetic field generated by a longitudinal oscillation of the nucleosomes, or by the physical interactions of the DNA–protein complexes. These results are in agreement with [20] showing that the telegraph−type equations do not take into account the mechanical and thermodynamic effects. Solutions for wave amplitude as a coordinate function $x - ct$ can be obtained for each region $U < \frac{a}{2}$, $\frac{a}{2} < U < \frac{a+1}{2}$ and $U > \frac{a+1}{2}$.

In the region $U < \frac{a}{2}$, depending on the values of m, solutions are given as follows:

if $m = 0$, we have

$$U(z) = Be^{\frac{\omega^2}{2\gamma_1} z}. \tag{41}$$

and,

if $m \neq 0$, we obtain

$$U(z) = B_+ e^{r_+ z} + B_- e^{r_- z}, \tag{42}$$

with

$$r_\pm = \frac{-\gamma_1 \pm \sqrt{\gamma_1^2 + m\omega^2}}{m}. \tag{43}$$

In the region $\frac{a}{2} \leq U \leq \frac{a+1}{2}$, depending again on the values of m, we obtain the following solutions:
if $m = 0$, we get

$$U(z) = a + Ce^{-\frac{\omega^2}{2\gamma_2}z} \tag{44}$$

and,
if $m \neq 0$, we have

$$U(z) = \begin{cases} a + C_+e^{R_+z} + C_-e^{R_-z} & R_+ \neq R_-, \\ a + C_0e^{Rz} + C_1ze^{Rz}, & R_+ = R_- = R, \end{cases} \tag{45}$$

with

$$R_\pm = \frac{-\gamma_2 \pm \sqrt{\gamma_2^2 - m\omega^2}}{m}. \tag{46}$$

In the region $U > \frac{a+1}{2}$,
if $m = 0$, it leads

$$U(z) = 1 - De^{\frac{\omega^2}{2\gamma_3}z}, \tag{47}$$

and,
if $m \neq 0$, we obtain

$$U(z) = \begin{cases} 1 - D_+e^{\mu_+z} - D_-e^{\mu_-z} & \mu_+ \neq \mu_-, \\ 1 - D_0e^{\mu z} + D_1ze^{\mu z}, & \mu_+ = \mu_- = \mu, \end{cases} \tag{48}$$

where

$$\mu_\pm = \frac{-\gamma_3 \pm \sqrt{\gamma_3^2 - m\omega^2}}{m}. \tag{49}$$

We define the following variables U_L, U_{R1} and U_{R2} via [1]

$$\begin{aligned} &U_L(-z) = U(z), \quad z \geq 0, \\ &U_{R1}(z) = a + U(z), \quad z \geq 0, \\ &U_{R2}(z) = 1 - U(z), \quad z \geq 0, \end{aligned} \tag{50}$$

and we have

$$\begin{aligned} &mU_L'' + 2\gamma_1U_L' - \omega^2U_L = 0, \ z < 0, \\ &mU_{R1}'' + 2\gamma_2U_{R1}' + \omega^2U_{R1} = 0, \ 0 < z < z_1, \\ &mU_{R2}'' + 2\gamma_3U_{R2}' + \omega^2U_{R2} = 0, \ z > z_1. \end{aligned} \tag{51}$$

We obtain a system of differential equations describing the three damped harmonic oscillators, one of which has a negative mass, and the other two having positive masses. The negative mass of the first oscillator is biologically explained by the fact that many biological systems are very repressive. They trigger a response that tends to oppose the solicitation. The first oscillator thus appears clearly as a low−pass filter, since it allows only signals whose wave velocity is lower than that imposed on it, and the rest is rejected.

Since we are interested in non−negative solutions, because U is assumed to be a concentration or density [2], it follows that the damped oscillator U_L representing the shape of the front of the wave must be critically damped to prevent this concentration from oscillating and ending up with negative values. The role of the first oscillator is thus to avoid that one finds oneself in a situation where the speed imposed by the stress is superior to that dictated by the medium. Therefore, the condition that this oscillator should be critically damped is verified.

Let us consider the case of the oscillators U_{R1} and U_{R2}. They can be slightly damped, since there is no problem if the concentration oscillates around a positive value. The condition for U_{R1} to be critically damped is: $\gamma_2 = \sqrt{m}\omega$, and the corresponding velocity is given by

$$c_{thr1} = v\frac{1}{\sqrt{1 + \frac{1}{4}(y - \frac{1}{y})^2}}, \tag{52}$$

where $y = \sqrt{\frac{\alpha}{k}}$. If $c < c_{thr1}$, the wave front shape exhibits spatial oscillations.

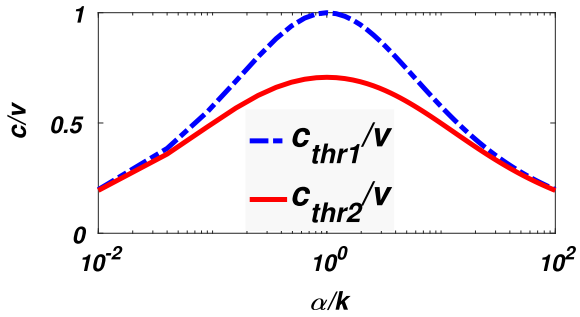

Fig. 6. The dependence of the respective ratios of c_{thr1} and c_{thr2} to the speed v dictated by medium on the damping−nonlinearity parameter ratio α/k.

The condition for U_{R2} to be critically damped is $\gamma_3 = \sqrt{m}\omega$, and the corresponding velocity is given by

$$c_{thr2} = v\frac{1}{\sqrt{1+\frac{1}{4}(y+\frac{1}{y})^2}}. \tag{53}$$

Fig. 6 shows a comparative study between v, c, c_{thr1} and c_{thr2}, and we see that $c_{thr2} \leq c_{thr1} \leq v$. Using this graph, we can determine explicit solutions of the following regions $c \leq c_{thr2}$, $c_{thr2} \leq c \leq c_{thr1}$ and $c \leq v$.

In the first region, $c \leq c_{thr2}$, depending on each of the three regions $z < 0$, $0 < z < z_1$ and $z > z_1$, solutions are given by

$$U(z) = \begin{cases} \frac{a}{2}e^{r_+ z} & z < 0, \\ a(1 - D_1\cos(\frac{2\pi}{\lambda_1}z - \delta_1)) & 0 \leq z \leq z_1, \\ 1 - D_2 e^{\mu z}\cos(\frac{2\pi}{\lambda_2}z - \delta_2) & z > z_1, \end{cases} \tag{54}$$

where

$$D_1 = \frac{1}{2\cos\delta_1}e^{Rz}, \tag{55}$$

$$D_2 = \frac{1 - a + \frac{a}{2\cos\delta_1}\cos(\frac{2\pi}{\lambda_1}z_1 - \delta_1)}{e^{\mu z_1}\cos(\frac{2\pi}{\lambda_2}z_1 - \delta_2)}, \tag{56}$$

$$\delta_1 = -\tan^{-1}\left(\frac{\lambda_1}{2\pi}(r_+ + R)\right), \tag{57}$$

$$\lambda_1 = \frac{2\pi m}{\sqrt{m\omega^2 - \gamma_2^2}}, \tag{58}$$

$$\lambda_2 = \frac{2\pi m}{\sqrt{m\omega^2 - \gamma_1^2}}, \tag{59}$$

$$R_\pm = R \pm i\frac{\lambda}{2\pi}, \tag{60}$$

$$\delta_2 = \frac{2\pi}{\lambda_2} - \tan^{-1}\left[\frac{\lambda_1}{2\pi}\left(\mu + \frac{\delta_N}{\delta_D}\right)\right], \tag{61}$$

$$\delta_N = a(-\frac{R}{2}\cos(\frac{2\pi}{\lambda_1}z_1 - \delta_1) + \frac{\pi}{\lambda}\sin(\frac{2\pi}{\lambda_1}z_1 - \delta_1))e^{Rz_1}, \tag{62}$$

$$\delta_D = (1 - a[1 - \frac{1}{2\cos\delta_1}\cos(\frac{2\pi}{\lambda_1}z_1 - \delta_1)])\cos\delta_1. \tag{63}$$

We have an oscillating wave front in space, which proves that there is a supply of energy from the outside environment in this region. If we consider this region as a sink, biophysically, this energy may come from locally ingested nutrients, drugs, or information transmitted into the region considered. This energy can be considered as a source [21]. The sink in this case can

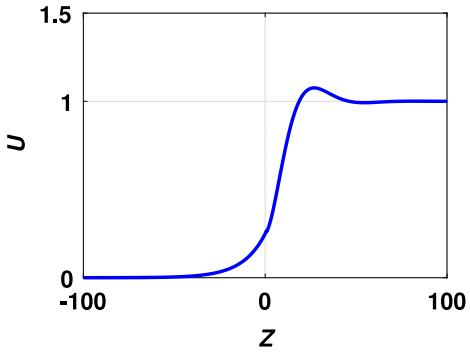

Fig. 7. Wave front shape with oscillations Eq. (54), using $\alpha = 3$, $a = 0.5$, $k = 1$, $c = 5$, $v = 10$ and $z_1 = \frac{a+1}{2}$.

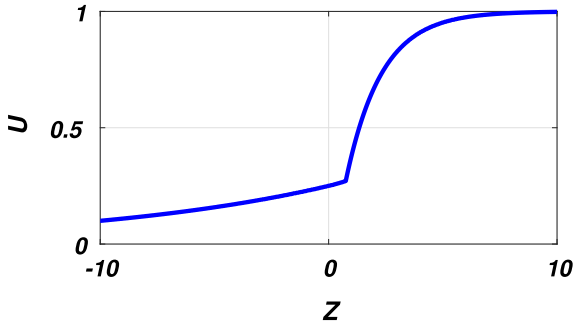

Fig. 8. Wave front shape with transition to no oscillations regime Eq. (64), with $\alpha = 3$, $a = 0.5$, $k = 1$, $c = 7$, $v = 10$ and $z_1 = \frac{a+1}{2}$.

be mechanical coupling imposing a coherent motion to the biological system as, for instance, chromatin. With this coherent motion, chromatin cannot undergo a segregation which is essential before any cell division. The source will therefore break this mechanical coupling, so that the motion of the chromatin becomes incoherent, and therefore, it can be subjected to free diffusion that will allow it to undergo segregation, and give rise to cell division. (See Fig. 7)

In the second region , $c_{thr2} \leq c \leq c_{thr1}$, m is positive, and we obtain

$$U(z) = \begin{cases} \frac{a}{2}e^{r+z}, & z < 0 \\ a(1 - \frac{1}{2\cos\delta}e^{Rz}\cos(\frac{2\pi}{\lambda}z - \delta)), & 0 \leq z \leq z_1, \\ 1 - D_- e^{\mu - z} & z > z_1, \end{cases} \tag{64}$$

where

$$\lambda = \frac{2\pi m}{\sqrt{m\omega^2 - \gamma_2^2}}, \tag{65}$$

$$\delta = -\tan^{-1}(\frac{\lambda(r_p + R_p)}{2\pi}), \tag{66}$$

$$C = -\frac{a}{2\cos\delta}, \tag{67}$$

$$D_- = (1 - a - Ce^{Rz_1}\cos(\frac{2\pi z_1}{\lambda} - \delta))e^{-\mu - z_1}. \tag{68}$$

The second region corresponds to a transition zone towards a state of no oscillations, which means that the mechanical coupling has been removed, and the energy used to break this coupling will initiate free diffusion processes in the second region. (See Fig. 8)

In the third region, $c \leq v$, m is still positive, the solution is given by:

$$U(z) = \begin{cases} \frac{a}{2}e^{r+z} & z < 0, \\ a + C_+ e^{R+z} + C_- e^{R-z} & 0 \leq z \leq z_1, \\ 1 - D_- e^{\mu - z} & z > z_1, \end{cases} \tag{69}$$

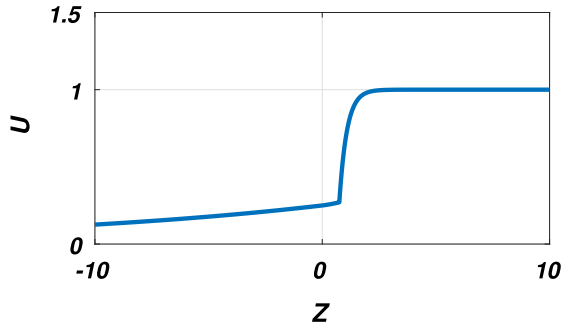

Fig. 9. Wave front shape without oscillations Eq. (69), for $\alpha = 3$, $a = 0.5$, $k = 1$, $c = 9.5$, $v = 10$ and $z_1 = \frac{a+1}{2}$.

where

$$C_+ = \frac{a(r_+ + R_+)}{2(R_- - R_+)}, \tag{70}$$

$$C_- = \frac{a(r_+ + R_-)}{2(R_+ - R_-)}, \tag{71}$$

$$D_- = \frac{1 - a - C_+ e^{R_+ z_1} - C_- e^{R_- z_1}}{e^{\mu - z_1}}. \tag{72}$$

Here, we realize that all oscillations have disappeared completely. It means that the process was successfully completed, and another cycle is on his way to start. (See Fig. 9)

4. Conclusion

We investigated the effects of transport memory of the wave fronts in the bistable reaction–diffusion which arises in biological system. We considered two hypotheses. Firstly, we assumed that these systems can be modeled as a chain of particles of identical masses, each one of them interacting with its two nearest neighbors through harmonic coupling, and secondly, we have considered that these systems can be found in a bistable regime. A model was proposed and nonlinear analysis was carried out. From this analysis, traveling front solution were obtained, connecting the hyperbolic points located at the two maxima of the potential, at $U = 0$ and $U = 1$, representing the invasion of one of the states by the other. We found that memory effects play an important role. When moving from the state $U = 0$ to the state $U = 1$, memory effects accelerate the speed of the traveling wave (see Fig. 2), and when moving from the state $U = 1$ to the state $U = 0$, memory effects play the role of a damping (see Fig. 3).

The piecewise linear approximation was carried out, and results gotten agreed with the behavior of the chromatin since it can be seen as clustered oscillators. The first oscillator behaving as a resistor, thus protecting against high wave-speeds. The other oscillators working together and can be classified into three regions. The first one is where the mechanical coupling is located. This mechanical coupling is there to impose coherent motion to the system, the problem is that this mechanical coupling prevents segregation (in the case of chromatin). Hence, the memory effects transported by the wave fronts in the bistable reaction–diffusion play a key role as it help break down this mechanical coupling for segregation to take place. The second region corresponds to a transition zone between the wave-like behavior and the diffusive behavior. In the third region, another cycle is yet to start.

Further work is in progress to investigate the memory effects combined with the stochastic version of the model that we have proposed.

References

[1] K.K. Manne, A.J. Hurd, V.M. Kenkre, Phys. Rev. E 61 (2000) 4177.
[2] G. Abramson, A.R. Bishop, V.M. Kenkre, Phys. Rev. E 64 (2001) 066615.
[3] V.M. Kenkre, P. Reineker, Exciton Dynamics in Molecular Crystals and Aggregates, Springer, Berlin, 1982.
[4] G. Abramson, V.M. Kenkre, A.R. Bishop, Physica A 305 (2002) 427.
[5] Y. Su, J. Shin, C. Zhong, S. Wang, P. Roychowdhury, J. Lim, D. Kim, G. Ming, H. Song, Nature Neurosci. 16 (2017) http://dx.doi.org/10.1038/nn.4494.
[6] A. Zidovska, D.A. Weitz, T.J. Mitchison, Proc. Natl. Acad. Sci. USA 110 (2013) 15555–15560; Proc. Natl. Acad. Sci. USA 64 (2001) 066615.
[7] R. Dockhorn, J.U. Sommer, Biophys. J. 100 (2011) 2539.
[8] Q. Zheng, J. Shen, Comput. Math. Appl. 70 (2015) 1082.
[9] C. Chen, S. Ei, Y. Lin, S. Kung, Comm. Partial Differential Equations 36 (2011) 998.
[10] P. Woafo, T.C. Kofane, A.S. Bokosah, Phys. Lett. A 160 (1991) 237.
[11] A. Sanchez, L. Vazquez, V.V. Konotop, Phys. Rev. A 44 (1991) 1086.
[12] J.W. Cahn, E.S.V. Vleck, SIAM J. Appl. Math. 59 (1998) 455.
[13] S. Aubry, J. Chem. Phys. 62 (1975) 3217; J. Chem. Phys. 64 (1976) 3392.

[14] J.A. Krumhansl, J.R. Schrieffer, Phys. Rev. B 11 (1975) 3535.
[15] J.M. Sancho, A. Sanchez, Eur. Phys. J. B 16 (2000) 127.
[16] H.C. Rosu, O. Cornejo-Perez, Phys. Rev. E 71 (2005) 046607.
[17] H.P. MacKean, Adv. Math. 4 (1970) 209.
[18] C.E. Elmer, Physica D 218 (2006) 11.
[19] Y. Zhao, Q. Zhan, Theor. Biol. Med. Model. (2012) 9.
[20] R. Appali, U.V. Rienen, T.A. Heimburg, Adv. Planar Lipid Bilayers Liposomes 16 (2012) 275.
[21] J.O. Indekeu, R. Smets, J. Phys. A 50 (2017) 315601.

Chaos, Solitons and Fractals 151 (2021) 111238

Contents lists available at ScienceDirect

Chaos, Solitons and Fractals

Nonlinear Science, and Nonequilibrium and Complex Phenomena

journal homepage: www.elsevier.com/locate/chaos

Dynamics and pattern formation of a diffusive predator - prey model in the subdiffusive regime in presence of toxicity

D.C. Bitang à Ziem [a,b,*], C.L. Gninzanlong [a], C.B. Tabi [c], T.C. Kofané [a,b,c]

[a] Laboratory of Mechanics, Department of Physics, Faculty of Science, University of Yaounde I, Yaounde, PO Box 812, Cameroon
[b] African Center of Excellence in Information and Communication Technologies, University of Yaounde I, Yaounde, PO Box 812, Cameroon
[c] Botswana International University of Science and Technology, Private Bag 16, Palapaye, Botswana

ARTICLE INFO

Article history:
Received 27 February 2021
Revised 23 June 2021
Accepted 27 June 2021

Keywords:
Toxicity induced stability
Subdiffusive regime
Strong memory effects and toxicity in prey-predator interactions

ABSTRACT

Motivated by the fact that the restrictive conditions for a Turing instability are relaxed in subdiffusive regime, we investigate the effects of subdiffusion in the predator - prey model with toxins under the homogeneous Neumann boundary condition. First, the stability analysis of the corresponding ordinary differential equation is carried out. From this analysis, it follows that stability is closely related to the coefficient of toxicity. In addition, the temporal fractional derivative does not systematically widen the range of parameters to maintain a point in the stability domain. Furthermore, we derive the condition which links the Turing instability to the coefficient of toxicity in the subdiffusive regime. System parameters are varied in order to test our mathematical predictions while comparing them to ecological literature. It turns out that the memory effects, linked to the transport process can, depending on the parameters, either stabilize an ecosystem or make a completely different configuration.

1. Introduction

During evolution, venomous animals have produced a panoply of peptide toxins, formidable weapons for the capture of prey. These venoms, considered as simple to complex mixtures of toxic components, are an invaluable source of very specific pharmacologicals agents for characterization of ion channel and receptor subtypes membranes [1]. The targets of these toxins are proteins involved in nervous conduction as well as nervous transmission, mainly ion channels. By their efficiency and selectivity of action, they offer significant therapeutic potential as evidenced by toxins whose effectiveness in neurological disorders is now being tested in therapeutic trials [1]. Toxins have also been developed by a range of prey as a defense against predation. Those species that advertise their toxicity to would-be predators with conspicuous warning signals are known as “aposematic”. Many aposematic prey species arm themselves with toxins that are harmful or unpleasant to predators, and advertise those defenses using a variety of conspicuous warning signals [2–4]. Although warning signals can be costly in terms of increased detection, they are also particularly salient to predators, allowing them to quickly learn about and identify toxic prey and reduce their attack rates on them [5–7]. Therefore, aposematic signals appear to have been selected to take advantage of the cognitive processes of predators, and in particular, how they learn about prey and make dietary decisions in a complex world [3,8]. Several researches have been carried out to investigate the role of toxins in prey-predator interactions using mathematical models. Some of the leading studies are the work of Chattopadhyay [9] which emphasised on the effects of toxic substances on two-species competitive system, considering that each species produces a substance toxic to the other only when the other is present. Further work on the presence of toxic substances was done by Kar and Chaudhuri [10], where they investigated the possibility of the existence of a bionic equilibrium and optimal harvesting policy on a model with two competiting fish species that are commercially exploited. In [11], Samanta investigated the effets of environmental toxins exposure. In this situation, predator are infected not only by the environmental exposure, but also indirectly during the feeding process. Other studies regarding the diffusion population model in the presence of toxic substance have been carried out by Aly [12]. He considered a Lokta-Volterra competitive system affected by toxic substances in two patches in which the per capita migration rate of each species is influenced not only by its own but also by the other one’s density. Thus far, few researchers have studied the combined effects of delay and toxicity in prey-predator interactions. Jana et al. [13] analyzed the stability

* Corresponding author at: Laboratory of Mechanics, Department of Physics, Faculty of Science, University of Yaounde I, PO Box 812, Yaounde, Cameroon.
E-mail addresses: danielcassidi7@gmail.com (D.C.B. à Ziem), gcarloslawrence@yahoo.fr (C.L. Gninzanlong), tabic@biust.ac.bw (C.B. Tabi), tckofane@yahoo.com (T.C. Kofané).

https://doi.org/10.1016/j.chaos.2021.111238
0960-0779/

and Hopf-bifurcation behaviors of a multi-delayed two-species competitive system affected by toxic substances with imprecise biological parameters. The asymptotic behavior of the reaction-diffusion model of plankton allelopathy with non-local delays was investigated by Li et al. [14]. It is worth pointing out that delay is used in mathematical modeling to describe memory effects [15–17]. Memory effects are important because they reflect the fact that the past is considered to explain the present [18]. Another approach to better describe these memory effects is fractional calculus which makes it possible to clearly distinguishes super diffusion, normal diffusion and subdiffusion. Recent studies point out the fact that nervous conduction and transmission, the main target of toxic substances are overwhelmingly dominated by subdiffusion [19–21].

Subdiffusion has acquired relevance in the past decades since it has been experimentally detected in several systems such as porous media [22], glasses [23], transport through cell membranes [19,20], and other biological systems [21]. Studies of subdiffusion in reaction-diffusion systems, using time fractional derivatives, have shown that the conditions for a Turing instability are not different from the normal conditions for special cases of subdiffusion [24,25]. However, Hernández et al. [26] came out with a new way of obtaining Turing patterns with subdiffusion.

Since the well - known Turing reaction - diffusion model was discovered [27], enormous efforts have been made to investigate nonlinear self - organization phenomena in nature. Recently, interest was given to the link between toxic substances and Turing bifurcation, Hopf bifurcation and Steady - State bifurcation [28]. This lead to the conclusion that the toxic coefficient is important for the occurrence of the complex spatial dynamics. Additionally, Zhang and Zhao [28] considered a typical reaction - diffusion system, which implies that the effects of reaction and diffusion are separable and combine additively to influence the total spatiotemporal evolution of the concentration field of a given species [29,30]. When it comes to subdiffusive entities undergoing reactions, reaction and diffusion processes are no longer separable because of the strong memory effects in the transport mechanism [29], which means that the non-Markovian nature of subdiffusion results in a nontrivial combination of reactions and spatial dispersal. In this situation, can toxicity still be considered as an important parameter responsible for complex spatial dynamics?

The answer to this question requires to investigate how strong memory effects in the transport process influence Turing pattern induced by toxic substances, which is the purpose of this paper.

The scheme of this paper is as follows. In Section 2, we start by examining the influence of toxic substances on the dynamics properties of the fractional - order ODE system. Section 3 is devoted to the analysis of a model describing an ecosystem where the preys produce substance that is toxic for the predators, and give general conditions for toxicity coefficient allowing Turing instability to appear. We verify the predictions of the analysis via numerical calculations in Section 4. In Section 5, we summarize our results and draw some conclusions.

2. Effect of toxic substances on the dynamics properties of the fractional - order ODE system

In this work, the following parabolic activator- inhibitor model with subdiffusion consisting of two variables is investigated:

$$\begin{aligned} {}^{c}\partial^{\eta}u/\partial t^{\eta} &= d_1\Delta u + ru\left(1-\frac{u}{K}\right) - \frac{muv}{a+u},\\ {}^{c}\partial^{\eta}v/\partial t^{\eta} &= d_2\Delta v + sv\left(1-\frac{hv}{u}\right) - \beta uv^2. \end{aligned} \tag{1}$$

The reaction terms in (1) were first proposed by Zhang and Zhao [28] to describe an ecosystem where the prey produces substances that are toxic to the predators. The term βuv^2 denotes the effect of toxic substances and β represents the efficiency of toxicity. u and v denote the sizes of the prey population and predator population, respectively. r, K, m, a, s, h, and β are all positive constants, and $\eta \le 1$. Note that in this form, the evolution of the uniform state is controlled by subdiffusion, even if the spatial term is not present. In here the time operator is the Caputo fractional derivative of order η [31]. The explicit form of this operator in one-dimensional systems reads

$$\frac{{}^{c}\partial^{\eta}P(X,t)}{\partial t^{\eta}} = \frac{1}{\Gamma(1-\eta)}\int_0^t (t-\tau)^{-\eta}\frac{\partial P(X,t)}{\partial \tau}d\tau, \tag{2}$$

where t and τ represent the integration time and the delay, respectively. In other words, the derivative in the Caputo's sense takes into account the past to determine the present, which, according to Barros et al. [18] is the defintion of memory effects.

We first study the manner in which toxic substances affect the stability and Hopf bifurcation of the ODE version of system (1). Omitting the diffusion terms, the following ODE is obtained from (1)

$$\begin{aligned} \frac{{}^{c}du^{\eta}}{dt^{\eta}} &= ru\left(1-\frac{u}{K}\right) - \frac{muv}{a+u},\\ \frac{{}^{c}dv^{\eta}}{dt^{\eta}} &= sv\left(1-\frac{hv}{u}\right) - \beta uv^2. \end{aligned} \tag{3}$$

An obvious steady state of system (3) is $E_1 = (K, 0)$, the predator - free equilibrium. Assuming that the other equilibrium $E^* = (u^*, v^*)$ of system (3) satisfies

$$\begin{cases} r\left(1-\frac{u^*}{K}\right) - \frac{mv^*}{a+u^*} = 0,\\ s\left(1-\frac{hv^*}{u^*}\right) - \beta u^*v^* = 0. \end{cases} \tag{4}$$

Eliminating v yields

$$\begin{aligned} &\beta r u^{*4} + \beta r\left(a-K\right)u^{*3} + r\left(hs - Ka\beta\right)u^{*2}\\ &\quad + s\left(Km + ahr - Khr\right)u^* - Kahrs = 0. \end{aligned} \tag{5}$$

The number and the signs of the roots can easily be predicted from (5), according to Descartes' rule of signs. In doing so, system (5) admits one or three positive roots $u = u^*$ if one of the following inequalities holds

$$a < K, \quad hs < Ka\beta, \quad Km + ahr < Khr, \tag{6}$$

$$a < K, \quad hs > Ka\beta, \quad Km + ahr < Khr. \tag{7}$$

That is to say, according to inequality (6), if $\beta > \frac{hs}{Ka}$, (5) has exactly one positive root. While inequality (7) states that if $\frac{h^2rs}{K^2\left(hr-m\right)} < \beta < \frac{hs}{Ka}$, (5) has eiter one positive root, or three positive roots. This result is in perfect agreement with the numerical result obtained by Zhang and Zhao [28]. Once we have determined u^*, v^* can easily be obtained from the second line of (4), yielding

$$v^* = \frac{su^*}{sh + \beta u^{*2}}. \tag{8}$$

Once we know the number of equilibria, a word should be said about their stability. The stability of the steady states is determined by the eigenvalues of the Jacobian matrix

$$J = \begin{pmatrix} r\left(1-\frac{2u^*}{K}\right) - \frac{mav^*}{\left(a+u^*\right)^2} & -\frac{mu^*}{a+u^*}\\ \left(\frac{sh}{u^{*2}} - \beta\right)v^{*2} & s\left(1-\frac{2hv^*}{u^*}\right) - 2u^*v^*\beta \end{pmatrix}, \tag{9}$$

and the associated characteristic equation is

$$\lambda^2 - T\lambda + \Delta = 0, \tag{10}$$

where

$$T = a_{11} + a_{22}, \qquad \Delta = a_{11}a_{22} - a_{12}a_{21}, \tag{11}$$

with

$$\begin{aligned} a_{11} &= r - \frac{2ru^*}{K} - \frac{mav^*}{\left(a+u^*\right)^2}, \\ a_{12} &= -\frac{mu^*}{a+u^*}, \\ a_{21} &= \frac{shv^{*2}}{u^{*2}} - \beta v^{*2}, \\ a_{22} &= s - \frac{2shv^*}{u^*} - 2\beta u^* v^*. \end{aligned} \tag{12}$$

If the trace T of the Jacobian matrix is negative, with Δ, its determinant, being positive, the steady state is stable. Since we are interested in the influence of the toxic coefficient on stability, we will therefore have.

$$\begin{aligned} &T < 0 \Rightarrow \beta > \alpha_2, \\ &\Delta > 0 \Rightarrow \beta < \alpha_3. \end{aligned} \tag{13}$$

Moreover, (6) states that $\beta > \alpha_1$. By combining these three constraints on the toxicity, and considering conditions (6), for $\eta = 1$, the steady state E^* will therefore be stable if

$$\max\{\alpha_1, \alpha_2\} < \beta < \alpha_3, \tag{14}$$

where

$$\begin{aligned} &\alpha_1 = \frac{hs}{Ka}, \qquad \alpha_2 = \frac{1}{2u^*v^*}\left[a_{11} + s\left(1 - \frac{2hv^*}{u^*}\right)\right], \\ &\alpha_3 = \frac{1}{2v^*(a_{12}u^* - a_{11}v^*)}\left[-a_{12}\frac{shv^{*2}}{u^{*2}} + a_{11}s(1 - 2\frac{hv^*}{u^*})\right], \end{aligned} \tag{15}$$

the Hopf bifurcation typically occurs at $\beta_H = \alpha_2$ for system (3). If, on the other hand, we consider conditions (7), steady states will be stable if β is bounded as follows

$$\alpha_2 < \beta < \max\{\alpha_1, \alpha_3\}. \tag{16}$$

However, for $\eta \in [0, 1]$, the steady state E^* is stable when

$$|\arg\lambda| > \frac{\eta\pi}{2}, \tag{17}$$

while it becomes asymptotically unstable for

$$|\arg\lambda| < \frac{\eta\pi}{2}, \tag{18}$$

for the roots λ in the Eq. (10).

Let us first consider the inequality (6). We choose $\beta = 0.17$, which is in agreement with (14). With this value of β, we have one positive and stable root for $\eta = 1$, as well as for $\eta \in [0, 1]$.

If we consider instead the inequality (7), and we choose $\beta = 0.09$ as in [28], we will have three positive equilibrium points E_1^*, E_2^* and E_3^*. The first equilibrium point is stable for $\eta = 1$, and for $\eta \in [0, 1]$.

For the second equilibrium point, if $\eta = 1$, $\Delta < 0$, the discriminant is always positive, i.e., $T^2 - 4\Delta > 0$, and both eigenvalues are real. However, one is positive and the other is negative. Trajectories approach the steady state along the eigenvector corresponding to the negative eigenvalue, but move away along the eigenvector corresponding to the positive eigenvalue. The steady state has one stable and one unstable direction. It is therefore unstable and called a saddle [32,33]. When $\eta \in [0, 1]$, this equilibrium point is stable, according to inequality (17). Regarding the third equilibrium point, its stability is guaranteed for both $\eta = 1$ and $\eta \in [0, 1]$. While remaining in inequality (7), according to Descartes' rule of signs, it is possible to have a unique positive root, yielding a positive equilibrium point that we call E_4^*. So, taking $\beta = 0.03$, for $\eta = 1$, the equilibrium point E_4^* has complex conjugate eigenvalues with a positive real part, $\lambda = T/2$. The steady state is unstable. Due to the presence of a nonzero imaginary part, perturbations grow in an oscillatory manner and spiral away from the steady state. The steady state is an unstable focus. If $\eta \in [0, 1]$, E_4^* is found to be unstable, according to (17). These results confirm the paramount role that the toxic coefficient plays on the stability of the system. In addition, it would be interesting to note that this stability, depending on the system parameters, can either be modified or maintained.

In this section, we conducted a study on the stability of fixed points in relation with toxicity. This work was already carried out in [28], but within the framework of a normal diffusion. The interest of carrying out this study again lies in the fact that the fractional derivative can modify the stability of a point.

3. Analysis of a system with toxic substances in a subdiffusive regime

We now proceed to analyze the case we are interested in, namely the modifications of Turing pattern induced by toxic substances in presence of strong memory effects in the transport process. In order to appreciate these modifications, it is convenient to use the approach developped by Hernández et al. [26], because it can help us to see every new results that will emerge. For this purpose, we start by linearizing around the fixed points. (1) is first written as follows

$$\begin{aligned} \frac{{}^c\partial^\eta u}{\partial t^\eta} &= d_1\Delta u + a_{11}u + a_{12}v, \\ \frac{{}^c\partial^\eta v}{\partial t^\eta} &= d_2\Delta v + a_{21}u + a_{22}v, \end{aligned} \tag{19}$$

where a_{ij} are the elements of the Jacobian matrix given by (12). Applying Fourier and Laplace transforms to (19) yields

$$\begin{aligned} s^\eta U - s^{\eta-1}U(k,0) &= -d_1k^2U + a_{11}U + a_{12}V, \\ s^\eta V - s^{\eta-1}V(k,0) &= -d_2k^2V + a_{21}U + a_{22}V, \end{aligned} \tag{20}$$

where U and V are given by

$$\begin{aligned} U &= \int_{-\infty}^{\infty}\int_{-\infty}^{\infty} e^{ikx}e^{-st}u(x,t)dtdx = \mathcal{F}(\mathcal{L}(u)), \\ V &= \int_{-\infty}^{\infty}\int_{-\infty}^{\infty} e^{ikx}e^{-st}v(x,t)dtdx = \mathcal{F}(\mathcal{L}(v)). \end{aligned} \tag{21}$$

where $\mathcal{F}$ and $\mathcal{L}$ represent the Fourier and Laplace transforms, respectively. Solving (20) yields

$$\begin{aligned} U(k,s) &= \frac{\left(s^\eta + d_1k^2 - a_{22}\right)s^{\eta-1}U(k,0) + s^{\eta-1}a_{12}V(k,0)}{S(k,s)}, \\ V(k,s) &= \frac{\left(s^\eta + d_2k^2 - a_{11}\right)s^{\eta-1}V(k,0) + s^{\eta-1}a_{21}U(k,0)}{S(k,s)}. \end{aligned} \tag{22}$$

The time evolution of $u(k,t) = \mathcal{L}^{-1}(U(k,s))$ is given by the singularities of (22) which is the zeros of the function

$$\begin{aligned} S(k,s) = s^{\eta+\alpha} + s^\eta\left(d_2k^2 - a_{22}\right) + s^\alpha\left(d_1k^2 - a_{11}\right) \\ + d_1d_2k^4 + (a_{11}a_{22} - a_{12}a_{21}) - k^2(a_{22}d_1 + a_{11}d_2). \end{aligned} \tag{23}$$

In order to analyze the stability of the system near the equilibrium point, we solve the equation

$$S(k, s_0) = 0, \tag{24}$$

where $s_0(k)$ will be studied numerically for different values of the toxic coefficient to determine when instabilities should appear in the system of (19), and if it is influenced by toxicity. In particular, the conditions for a Turing instability are

$$Re[s_0(k=0)] < 0, \tag{25}$$

and

$$Re[s_0(k)] > 0. \tag{26}$$

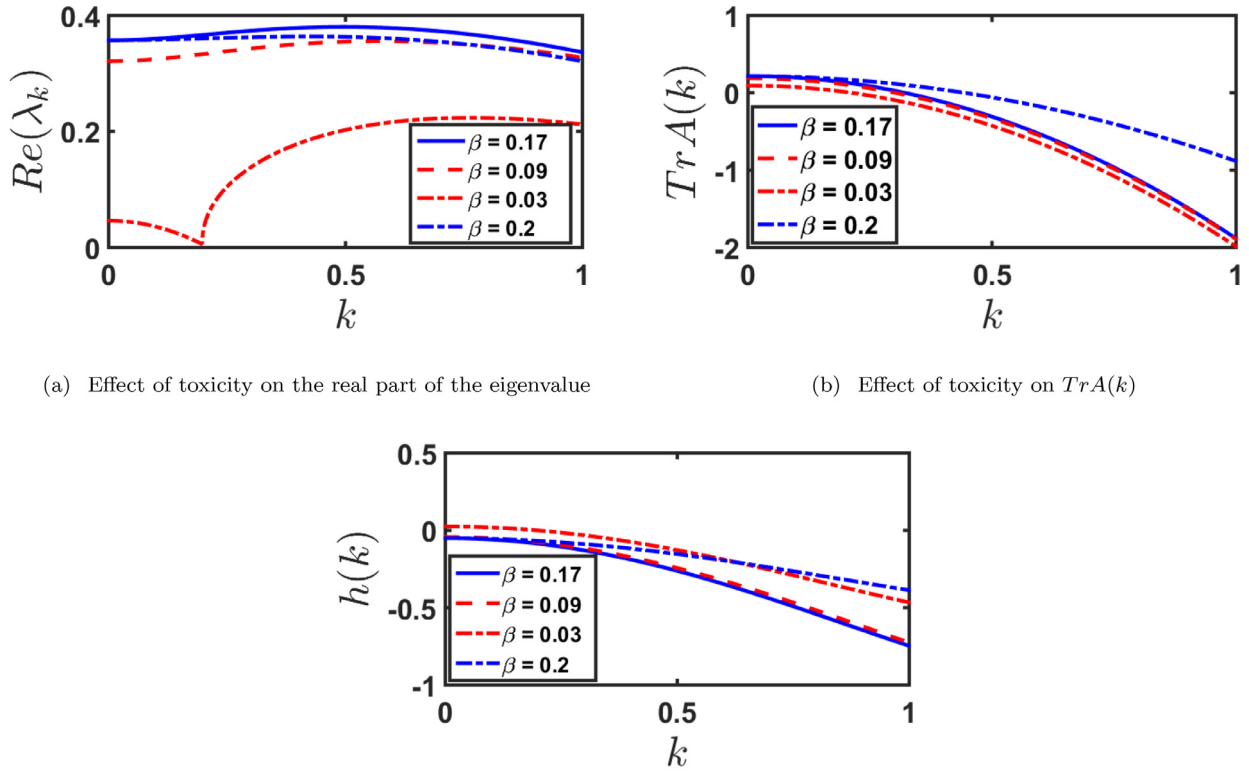

(a) Effect of toxicity on the real part of the eigenvalue

(b) Effect of toxicity on $TrA(k)$

(c) Effect of toxicity on $h(k)$

Fig. 1. Efficiency of the toxic substances on system's variables. Simulations were performed with $K = 2$, $s = 0.25$ and $h = 1$, $m = 1.5$, $r = 0.7$. Continuous blue line corresponds to $a = 0.1$, $\beta = 0.1$; continuous red line corresponds to $a = 0.05$, $\beta = 0.3$ dashed blue line corresponds to $a = 0.1$, $\beta = 0.5$, $d_1 = 0.008$ and $d_2 = 0.3$ and dashed red line corresponds to $a = 0.05$, $\beta = 0.1$. (For interpretation of the references to colour in this figure legend, the reader is referred to the web version of this article.)

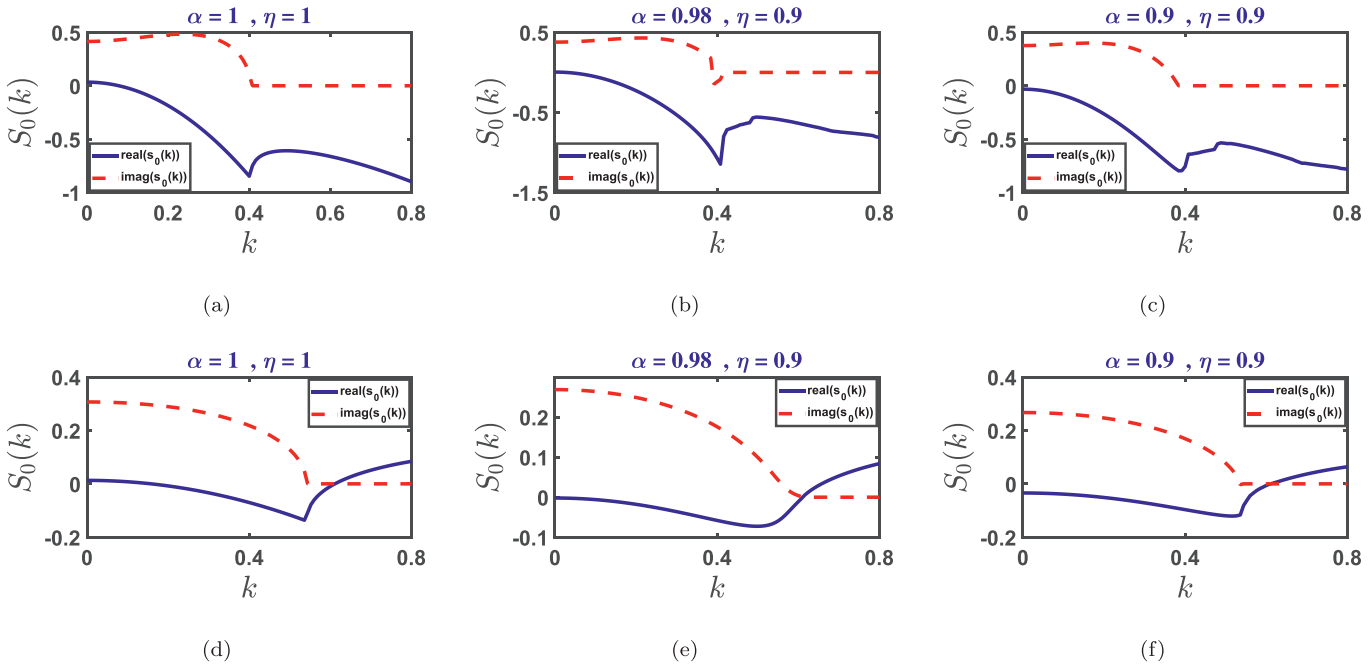

(a) (b) (c)

(d) (e) (f)

Fig. 2. Conditions for the Turing instabilities mentioned in (26) for different value of the derivative order index. Simulations were performed with $K = 2$, $s = 0.25$ and $h = 1$, $m = 1.5$, $r = 0.7$, $d_1 = 0.008$. In (a), (b) and (c), $a = 0.05$, $\beta = 0.1$, with $u(x, 0) = 0.4221 + 0.01\cos(x)$ and $v(x, 0) = 0.3654 + 0.01\cos(x)$. While in (d), (e) and (f), $a = 0.1$, $\beta = 0.5$, $d_2 = 0.03$, with $u(x, 0) = 0.0830 + 0.01\cos(x)$, and $v(x, 0) = 0.0818 + 0.01\cos(x)$.

Now, let us use the approach proposed by Hernández *et al*. [26] to have a Turing instability in the case where $\alpha = \eta < 1$. For this purpose, we start with the Fourier transform of (19), i.e.,

$$\frac{{}^{c}\partial^{\eta}}{\partial t^{\eta}}\begin{pmatrix}\widetilde{u}\\ \widetilde{v}\end{pmatrix} = \begin{pmatrix}-d_1k^2+a_{11} & a_{21}\\ a_{12} & -d_2k^2+a_{22}\end{pmatrix}\begin{pmatrix}\widetilde{u}\\ \widetilde{v}\end{pmatrix} = A(k)\begin{pmatrix}\widetilde{u}\\ \widetilde{v}\end{pmatrix}.$$

The eigenvalues of the stability matrix $[A(k)]$ are given by

$$\lambda_1 = \frac{TrA(k)}{2} + \frac{\left([TrA(k)]^2-4h(k)\right)^{1/2}}{2}, \qquad \lambda_2 = \frac{TrA(k)}{2} - \frac{\left([TrA(k)]^2-4h(k)\right)^{1/2}}{2}, \tag{27}$$

where

$$TrA(k) = -(d_1+d_2)k^2 + (a_{11}+a_{22}), \qquad h(k) = d_1d_2k^4 - \left(a_{11}d_2 + a_{22}d_1\right)k^2 + a_{11}a_{22} - a_{12}a_{21}. \tag{28}$$

The stability of the system is completely determined by the nature of the eigenvalues. Real and negative eigenvalues yield a stable system, meaning that no Turing instabilities are possible. Meanwhile if both are real and one of them is positive (the other being negative), the system will no longer be stable, and the condition for this are exactly similar to the case $\eta = 1$. However, complex roots go with a critical value of η. This critical value η_c only exists if $TrA(k) > 0$, which is given by

$$\eta_c(k) = \frac{2}{\pi}arctan\left(\sqrt{\frac{4h(k)}{[TrA(k)]^2}-1}\right). \tag{29}$$

η_c is a critical value of the of the anomalous exponent or bifurcation parameter that separates a regime of stationary Turing patterns from an oscillatory cellular instability, commonly known as a Hopf - Turing bifurcation [24]. The Turing conditions are fullfiled when the stationary homogeneous state ($k = 0$) is stable, and the system becomes unstable under perturbations with finite wavelength. In other words, when reactions take place in the presence of subdiffusion, the condition (25) can be satisfied in two ways, either

$$\beta > max\{\alpha_2, \alpha_3\} \tag{30}$$

or

$$\beta < \alpha_2, \qquad 4u^{*2}v^{*2}\beta^2 + \alpha_4\beta + \alpha_5 < 0, \qquad \eta_c(0) > \eta, \tag{31}$$

where

$$\alpha_4 = 4v^*\left(-a_{11}u^* - a_{12}v^* + su^*\left(1-\frac{2hv^*}{u^*}\right)\right), \qquad \alpha_5 = a_{11}^2 - 2a_{11}s\left(1-\frac{2hv^*}{u^*}\right) + \frac{4a_{12}shv^{*2}}{u^{*2}} + s^2\left(1-\frac{2hv^*}{u^*}\right)^2. \tag{32}$$

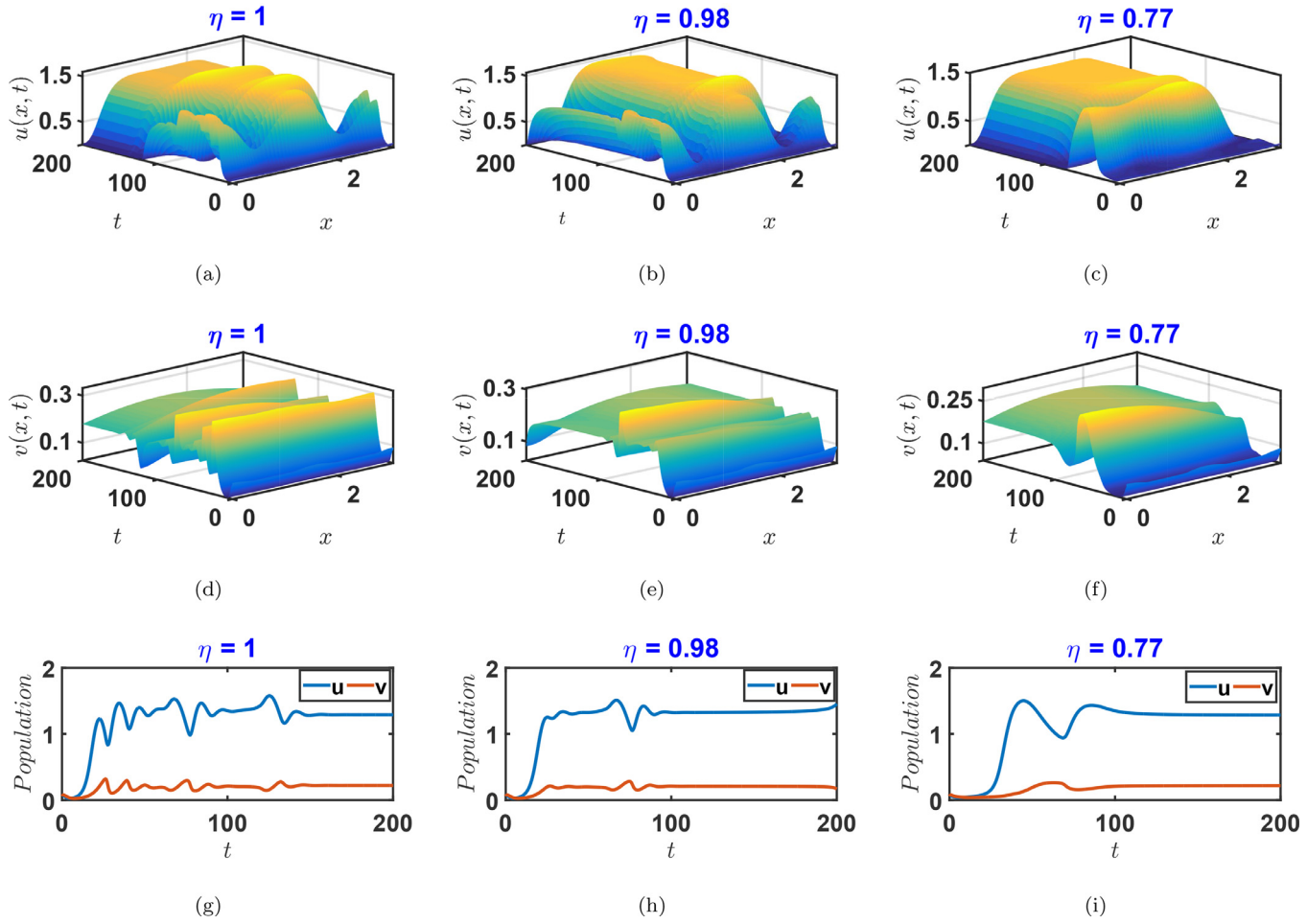

Fig. 3. Efficiency of the toxic substances on prey's density. Simulations were performed with $K = 2$, $s = 0.25$ and $h = 1$, $m = 1.5$, $r = 0.7$. $a = 0.05$, $\beta = 0.1$, $d_1 = 0.008$, $d_2 = 1$. The initial values are $u(x, 0) = 0.0814 + 0.01\cos(4x)$, $v(x, 0) = 0.0812 + 0.01\cos(4x)$.

Condition (31) cannot be fullfiled for the classical diffusion.

To fulfill the condition in (26) it is necessary that

$$\beta > \frac{1}{2Du^*v^*}\left[a_{11} + Ds\left(1 - \frac{2hv^*}{u^*}\right)\right], \tag{33}$$

where $D \neq 1$ is the ratio of diffusion coefficients, and either

$$a_{11} > 0, \qquad \beta > \frac{s}{2u^*v^*}\left(1 - \frac{2hv^*}{u^*}\right), \tag{34}$$

or

$$a_{11} < 0, \qquad \beta < \frac{s}{2u^*v^*}\left(1 - \frac{2hv^*}{u^*}\right). \tag{35}$$

In Fig. 1, we depict the influence of the toxic substances on the parameter that constitute the anomalous exponent. It is clear that the slight variation of the efficiency of the toxicity modifies this parameter, yielding a modification of the anomalous exponent itself. However, it would be premature to assert, based solely on Fig. 1, that this modification would systematically lead to a modification in the Turing instabilities. In order to decide on this, it would be necessary that one of the two relations (25), or (26) should be satisfied. If at least one of the two is verified, then the relationship between the degree of toxicity and the Turing instabilities will be clearly established, as depicted in Fig. 2 which displays clearly the efficiency of toxicity on the Turing instabilities. These results are a direct consequence of Hernandez's work [26] on subdiffusion, where the existence of Turing structures has been demonstrated. In this work, we will take a few cases to study the phenomenon of subdiffusion under the influence of toxicity.

In the next section, we will try to numerically analyze the different possible scenarios by varying a few parameters, with the aim being to see how memory affects different ecosystems.

4. Numerical results and discussions

In this section, our numerical predictions are verified via direct numerical simulations of system (1). This system describes an ecosystem where preys produce a substance that is toxic to predators. In the process, suitable initial and boundary conditions have been use along with explicit and implicit schemes for time and centered difference for space derivatives. The fractional derivatives were approximated using a scheme base on the Grunwald-Letnikov definition [26,34].

We provide now some simulations as evidence of the analytical predictions derived in the previous sections.

Example 1. Consider system (1) with the parameter values $r = 0.7$, $K = 2$, $s = 0.25$, $m = 1.5$, $h = 1$, $d_1 = 0.008$, $d_2 = 1$, $a = 0.1$ and $\beta = 0.1$. For this set of parameters, we first have to make sure that all the above mentioned conditions are met. This can trivially be done numerically by checking if (26) is fullfiled. Upon this, the Turing patterns obtained for this set of parameters are depicted in Fig. 3.

In this case, we observe that before taking into account the memory effect ($\eta = 1$), there are oscillations both in predators and in preys, which means that predators indiscriminately consume

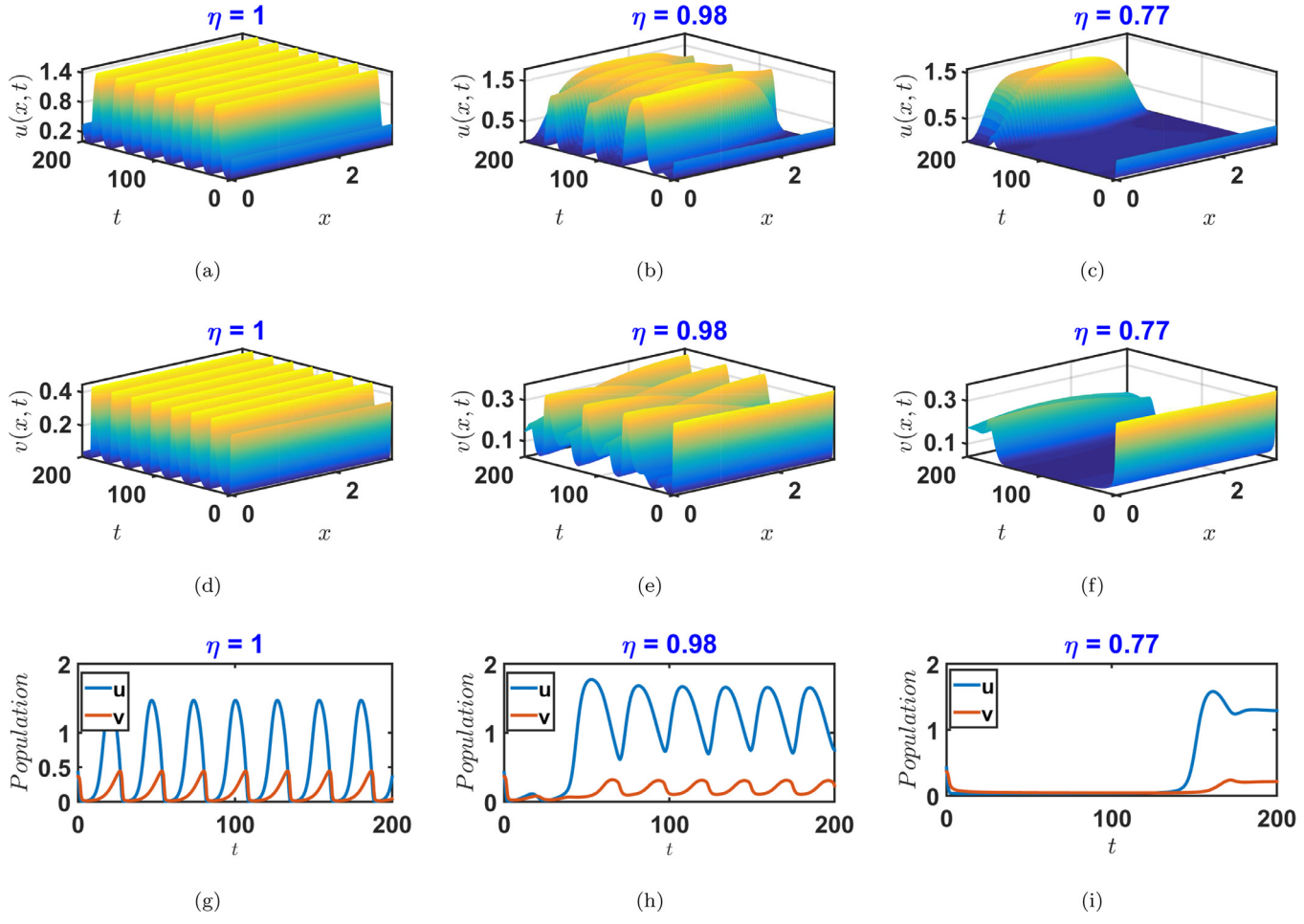

Fig. 4. Efficiency of the toxic substances on prey's density. Simulations were performed with $K = 2$, $s = 0.25$ and $h = 1$, $m = 1.5$, $r = 0.7$. $a = 0.05$, $\beta = 0.1$, $d_1 = 0.008$, $d_2 = 1$, with the initial values being $u(x, 0) = 0.4221 + 0.01\cos(x)$, $v(x, 0) = 0.3654 + 0.01\cos(x)$. Here we changed the initial values.

toxic preys. However, if the memory effect is triggered ($\eta < 1$), we observe that after a certain time, there is stabilization both in preys and predators. This stabilization can be explained in two ways. Either the predators have known how to recognize the less toxic preys, and therefore consume only those preys whose toxicity is reduced, or the predators completely abstain from ingesting the toxic preys. This behavior has been observed in European starlings which, when their body masses have been experimentally reduced become more willing to eat prey items that have been injected with quinine, which is toxic to birds in high doses [35,36]. It is now clear that memory effects play a key role in ways in which naive predators learn to associate warningly preys with their defenses and remember to avoid them in future encounters. This field underpins an extensive body of evolutionary theory [37–41]. Moreover, it is obvious that memory effects regulate the effect of toxic substances on predators. In other word, predators are affected by toxic substances for a certain time, then, they become used to it, and the ecosystem becomes locally stable as shown in Fig. 3 $(e) - (f)$ and $(h) - (i)$.

Example 2. Let $a = 0.05$, $d_1 = 0.1$, and the other parameters remain as in the first example. As previously, we make sure that condition (26) is satisfied. For this set of parameters, we have the structures of Fig. 4.

Despite the toxicity of preys, the cohabitation between predator and prey takes place without any problems, even if the number of predators remains relatively low. However, when we take into account the memory effect, we realize that the number of preys decreases considerably, while that of predators remains relatively constant. By further reducing the fractional order of the derivative, we observe a complete stabilization of the two entities (predators and preys). Albeit the drastic fall in their respective population, no species will disappear due to the effect of fractional - order parameter or memory effect. This scenario is similar to the one described in Ref[42]. where predators deliberately choose to swallow toxic preys, choice which is a trade-off between the benefits of obtaining nutrients and the costs of ingesting toxins. This trade-off is affected by the fact that: animals will consume more toxic preys if they are food-deprived. Indeed, animals face constant decisions about what to eat and what not to eat. While some items are never worth eating, there are many cases where the decision to eat or not should depend on the environment and the individual's current state [43–45]. For example, many potential preys available to wild birds are chemically defended, and so contain toxins that will be harmful in the long term or if eaten in excess [46,47]. However, such preys also contain valuable nutrients. In such cases, having lower energy reserves or poorer foraging prospects shifts the balance of costs and benefits in favour of consumption [45].

Example 3. Once more, we consider system (1) with the parameter values $\beta = 0.3$, $a = 0.05$, the others remain unchanged. In this case also, the validity of (26) is checked. The resulting structures are shown in Fig. 5. This case presents some similarities with the one depicted in *example* 2. The preys are not really affected by the predators, which is similar to the case discussed in Ref. [48]. Here,

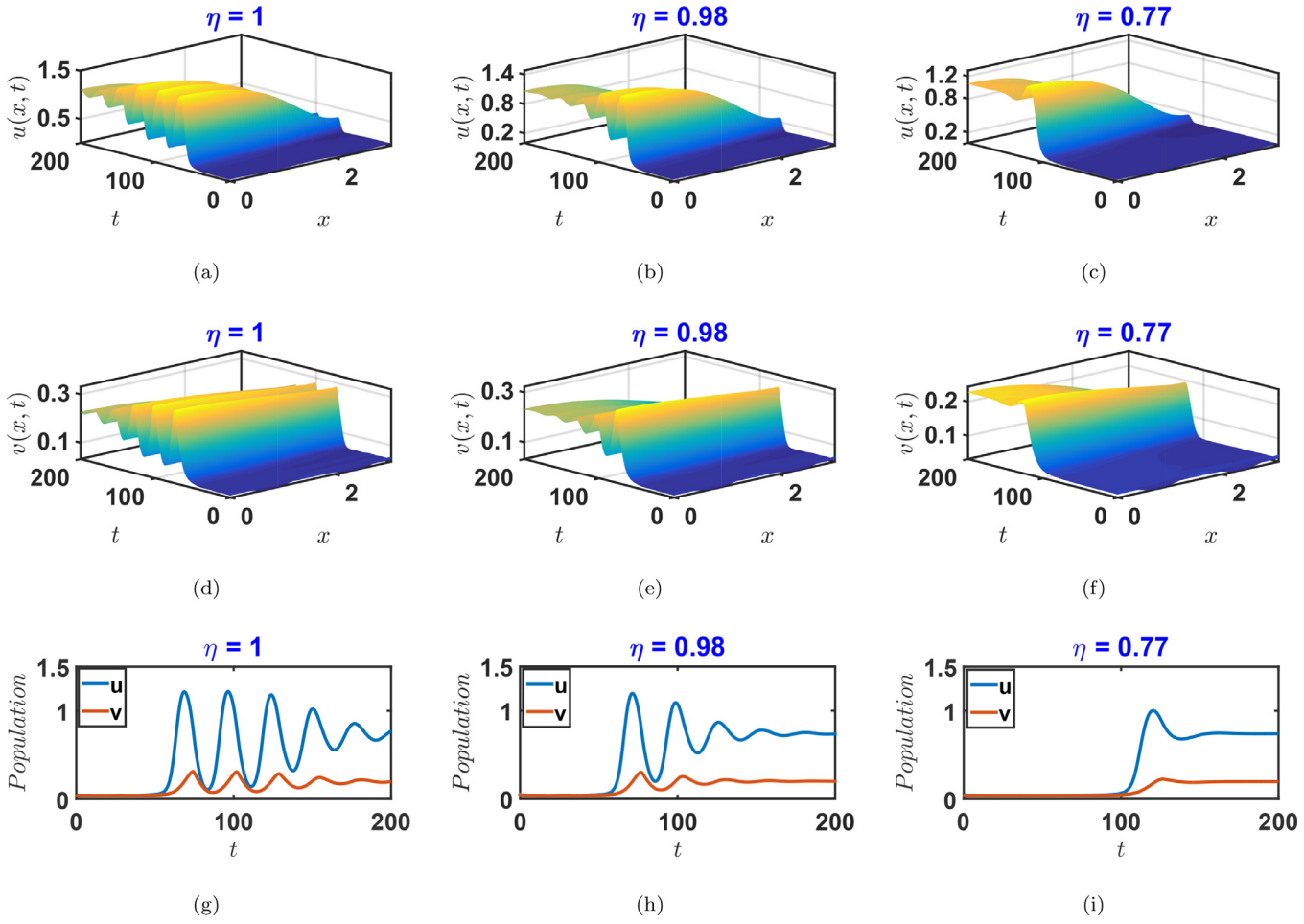

Fig. 5. Efficiency of the toxic substances on prey's density. Simulations were performed by changing the values of initial conditions and the toxic coefficient, yielding $K = 2$, $s = 0.25$ and $h = 1$, $m = 1.5$, $r = 0.7$. $a = 0.05$, $\beta = 0.3$, $d_1 = 0.08$, $d_2 = 1$, and $u(x, 0) = 0.0422 + 0.01\cos(4x)$, $v(x, 0) = 0.0421 + 0.01\cos(4x)$.

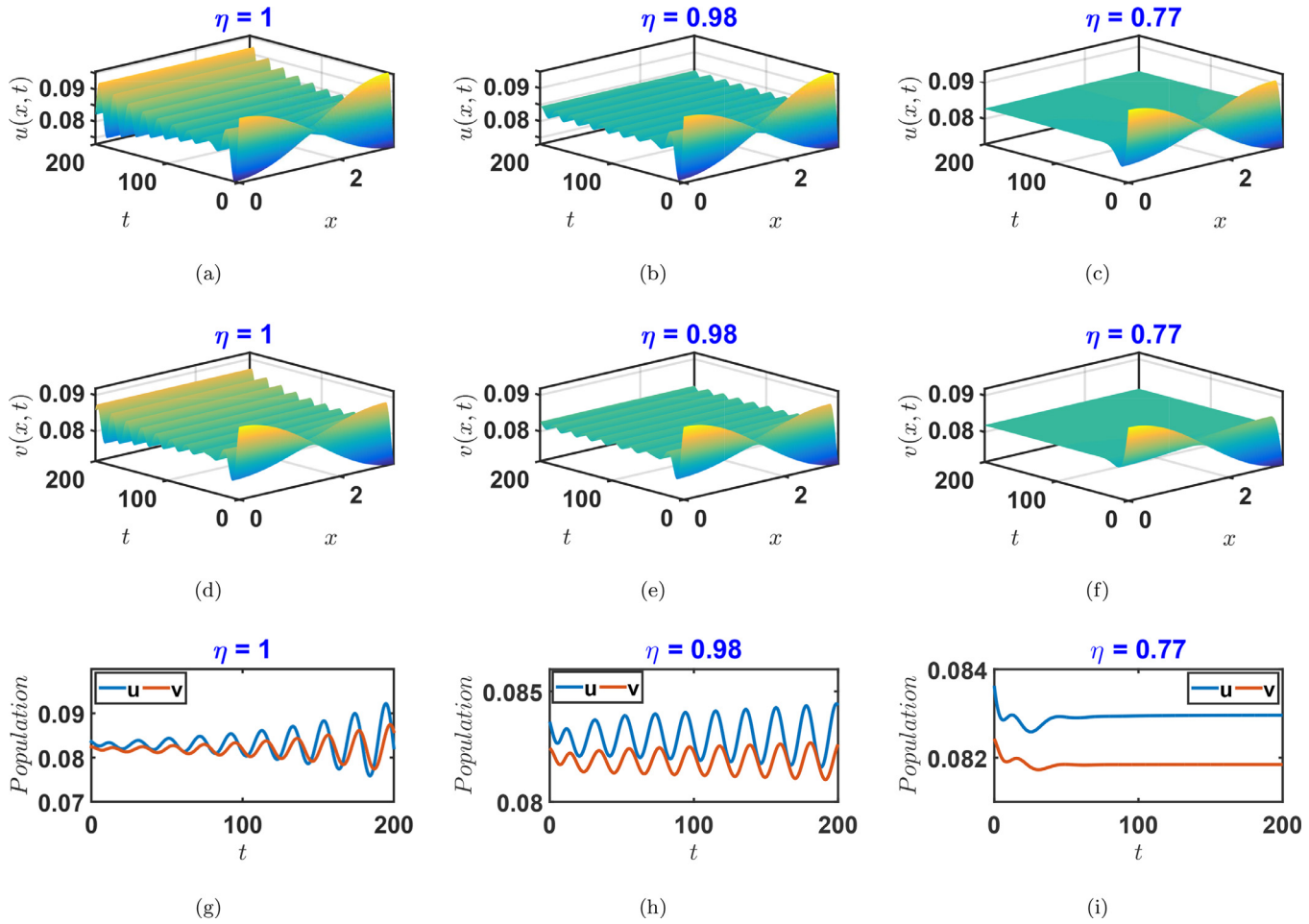

Fig. 6. Efficiency of the toxic substances on prey's density. Simulations were performed by changing the values of a, the coefficient of diffusion, the coefficient of toxicity, and initial conditions yields $K = 2$, $s = 0.25$ and $h = 1$, $m = 1.5$, $r = 0.7$. $a = 0.1$, $\beta = 0.5$, $d_2 = 0.03$, $d_1 = 0.1$, $u(x, 0) = 0.0830 + 0.01\cos(x)$, $v(x, 0) = 0.0818 + 0.01\cos(x)$.

the first conspicuous mutants would have to survive greater levels of predation than previously thought, because even when the learning process is complete, educated predators may still be prepared to eat aposematic prey. There may be another reason for this phenomenon. Indeed, a predator's ability to moderate and process toxins would be a key factor in limiting attack rates on chemically defended preys, and one that could have significant implications for the survival advantage of being aposematic [48].

Example 4. The set of parameters used here is almost the same as in the previous cases, except for $a = 0.1$, $\beta = 0.5$, $d_1 = 0.1$ and $d_2 = 0.03$. For these parameter values, condition (26) is also met. The resulting structures of Fig. 6. reveal that predators and prey may be simultaneously exposed to toxins. Since the natural dispersive force of the movement of each species is weak ($\frac{d_2}{d_1} < 1$), we can conclude that this configuration corresponds to environmental toxins exposure. Indeed, if toxin came from either preys or predators, it could not be affected as much. This means that toxin comes from the environment. The impact of environmental toxins on predator-prey dynamics has recently been investigated [49]. Since mobility is reduced, we are in a situation of confinement in a toxic environment. The direct effects of toxins typically reduce organism abundance by increasing mortality or reducing fecundity. Such direct effects, therefore, alter both bottom-up food availability and top-down predatory ability. However, the indirect effects, when mediated through predator-prey interactions, may lead to counterintuitive effects. Environmental toxins also reduce population variability by preventing populations from fluctuating around a coexistence equilibrium [49] as depicted in Fig. 6 (f) and (i).

5. Conclusion

The main objective of this work, was to answer the question whether toxic coefficient β, in the presence of memory can still be considered as an important parameter that can give rise to complex spatial dynamics. To this end, we have examined the influence of toxic substances on the dynamics properties of the fractional-order ODE system (3), then we have analyzed the system describing an ecosystem where preys produce substance that is toxic for predators in the subdiffusive regime, and give general conditions for toxicity coefficient allowing Turing instability to appear. We have numerically studied in the generic model Eq. (1). Particularly, investigation have been conducted with emphasis on the effect of subdiffusion on pattern formation in a context where preys release toxin to prevent attacks from predators. Insisting on the formation of Turing patterns, it appears clearly that the effect of toxic coefficient can either be altered by the memory effects by canceling existing Turing structures or by creating new ones.

This study allows us to understand the behavior of toxins in a subdiffusive environment such as neuron. In fact, nervous transmission and conduction, the targets of toxins being overwhelmingly dominated by subdiffusion where strong memory effects play a crucial role in transport mechanism [29] can be modeled by bacterial dynamics [50] whose mathematical description is mainly done by prey-predator models.

We could not finished this work whitout mentioning the importance of the parameter in the ecosystem. Each scenario is reallistic, one has to adequately choose the parameter values. As an illustra-

tion, we have proposed four examples. In each of them, by changing the value of certain key parameters, the system configuration changed. In each configuration obtained, memory plays more of a stabilizing role while preserving the ecosystem, regardless of the value of the toxic coefficient. This findings suggest that the memory plays a key role in conservation.

Declaration of Competing Interest

The authors declare that they have no known competing financial interests or personal relationships that could have appeared to influence the work reported in this paper.

CRediT authorship contribution statement

D.C. Bitang à Ziem: Conceptualization, Data curation, Validation, Visualization, Writing – review & editing. **C.L. Gninzanlong:** Data curation, Software. **C.B. Tabi:** Writing – review & editing. **T.C. Kofané:** Supervision, Validation.

References

[1] Tiaho F, Becq F, de venin HNT. Toxines de venin: des armes biologiques redoutables au service de la santé humaine. Med Sci (Paris) 2001;17(8–9):947–51. And references therein

[2] Poulton EB. The colours of animals: their meaning and use especially considered in the case of insects. London: Kegan Paul, Trench, Trübner and Co, Ltd; 1890.

[3] Mappes J, Marples N, Endler J.A. The complex business of survival by aposematism. Trends Ecol Evol. 2005. 20, 598–603,

[4] Halpin CG, Skelhorn J, Rowe C. Predators' decisions to eat defended prey depend on the size of undefended prey. Anim Behav 2013;85:1315–21.

[5] Gittleman J, Harvey PH. Why are distasteful prey not cryptic? Nature 1980;286:149–50.

[6] Alatalo RV, Mappes J. Tracking the evolution of warning signals. Nature 1996;382:708–10.

[7] Lindström L, Alatalo RV, Mappes J, Riipi M, Vertainen L. Can aposematic signals evolve by gradual change? Nature 1999;397:249–51.

[8] Stevens M, Ruxton G.D. Linking the evolution and form of warning coloration in nature. 2012. Proc R Soc Lond B, 279, 417–426

[9] Chattopadhyay J. Effect of toxic substances on a two-species competitive system. Ecol Modell 1996;84(1–3):287–9.

[10] Kar TK, Chaudhuri KS. On non-selective harvesting of two competing fish species in the presence of toxicity. Ecol Modell 2003;161(1–2):125–37.

[11] Samanta GP. A two-species competitive system under the influence of toxic substances. Appl Math Comput 2010;216(1):291–9.

[12] Aly S. Competition in patchy space with cross-diffusion and toxic substances. Nonlinear Anal Real World Appl 2009;10(1):185–90.

[13] Jana D, Dolai P, Pal AK, Samanta GP. On the stability and Hopf-bifurcation of a multi-delayed competitive population system affected by toxic substances with imprecise biological parameters. Model Earth Syst Environ 2016;2(3):110.

[14] Li Z, Chen F, He M. Asymptotic behavior of the reaction-diffusion model of plankton allelopathy with nonlocal delays. Nonlinear Anal Real World Appl 2011;12(3):1748–58.

[15] Bitang A Ziem DC, Mvogo A, Kofane TC. Effects of transport memory in wave fronts in a bistable reaction-diffusion system. Physica A 2019;517:36–46.

[16] Abramson G, Bishop AR, Kenkre VM. Effects of transport memory and nonlinear damping in a generalized Fisher's equation. Phys Rev E 2001. 066615-1-64066615-6.

[17] Manne KK, Hurd AJ, Kenkre VM. Nonlinear waves in reaction-diffusion systems: the effect of transport memory. Phys Rev E 2000;61:4177–84.

[18] Barros L.C.D, Lopes M.M, S.F, et al. The memory effect on fractional calculus: an application in the spread of COVID-19. 2021. Comp Apply Math, 40, 72, 10.1007/s40314-021-01456-z.

[19] Richie K, Shan X-YJK, Iwasawa T, Kusumi A. Detection of non-Brownian diffusion in the cell membrane in single molecule tracking. J Biophys 2005;88:2266–77.

[20] Goychuk I, Hänggi P. Fractional diffusion modeling of ion channel gating. Phys Rev E 2004;70. 051915-1-051915-9

[21] Metzler R, Klafter J, Jortner J, Volk M. Multiple time scales for dispersive kinetics in early events of peptide folding. Chem Phys 1998;293:477–84.

[22] Drazer G, Zanette DH. Experimental evidence of power-law trapping-time distributions in porous media. Phys Rev E 1999;60(5):5858–64.

[23] Hilfer R. Experimental evidence for fractional time evolution in glass forming materials. Chem Phys 2002;284:399–408.

[24] Gafiychuk VV, Datsko BY. Stability analysis and oscillatory structures in time-fractional reaction-diffusion systems. Phys Rev E 2007;75. 055201-1-055201-4

[25] Langlands TAM, Henry BI, Wearne SL. Turing pattern formation with fractional diffusion and fractional reactions. J PhysCondens Matter 2007;19. 0651151-15

[26] Hernández D, Varea C, Barrio R.A. Dynamics of reaction-diffusion systems in a subdiffusive regime. 2009. Phys Rev E, 79, 026109.

[27] Turing AM. The chemical basis of morphogenesis. Philos Trans R Soc London Ser-B 1952;237:37–72.

[28] Zhang H, Zhao H. Dynamics and pattern formation of a diffusive predator-prey model in the presence of toxicity. Nonlinear Dyn10.1007/s11071-018-4683-2.

[29] Yadav A, Horsthemke W. Kinetic equations for reaction-subdiffusion systems: derivation and stability analysis. Phys Rev E 2006;74. 0661181-10.

[30] Yadav A, Milu SM, Horsthemke W. Turing instability in reaction-subdiffusion systems. Phys Rev E 2008;78. 026116-1-026116-8.

[31] del Castillo-Negrete D, Carreras BA, Lynch VE. Nondiffusive transport in plasma turbulence: a fractional diffusion approach. Phys Rev Lett 2005;94:065003.

[32] Méndez V, Fedotov S, Horsthemke W. Reaction - transport systems. mesoscopic foundations, fronts, and spatial instabilities. New York: Springer; 2010.

[33] Guckenheimer J, Holmes P. Nonlinear oscillations. New York: dynamical systems and bifurcation of vector fields Springer-Verlag; 1983.

[34] Podlubny I. Fractional differential equations. New York: Academic Press; 1999.

[35] Barnett CA, Bateson M, Rowe C. State-dependent decision making: educated predators strategically trade off the costs and benefits of consuming aposematic prey. Behav Ecol 2007;18(4):645–51. doi:10.1093/beheco/arm027.

[36] Barnett CA, Skelhorn J, Bateson M, Rowe C. Educated predators make strategic decisions to eat defended prey according to their toxin content. Behav Ecol 2012;23(2):418–24. doi:10.1093/beheco/arr206.

[37] Speed MP. Muellerian mimicry and the psychology of predation. Anim Behav 1993;45:571–80.

[38] Müller F. Ituna and Thyridia: a remarkable case of mimicry in butterflies. Proc Ent Soc 1878. 1879:xx-xxiv.

[39] Speed MP. Can receiver psychology explain the evolution of mimicry? Anim Behav 2001;61:205–16.

[40] Batesian SMP. quasi-batesian or Muüllerian mimicry? Theory and data in mimicry research. Evol Ecol 2001;13:755–76.

[41] Servedio MR. The effects of predator learning, forgetting, and recognition errors on the evolution of warning coloration. Evol Int J Org Evol 2000;54:751–63.

[42] Bloxham L, Bateson M, Bedford T, Brilot B, Nettle D. The memory of hunger: developmental plasticity of dietary selectivity in the european starling. Sturnus vulgaris Anim Behav 2014;91:33–40.

[43] Kokko H, Mappes J, Lindström L. Alternative prey can change model-mimic dynamics between parasitism and mutualism. Ecol Lett 2003;6(12):1068–76.

[44] Sih A, Christensen B. Optimal diet theory: when does it work, and when and why does it fail? Anim Behav 2001;61(2):379–90.

[45] Stephens DW, Krebs JR. Foraging theory. Princeton: Princeton University Press; 1986.

[46] Eisner T, Eisner M, Siegler. Secret weapons: defences in insects, spiders, scorpions, and other many-legged creatures. Cambridge: Harvard University Press; 2005.

[47] Eisner T, Meinwald J. Defensive secretions of arthropods. Science 1966;153(3742):1341–50.

[48] Skelhorn J, Rowe R. Predators' toxin burdens influence their strategic decisions to eat toxic prey. Curr Biol 2007;17:479–1483.

[49] Huang Q, Wang H, Lewis MA. The impact of environmental toxins on predator-prey dynamics. J Theor Bio 2015;378:12–30.

[50] Ram A, Lo AW. Is smaller better? A proposal to use bacteria for neuroscientific modeling. Front Comput Neurosci 2018;12:7. doi:10.3389/fncom.2018.00007.